Nitrogen in the Orgueil meteorite: Abundant ammonium among other reservoirs of variable isotopic compositions

Lucie Laize-Générat, Lison Soussaintjean, Olivier Poch, Lydie Bonal, Joël Savarino, Nicolas Caillon, Patrick Ginot, Anthony Vella, Alexis Lamothe, Rhabira Elazzouzi, et al.

Nitrogen in the Orgueil meteorite: abundant ammonium among other reservoirs of variable isotopic compositions

Lucie Laize-Générat[a]*, Lison Soussaintjean[a,b]*, Olivier Poch[a]**, Lydie Bonal[a], Joël Savarino[c], Nicolas Caillon[c], Patrick Ginot[c], Anthony Vella[c], Alexis Lamothe[c], Rhabira Elazzouzi[c], Laurène Flandinet[a], Lionel Vacher[a], Matthieu Gounelle[d], Martin Bizzaro[e], Pierre Beck[a], Eric Quirico[a], Bernard Schmitt[a]

[a]Univ. Grenoble Alpes, CNRS, IPAG, 38000 Grenoble, France

[b]now at Climate and Environmental Physics, Physics Institute & Oeschger Centre for Climate Change Research, University of Bern, Bern, Switzerland

[c]Univ. Grenoble Alpes, CNRS, IRD, G-INP, Institut des Géosciences de l'Environnement, Grenoble, France

[d]Muséum National d'Histoire Naturelle, IMPMC, Paris, France

[e]University of Copenhagen, Centre for Star and Planet Formation, Globe Institute, Copenhagen, Denmark

* Equal contribution to this work

** Corresponding author (olivier.poch@univ-grenoble-alpes.fr)

Manuscript accepted in Geochimica et Cosmochimica Acta on 01/10/2024

Abstract

Nitrogen, because of its abundance and variety of carrier phases, is a unique tracer of physico-chemical processes occurring throughout star and planet formations. The refractory organic matter is commonly considered as the main carrier of nitrogen in the most primitive

objects of our Solar System. However, nitrogen in the form of ammonium (NH_4^+) was observed in the Ivuna-type carbonaceous (CI) chondrites Alais in 1834, and Orgueil just after its fall in 1864, as well as more recently on Ceres, comet 67P/Churyumov-Gerasimenko, and possibly on some asteroids. In the present study, we have measured the nitrogen content and isotopic composition in various nitrogen-bearing phases of several samples of the Orgueil meteorite, with different degrees of terrestrial weathering. Water-soluble NH_4^+ is present in Orgueil at a mean concentration of 0.07 ± 0.01 wt.%, with a mean isotopic composition of $\delta^{15}N$ = +72 ± 9 ‰ ($^{14}N/^{15}N$ = 254 ± 2), confirming its extra-terrestrial origin. In the most terrestrially altered sample of Orgueil that we analysed, the isotopic composition is $\delta^{15}N$ = +50 ± 12 ‰ ($^{14}N/^{15}N$ = 259 ± 3). NH_4^+ is in species that are thermally stable up to 383 K, possibly ammonium inorganic/organic salts and ammoniated phyllosilicates. We also show that the nitrogen in Orgueil is distributed among the insoluble organic matter (IOM) (35 ± 5 %), ammonium (27 ± 5 %), and other minor water-soluble species (e.g., nitrate, amines etc.: < 6 %). The remaining nitrogen (34 ± 14 %) is mainly in an unidentified organic matter (UOM), which may be IOM lost during its extraction and/or acid hydrolysable functional groups bounded to the IOM and/or organic nitrogen trapped within minerals. The three main carriers of nitrogen in Orgueil have $\delta^{15}N$ (and $^{14}N/^{15}N$) values of +32 ± 1 ‰ (264 ± 0.3) for IOM, +39 ± 16 ‰ (262 ± 4) for UOM, and +72 ± 9 ‰ (254 ± 2) for NH_4^+.

Although IOM and NH_4^+ have significantly different $\delta^{15}N$, we cannot exclude that these phases could be compositionally related because IOM is heterogeneous in ^{15}N. Ammonium could have been produced via heating and/or aqueous alteration processes of organic matter in the CI parent body. Alternatively, or additionnally, ammonium could be a tracer of the accretion and/or later deposit of NH_3 ice, NH_3 hydrates, and/or NH_4^+ salts on the CI parent body.

As shown by previous studies, Ryugu grains sampled by the Hayabusa2 mission (JAXA) have heterogeneous compositions at the millimeter scale, with nitrogen concentrations

and $\delta^{15}N$ similar or lower than Orgueil, possibly because of different parent body processing. The present study suggests that the lack or loss of ^{15}N-rich NH_4^+ in some Ryugu grains may explain some of these differences with Orgueil.

Keywords: Orgueil; Carbonaceous chondrites; Isotope; 15N/14N ratio; Nitrogen

1. Introduction

Nitrogen is one of the most abundant elements in the universe; it can exist in a large variety of species or phases. In this regard, nitrogen is a unique tracer of physico-chemical processes occurring at each step of star and planet formation.

Earth and several icy bodies of the Solar System (Titan, Triton, Pluto) have N_2-dominated atmospheres. On Earth, the geochemical cycle of nitrogen plays fundamental roles in the evolution and maintenance of the biosphere, as nitrogen is one of the essential elements with C, H, and O constituting the molecular building blocks of life. However, the incorporation and evolution of these elements in the early Solar System and finally in Solar System bodies are still poorly understood. This is especially the case of nitrogen, whose elemental ratio relative to silicon and isotopic composition show larger variations among Solar System bodies than carbon and oxygen do (Geiss, 1987; Lodders, 2004; Pontoppidan et al., 2014; Füri and Marty, 2015; Bergin et al., 2015; Lyons et al., 2018). Some of these variations may be due to differences in the abundances and/or nature of the nitrogen-bearing species accreted by these bodies and/or delivered later.

Up to now, nitrogen in primitive small bodies is considered to be mainly carried by their refractory organic matter (Aléon, 2010; Alexander et al., 2017; Fray et al., 2017). However, nitrogen in the form of ammonium (NH_4^+) has recently been identified on the dwarf planet

Ceres and on the nucleus of comet 67P/Churyumov-Gerasimenko, which appear to be entirely covered with ammoniated phyllosilicates and ammonium salts, respectively (King et al., 1992; De Sanctis et al., 2015; Poch et al., 2020). Ammonium is also thought to be present at the surfaces of various asteroids (Poch et al., 2020; Rivkin et al., 2022). Consequently, the nitrogen contained in these objects is not only in the form of refractory organic matter but also present as ammonium (e.g., NH_4^+ in organic and inorganic salts, and/or NH_4^+-bearing minerals). If the concentrations of ammonium – currently unknown – are high, some of these objects may contain more nitrogen than previously thought (Poch et al., 2020; Altwegg et al., 2020). This would have implications for the distribution and evolution of nitrogen in the early Solar System, its incorporation into planets, and possibly, the emergence of life as ammonium is known to promote the synthesis of multiple prebiotic molecules (Weber, 2007; Dziedzic et al., 2009; Callahan et al., 2011; Burcar et al., 2016).

These recent identifications of ammonium on small bodies raise the question of its presence in carbonaceous chondrite meteorites, which are fragments of some of the most primitive small bodies of the Solar System. Very few studies have searched for ammonium in carbonaceous chondrites. The highest concentration of ammonium was reported in the Orgueil meteorite immediately after its fall in 1864 (Daubrée, 1864; Pisani, 1864; Cloëz, 1864). Orgueil belongs to a rare group of carbonaceous chondrites, the Ivuna-type carbonaceous (CI) chondrites, designated as chemically primitive meteorites because their bulk compositions are the closest to that of the solar photosphere (Lodders, 2021). Although chemically primitive, the CI chondrites are made of highly aqueously altered minerals (Gounelle and Zolensky, 2014). Soluble ammonium was detected in Orgueil independently by Cloëz (1864) and Pisani (1864) at a concentration of about 0.1 wt.% (Cloëz, 1864), among several substances that are soluble in water (chlorides, sulfates etc.) that account for 3-5 wt.% of the meteorite. Cloëz (1864) reported the presence of ammonium chloride ($NH_4^+Cl^-$), in a solution obtained after leaching

the meteorite with rectified alcohol, and as part of a white deposit crystallizing on the surface of the stone when heated. Later, Ansdell and Dewar (1886) also observed the crystallization of abundant ammonium sulfate ($(NH_4^+)_2SO_4^{2-}$) on the cold parts of the tube in which they had heated a powdered sample of the Orgueil meteorite. Following the analyses of Wiik (1956), who did not report ammonium, Urey (1966) hypothesized that ammonium escaped from the stone during the century of storage: $NH_4^+Cl^-$ would have been hydrolyzed by water vapour to form ammonia (NH_3) and HCl. HCl would react with minerals, and NH_3 would escape from the meteorite. Vdovykin (1970) pointed out that the reaction of HCl with minerals is possibly confirmed by the detection of up to 3 % chlorine in rounded particles of iron hydroxide observed in Orgueil by Nagy et al. (1963).

The terrestrial alteration of the Orgueil meteorite by water vapour and oxygen was documented since its fall. Pisani (1864) reported the probable transformation of Orgueil iron sulfides in sulfates. One century later, Dufresne and Anders (1962) identified white veins of sulfate salts. These salts may have been originally present in the meteorite and/or they were produced by the oxidation of sulfides, and they were dissolved and remobilised due to the interaction of the meteoritic material with humidity during its storage (Gounelle and Zolensky, 2001). The analysis of Ryugu samples confirms that pristine CI material is indeed devoid of sulfate veins (Nakamura et al., 2023). Because some ammonium salts can be relatively volatile, hygroscopic and water-soluble, they could also be dissolved, remobilised, volatilised, or leached by terrestrial water, during storage of the meteorite under ambient conditions. After Urey (1966), Gounelle and Zolensky (2014) also hypothesized that these ammonium salts are no longer present in Orgueil. However, the fact that neither Wiik (1956) nor later studies reported the presence of ammonium in Orgueil may also be because it was simply not searched for.

More recently, Pizzarello and collaborators reported the release of NH_3 after hydrothermal treatment at 100°C of powders of Murchison meteorite (0.002 wt.%) (Pizzarello et al., 1994) and of two Renazzo-type carbonaceous (CR) chondrites (0.02 and 0.03 wt.%) (Pizzarello and Holmes, 2009). However, the experimental conditions used in these studies (hydrochloric acid at 100°C for 24 h) may have resulted in the release of NH_3 from the decomposition of organic matter and/or of volatile ammonium salts, precluding the identification of the original ammonium-bearing phases. In a following study, hydrothermal treatment (water at 300°C and 100 MPa for six days) of the insoluble organic matter (IOM) of Orgueil and several other carbonaceous chondrites was found to release NH_3 enriched in ^{15}N compared to the IOM and comprising 14 % of the total nitrogen in the case of Orgueil (Pizzarello et al., 2011; Pizzarello and Williams, 2012). Mautner (2014) carried out milder extractions (H_2O at 20°C for 4 days) of soluble ions from several carbonaceous chondrites and reported NH_4^+ concentrations ranging from 0.001 wt.% to 0.03 wt.% in CK, CO, CV, CR, and CM chondrites. However, the extraterrestrial origin of the NH_4^+ was not confirmed by isotopic analysis, and Orgueil was not measured (Mautner, 2014). Very recently, Yoshimura et al. (2023) reported 0.061 ± 0.006 wt.% NH_4^+ in Orgueil, after solubilisation for 20 h in ultra-pure water at 105°C. This study confirms the presence of water-soluble NH_4^+ in this meteorite, even after 159 years of residency on Earth, but it did not confirm its extraterrestrial origin.

In the present study, we aim to provide answers to the following questions: Does this ammonium detected in Orgueil result from terrestrial contamination or is it of extraterrestrial origin? How much of the total (bulk) nitrogen is present as ammonium? How is Orgueil nitrogen distributed between the different nitrogen-bearing phases (ammonium, soluble and insoluble organic matter)? Are there any genetic links between these nitrogen-bearing phases?

With these goals in mind, we have analysed several samples of the Orgueil meteorite, from two different sources and curation conditions, to determine their nitrogen contents and

isotopic compositions. For each sample, we have extracted and characterised bulk nitrogen, nitrogen in IOM, and nitrogen in water-soluble ammonium. To avoid terrestrial contamination and physico-chemical transformations that would volatilise some ammonium species and/or produce ammonium from the decomposition of organic compounds, we have developed a contamination-free and cryogenic protocol to extract the water-soluble ammonium contained in the meteorite. In section 2 of this paper, we first present the studied samples, and the experimental protocols used to extract and characterise the nitrogen content and isotopic composition of the bulk meteorite, the IOM, and the water-soluble ammonium. The results of these analyses are presented in section 3, along with the quantification of other organic and inorganic water-soluble ions. We also establish how nitrogen is distributed among the various nitrogen-bearing phases in Orgueil: NH_4^+, IOM, and other phases, including a yet unidentified material mainly made of organic matter. In section 4, we discuss the degree of terrestrial alteration of the nitrogen-bearing phases in Orgueil and we compare these results to previous studies, including those performed on Ryugu grains. We also discuss their implications for the history of Orgueil and the parent body of CI chondrites in general. Finally, section 5 summarises the main conclusions.

2. Materials and Methods

2.1. Samples

Given that Orgueil is known to have been altered by the terrestrial environment (Gounelle and Zolensky, 2001), and because ammonium might be present in volatile phases that are easily lost, we have selected two samples of Orgueil that have been stored under different conditions.

The sample that we have named “Orgueil-Flask” (OF) is material collected just after the fall in 1864 by a teacher in the Orgueil village in France, and kept in a tightly sealed flask in their attic as far as we know. The teacher’s family discovered the flask in 2017, and it was probably opened between 2017 and 2018. We have selected this sample because of its optimal storage conditions, which minimised its exchanges with the terrestrial atmosphere. By contrast, the sample named “Orgueil Museum” (OM) is a chip from a 2.5 kg fragment kept in a sealed (but possibly leaking) bell-jar exhibited in the Museum Victor Brun of Montauban (France). This fragment of Orgueil has its fusion crust covered by abundant sulfate veins and efflorescences, indicative of terrestrial weathering (Gounelle and Zolensky 2001).

We performed analyses on five pieces of each sample, named OFa to OFe and OMa to OMe, listed with their respective masses in Table 1.

2.2. Spectroscopy measurements

To compare the degree of terrestrial alteration of OF and OM, we have measured the visible and infrared reflectance spectra over the wavelength range from 0.38 to 4.2 µm on an individual chip (larger than 2 mm) of each sample (Soussaintjean et al., 2021), using the spectro-gonio radiometer SHADOWS (Spectrophotometer with cHanging Angles for the Detection Of Weak Signals) (Potin et al., 2018). This instrument enables the measurement of dark samples available in small quantities. The samples were illuminated with a monochromatic beam $\leq$ 1.7 mm in diameter, at normal incidence, and at an emergence angle of 30°. The reflectance was measured by steps of 20 nm over the entire wavelength range. The spectral resolution was of 5 nm from 0.38 to 0.66 µm, 10 nm from 0.68 to 1.58 µm, 20 nm from 1.60 to 2.82 µm, and 41 nm from 2.84 to 4.20 µm. Surfaces of Spectralon and Infragold (LabSphere Inc.) were measured, from 0.38 to 2.00 µm and from 1.20 to 4.8 µm, respectively, under the

same conditions as the samples and used as references to calibrate the signal measured on the samples, and to obtain absolute values of reflectance factors, as described in Potin et al. (2018).

2.3. Measurements of elemental and isotopic bulk compositions

The total amounts and isotopic compositions of nitrogen and carbon contained in the bulk samples were measured by isotope ratio mass spectrometry (IRMS). To ensure that these measurements are representative of the bulk composition of each sample, one chip was crushed and homogenised in an agate mortar, and then two or three replicates of about 3 mg of this powder were put in tin capsules for IRMS analysis (Table 1). The IRMS system is a delta V advantage combined with a Thermo Scientific EA IsoLink CNSOH gas chromatography. Due to the injection of oxygen, the temperature of the combustion furnace (set to 1020 °C) reaches about 1800 °C for a few seconds and the nitrogen and carbon present in the samples are oxidised to NO_x and CO_2. The NO_x is then reduced in a quartz tube reactor filled with chromium oxide, reduced copper, and silvered cobalt oxide. The produced N_2 and CO_2 are separated by chromatography and their isotopic compositions measured with the delta V advantage IRMS. The total amount of nitrogen and carbon are determined by calibration with a commercial High Organic Sediment standard OAS (B2151) with a known concentration of 0.52 wt.% nitrogen and 7.45 wt.% carbon. The measured isotopic compositions were corrected for blanks (using empty tin capsules) and are reported as relative differences in isotope ratios, $\delta^{15}\mathrm{N}\ (‰) = \left(\frac{^{15}\mathrm{N}/^{14}\mathrm{N}_{\mathrm{sample}}}{^{15}\mathrm{N}/^{14}\mathrm{N}_{\mathrm{reference}}} - 1\right) \times 1000$, $\delta^{13}\mathrm{C}\ (‰) = \left(\frac{^{13}\mathrm{C}/^{12}\mathrm{C}_{\mathrm{sample}}}{^{13}\mathrm{C}/^{12}\mathrm{C}_{\mathrm{reference}}} - 1\right) \times 1000$, the references being terrestrial atmospheric N_2 ($^{15}N/^{14}N_{reference} = 3.676 \times 10^{-3}$) (Mariotti et al., 1984) and Vienna Pee Dee Belemnite, VPDB, ($^{13}C/^{12}C_{reference} = 0.0111802$) (Gonfiantini, 1984). The accuracy of $\delta^{15}N$ and $\delta^{13}C$ measurements were estimated as the standard deviation (σ) of the residuals between the measured values and the true values of standards. One certified standard

and one internal standard were routinely included during the analysis runs and used as reference materials to determine the $\delta^{15}N_{raw}$ and $\delta^{13}C_{raw}$ values of samples: B2151 purchased from Elemental Microanalysis Ltd ($\delta^{15}N$ = +4.32 ± 0.20 ‰, $\delta^{13}C$ = -28.85 ± 0.20 ‰) and a mixture of urea and $BaSO_4$ ($\delta^{15}N$ = -2.91 ± 0.04 ‰, $\delta^{13}C$ = -37.02 ± 0.06 ‰) (for OFd) or urea and Ag_2S (for OFe and OMb).

To estimate the nitrogen and carbon isotopic composition of the water-soluble fractions, the solid powders remaining after the leachings described in the next section were also analysed via this IRMS with three replicates of 3 mg each.

2.4. Extraction of insoluble organic matter

To extract the IOM, we have followed an extraction protocol inspired by Gardinier et al. (2000), based on the initial work of Durand and Nicaise (1980). One should note that there is no unified protocol to isolate the IOM, but it varies from one study to another depending on experience and amount of sample available. Fragments totalling between 38 mg and 81 mg of meteorite (see Table 1) were manually ground and homogenised in an agate mortar. The powder was then leached with ultra-pure-water (UPW) in a glass tube to wash out the water-soluble compounds present in the meteorite powder (2 mL of UPW, stirring for 4 to 6 h, under air). The remaining powder was leached with a toluene-methanol solution (2/3:1/3) dissolving soluble organic molecules during 18 h. The leached powder was then transferred in a Teflon or polypropylene tube depending on the sample, where it underwent the following steps under air. To remove carbonates, metal oxides as well as metal complexes, the powder was treated with hydrochloric acid (HCl) at a concentration of 6 mol L^{-1}. In contact with the powder, the HCl solution becomes yellowish. The HCl step was repeated 4 times, until the yellowish coloration disappeared after 72 hours. The HCl solution was then removed and the powder was rinsed with

UPW. To remove the silicates, the powder was treated with a hydrofluoric acid (HF)/HCl solution (9 mol L^{-1}/4 mol L^{-1}). The HF/HCl step was repeated 2 times (3 successive baths, total duration of about 26 h). Then the HF/HCl solution was removed and the solid was rinsed with UPW four times. To remove the potentially formed fluorochemicals, the solid was treated in a HCl/boric acid (H_3BO_3) solution (3 mol L^{-1}/0.4 mol L^{-1}) for 16 h. The solution was removed and the solid was rinsed twice with UPW, 3 to 4 times until the pH of the solution reaches that of the UPW (around pH 4). The solid was then washed with dioxane for 4 h to extract some remaining compounds soluble in organic solvents such as sulfides, sulfites, and sulfates. Finally, the compounds soluble in organic solvents potentially remaining were removed by a toluene-methanol solution (2/3:1/3) for 2 h, and the powder was dried under a laminar flow hood overnight. Each of these chemical steps were done at ambient temperature. The elemental (N, C) and isotopic compositions of the insoluble residue were measured by injecting two replicates of 600 µg in the IRMS, as described in section 2.2. The same protocol was applied to the powders of OFb, OFc, and OMa remaining after the leaching treatment in order to measure if and how the leaching influenced the insoluble residue and the IOM it contains.

2.5. Extraction of water-soluble NH_4^+ and other ions

The extraction of NH_4^+ was performed by cryogenic grinding of the meteorite, followed by leaching of the powder in ultra-pure liquid water to dissolve NH_4^+. The flowchart of the extraction protocol is shown in Figure 1, with pictures of the samples at different steps in Figure S1. By reducing the grain size, the grinding and the ultrasonication allow the water to penetrate the sample, and enhance the dissolution of water-soluble species.

We have determined the minimum mass of Orgueil meteorite necessary to be able to measure the abundance and isotopic composition of ammonium, by considering several

constraints. First, we considered the concentration of ammonium potentially extractable from Orgueil to range from 0.002 wt.% (the concentration of NH_3 released from hydrothermal treatment of Murchison by Pizzarello et al. (1994)), to 0.1 wt.% (the concentration reported by Cloëz (1864)). Second, the concentration of NH_4^+ dissolved in water must be higher than the IRMS detection limit (10 nmol mL^{-1}) to measure its isotopic composition. Third, the dimension of the grinding bowl we used (25 mL), constrained the volume of material to provide optimal grinding conditions, and the volume of water in which the meteorite powder is finally dissolved (10 or 12 mL). From these three constraints, we expected to need from about 30 mg to 450 mg of Orgueil. Finally, the sample volume must be large enough to have a composition representative of the bulk meteorite, and to have the better chance to preserve ammonium. Because of its affinity with water (solubility, hygroscopy), ammonium may have been distributed heterogeneously in the whole meteorite by water-related processes on the parent body and on Earth. Morever, because of their volatility and water affinity, some ammonium-bearing species could be better preserved in a sample with a lower surface/volume ratio, less sensitive to heat and humidity. Therefore, for OFa, OFb, and OMa, that were analysed first, we decided to grind a total mass of 300 mg (close to 450 mg, but being thriftier in the use of this precious meteorite) made of fragments as large as possible (in 3 to 12 chips depending on the sample). The concentration of ammonium extracted from OFa, OFb and OMa was large enough to allow us to reduce the mass of meteorite used for the grinding of OFc to 150 mg (in 3 chips).

Because we aimed at quantifying soluble ammonium concentrations, we intentionally did not wash the meteorite samples before analyses to avoid losing this compound. Nevertheless, throughout the experimental protocol, precautions were taken to avoid contamination by terrestrial ammonium that would affect the isotopic analyses. Meteorite fragments and extraction solutions were handled in a glove box under an argon atmosphere (Ar > 99.999 %). The water used was exclusively ultra-pure water (UPW), containing extremely

few ions that could contaminate the samples (≈ 0.1 ppb of NH_4^+). All the equipment used was rinsed three times with UPW, and the grinding jar and balls were heated for at least 30 minutes at 120 °C in an oven to desorb most impurities.

Grinding the meteorite fragments can lead to heating of the samples and potential evaporation of the NH_4^+ and/or decomposition of organic molecules into ammonium or ammonia (Pizzarello *et al.*, 1994, 2009, 2012). To avoid these problems, the meteorite fragments were ground at low temperature (between 77 K and 273 K) in a 25 mL hermetic stainless-steel jar, containing two 15-mm stainless-steel balls and 6 mL of UPW ice particles. The water ice was added in order to optimise both the grinding conditions (the jar volume must be shared by 1/3 of sample, 1/3 of balls and 1/3 of argon atmosphere) and the final dissolution of the solutes after warming up. Because of the smaller mass of OFc, 8 mL of UPW ice particles were added to this sample. First, the open jar and balls were cooled in liquid nitrogen inside the glove box. Then, the ice particles were added by dripping UPW directly into the grinding jar, using a 1000 µL micropipette. Finally, a controlled mass of meteorite fragments was added before sealing the jar. The hermetically closed jar was shaken at 30 Hz for two minutes using a ball mill (Retsch© MM200), then immersed again in liquid nitrogen to mitigate the sample heating, and shaken for a further four minutes. These grinding times were determined by preliminary tests such that the sample temperature never exceeded 273 K. Finally, the grinding jar was warmed to room temperature to melt the ice and initiate the dissolution of soluble compounds, and a colloidal grinding was performed for five seconds at 30 Hz. Preliminary tests have shown that this grinding protocol results in grains smaller than 25 µm, so the grinding increases the surface in contact with the liquid water by at least three orders of magnitude.

After the grinding steps, the jar was immersed in a cold ultrasonic bath for 10 minutes, to disaggregate the grains even more and enhance the dissolution of ions. Colloidal suspensions were observed after ultrasonic bath (Figure S2), indicating the disaggregation of sub-

317 micrometre-size grains. To limit the potential loss of volatiles and/or the decomposition of
318 organics into ammonium and ammonia (Oba et al., 2020), the water of the ultrasonic bath was
319 pre-cooled with ice cubes and maintained at a temperature between 271 K and 281 K.

320 The suspension of meteorite powder in water (6 mL for OFa, OFb and OM, 8 mL for
321 OFc) was then recovered in a centrifuge tube. To recover the solid material remaining in the jar
322 and on the griding balls, they were rinsed with 4 mL UPW, and the closed jar was ultrasonicated
323 for a further 10 minutes. Then, these 4 mL were transferred to the centrifuge tube, resulting in
324 a suspension of 10 mL for OFa, OFb and OMa, and 12 mL for OFc. To recover any remaining
325 solid material, the jar and balls were rinsed a second time with 5 mL UPW, then ultrasonicated
326 for a further 10 minutes, and this suspension was transferred into a second centrifuge tube.

327 To dissolve as much as possible water-soluble ions contained in the meteorite, the
328 following steps were performed: (1) The tube was ultrasonicated again for 10 minutes under
329 cold conditions (271-281 K). (2) To separate the solid and liquid phases, the suspension was
330 centrifuged for 8 minutes at 2150 g for OFa, OFb and OM. To increase the efficiency of the
331 centrifugation, the 12 mL suspension of OFc was centrifuged for 8 minutes at 5580 g. (3) The
332 supernatant liquid was filtered using a 0.2 µm filter (0.1 µm for OFa) and transferred to a new
333 tube to be analysed for all ions. (4) To continue the leaching of the remaining powder, 10 mL
334 of UPW was added in the tube before repeating steps 1 to 3 on this new suspension. These four
335 steps (ultrasonication, centrifugation, filtration, and recovery) were repeated 10 times, leading
336 to 10 solutions of 10 mL (12 mL for OFc). The same steps were performed on the second
337 centrifuge tube (containing the second rinse of the jar and balls) and repeated 7 times for OFa,
338 10 times for OFb,c and 5 times for OMa. During step 3, a maximum of the liquid volume is
339 collected, but a small volume remaining with the powder is added to the next solution in step
340 4. This volume of liquid and the quantity of ions it contains have to be considered in the
341 calculation of the total quantity of ion extracted for the main extractions. This correction was

not applied on the extractions of the second rinse of the jar and balls as they contained barely no remaining water from one extraction to another.

Preliminary tests have shown that this extraction protocol allows us to dissolve 75 % of the soluble ammonium ions contained in the form of ammonium salts and/or ammonium adsorbed in phyllosilicate minerals (Text S1, Figure S3). This amount reached 100 % when the extraction n°1 was performed by mechanical stirring for 15 hours, before nine other 10-min long ultrasonic extractions. To avoid any chemical transformation (especially production or consumption of NH_4^+), which could happen during such a long first extraction, we have only performed 10-min extractions for the Orgueil samples, except for OFa. We left the 4^{th} OFa suspension to solubilise for 15 hours before continuing the extraction steps. However, the amount of ammonium released after this 4^{th} step was not significantly enhanced (see Figure S4 and Figure S5).

Before or between analyses, samples were stored in a freezer (< 255 K) to avoid any potential chemical reactions or loss of volatile compounds.

2.6. Quantification of NH_4^+ and other ions

NH_4^+ and other cations and anions (listed in Table S1) present in the solutions obtained by leaching of the Orgueil powder were analysed in a clean room using either a Dionex© ICS3000 dual ion chromatography system (ICS3000) or a couple of ThermoScientific © Integrions HPIC system with the anion system connected with a ThermoScientific © ISQ EC mass spectrometer (ICMS). To dissolve crystalline solids that could have precipitated during the storage of the most concentrated samples, the solutions were ultrasonicated for 10 minutes under ambient temperature just before their analysis. The ICS3000 separates the ions on an AG11HC and AS11HC 2 mm columns for the anions and CG16 and CS16 2 mm for the cations.

The flow rate of the eluent was set to 0.38 mL min^{-1} for anions (1 to 48 mM gradient of KOH) and to 0.4 mL min^{-1} for cations (isocratic MSA). The column temperature was set to 60°C. The ICMS (Integrions & ISQ) is using AS11HC-4µm & AG11HC-4µm columns for anions, and CS16-4µm & CG16-4µm columns eluent for cations separation. The flow rate of eluents was set to 0.38 mL min^{-1} for anions (1 to 48 mM gradient of KOH) and to 0.16 mL min^{-1} for cations (MSA). For inorganic ions, the detection is performed by conductivity, whereas organic anions are detected with a Thermofischer ISQ EC mass spectrometer (-2700V, individual tuned scan windows). These two systems allow measurements down to the sub-ppb level. Despite the similar affinity of Na^+ and NH_4^+ ions leading to a partial overlap of their two peaks, the cationic column was found to be effective in separating both compounds for solutions with a sodium/ammonium ratio up to 10^4. Calibration curves for determining the ion concentration from chromatographic peak area were obtained by analyses of solutions of controlled concentrations (from 1 ppb to 5000 ppb depending on the expected ion concentration in the solutions) before, during and after the sample analyses.

We compute the total amount of a water-soluble ions by adding up the quantities measured in the 10 extraction solutions, corrected for the quantity of ions remaining from one solution to the next one (based on experimental observations, we assume that a maximum of 0.5 mL of solution remains from one extraction to the next one), and the quantities measured in the second rinse extraction solutions.

To check for contamination sources, we have conducted 15 “blank experiments” by applying the extraction and analytical protocol only to UPW ice (without meteorite). We have calculated the Limit of Blank (LoB) (defined as the mean concentration of an ion measured in the blanks minus 1.645 times the standard deviation of these concentrations; Armbruster and Pry, 2008) of NH_4^+, NO_3^-, NO_2^-, and other ions (those marked with a symbol in Table 2). The concentrations of these ions were corrected by their LoB. For NH_4^+, the LoB is negligible

391 compared to the concentrations extracted from the meteorite, but it is not the case for NO_2^- (for
392 all samples) and for NO_3^- (for some samples) (Table S2), as discussed in section 3.2.1.

393

394 **2.7. Measurement of nitrogen isotopic composition in NH_4^+**

395 The isotopic composition of nitrogen in NH_4^+ was measured in the solution obtained
396 after the first leaching step described in section 2.5 (extraction solution n°1). The chemical
397 "azide method" (McIlvin and Altabet, 2005; Zhang et al., 2007) was used to convert $NH_4^+{}_{(aq)}$
398 into $N_2O_{(g)}$ and then into $N_{2(g)}$ for the IRMS measurement. About 50 nmol of NH_4^+ was
399 quantitatively oxidised to nitrite (NO_2^-) by a hypobromite solution. Then, NO_2^- was reduced to
400 $N_2O_{(g)}$ using a 1:1 by volume mixture of 2 M sodium azide and 100 % acetic acid. One should
401 note that any NO_2^- already present in the blank and/or in the meteorite extraction solution will
402 also be reduced to N_2O. Moreover, other nitrogen-bearing water-soluble organic molecules,
403 such as amino acids and amines, may also be partially oxidised into NO_2^- (Zhang et al., 2007).
404 We have checked the potential influences of these other sources of NO_2^- on the isotopic
405 measurement by analysing the first extraction solution of OFc before and after isolation of NH_4^+
406 on a cationic column, as described in the work of Lamothe et al. (2023). Briefly, the sample
407 solution containing 50 nmol of NH_4^+ is introduced into a Bio Rad AG 50W column filled with
408 a cation exchange resin in which NH_4^+ is selectively trapped. Subsequently, the trapped NH_4^+
409 is eluted by passing a concentrated sodium chloride solution through the column, releasing the
410 NH_4^+ in a solution in which NO_2^- and other anions are eliminated. We cannot exclude that other
411 nitrogen-bearing cations, such as amino acids and amines, might also be trapped and eluted
412 with NH_4^+.

413 The analytical procedure applied to analyse the isotopic composition of N_2O has been
414 described previously by Morin et al. (2009). Briefly, N_2O was decomposed into N_2 and O_2 in a

gold tube heated to 900°C, then O_2 and N_2 were separated in a gas chromatography column (10 m length, molecular sieve 5 Å), before being injected into the ionization chamber of a ThermoFinnigan© MAT 253 IRMS.

To obtain the $\delta^{15}N$ of the NH_4^+ from the meteorite sample ($\delta^{15}N_{meteorite}$), the measured $\delta^{15}N$ of N_2 ($\delta^{15}N_{measured}$) must be corrected from the influences of contaminations and isotopic fractionations potentially occurring at several steps of the extraction and analytical protocol. International isotopic standards were used for these calibrations: ammonium sulfate salts IAEA-N-1, USGS25, USGS26 and IAEA-305B with a $\delta^{15}N$ of +0.43 ‰, -30.41 ‰, +53.75 ‰, and +375.3 ‰, called J, K, L, and M respectively. We applied the principle of identical treatment, by which samples and standards are processed in an identical manner (Werner and Brand, 2001). $\delta^{15}N_{measured}$ is corrected for the influences of contamination and isotopic fractionations occuring between the conversion of NH_4^+ and the detection of N_2, as detailed in Lamothe et al. (2023). This first corrected value is called $\delta^{15}N_{first\ correction}$. In addition, to obtain $\delta^{15}N_{meteorite}$ we must correct $\delta^{15}N_{first\ correction}$ from the isotopic fractionation induced during the extraction of the NH_4^+ from the meteorite and during its isolation on a cationic resin when used. For this, the whole extraction protocol described in section 2.5 was run on reference samples consisting of a mineral powder and of UPW ice particles containing an isotopic standard, at concentrations similar to the samples. Ideally, the properties of the mineral powder and of the isotopic standards should also be identical to those of the samples, which is not feasible in practice. Therefore, we have performed several series of calibration experiments, varying the isotopic standard used, its concentration, and the nature of the mineral powder. As Orgueil is mainly composed of smectite phyllosilicates (King et al., 2015; Viennet et al., 2023), we used nitrogen-free Na-montmorillonite smectite phyllosilicate powder (SWy-3, purchased from the Clay Mineral Society), or a leached powder of Orgueil, in different series of experiments (Table S3). As detailed in the Text S2, an isotopic fractionation does occur in presence of mineral powder

(no isotopic fractionation is observed in the absence of mineral powder). The isotopic fractionation depends on the ratio between the concentration of NH_4^+ and the mass of powder, and it appears to be comparable for both powders, although possibly slightly higher for Orgueil (Text S2, Figure S6). Following these experiments, the best equation to correct $\delta^{15}N_{\text{first correction}}$ was found to be $\delta^{15}N_{\text{meteorite}} = 0.874 \times \delta^{15}N_{\text{first correction}} + 4.568$ (Figure S6, Table S4). As detailed in Text S2, this calibration may not be perfect, because several sources of uncertainties are difficult to clear up. The values given in this work should thus be considered as present-day best estimates.

3. Results

3.1 Degree of terrestrial alteration of the raw samples

Reflectance spectra of the Orgueil samples are presented in Figure 2. The surface of the OM sample being heterogeneous, two spectra were measured: one with the illumination spot on a visually dark area, and another on a brighter area. In the visible range, OM is brighter than OF by 60 % to 380 %. Examination of the chip surfaces with an optical microscope shows that they are covered by white translucent crystals, with a denser coverage on OM. In the infrared range, the 3-µm absorption feature is mainly due to stretching modes of adsorbed H_2O and structural OH and H_2O in minerals. In addition, the spectrum of the brighter area of OM shows absorption bands at ≈1.46 µm, 1.94 µm, and ≥ 2.44 µm mainly attributed to H_2O in calcium- and magnesium-sulfate minerals (Cloutis et al., 2011). The band at 1.94 µm is the strongest of these three, and is present in all spectra, although much more pronounced in OM's spectra. Since sulfates are known to be remobilised and/or produced through reactions between Orgueil and atmospheric water (forming veins and efflorescences at the meteorite surface, cf. Gounelle

and Zolensky, 2001), these observations indicate that OM has been more terrestrially altered than OF.

3.2 Water-soluble ions

3.2.1. Quantification

The first extraction solution is the most concentrated, and the following solutions contain progressively less ions as the meteorite sample is leached. Figure S4 shows that the first extraction solutions contain 72-87 % (depending on the ion and sample) of the total amount of ions extracted. This figure also shows that during the successive dissolutions, the cumulative extracted amount does not always reach a plateau, indicating that some soluble ions remain in the leached powder (see also the last paragraph of section 2.5). In addition, it is possible that some ions remain chelated and/or are trapped onto the surface of the used containers. Therefore, the ion concentrations reported here should be considered as lower limits.

The abundances of water-soluble ions leached from the Orgueil samples are presented in Table 2 and Figure 3. The total amount of water-soluble ions varies from 7.7 wt.% to 10 wt.% of the bulk meteorite, with a mean value of 9.0 ± 1.8 wt.%, very close to those found by Fredriksson and Kerridge (1988) and Yoshimura et al. (2023) via extraction in boiling water (8.9 wt.% and 9.2 wt.%, respectively). The amounts obtained for OFa, OFb and OFc, from the same Orgueil sample (OF), almost encompass this variability, indicating that the differences of ion concentrations between samples are probably mainly due to the heterogeneity of composition in the Orgueil meteorite at the millimetre to centimetre scales. Figure S1a shows the heterogeneity of the OFa grains: one has brighter surface patches, probably salt-rich, while others have not.

Among all ions, sulfates SO_4^{2-} are the most abundant (5.6-7.8 wt.%, 582-815 µmol g^{-1} of meteorite) and account for 40-50 mol% of total water-soluble ions. Other major ions are Mg^{2+}, Na^+, and Ca^{2+}, with individual concentrations ranging between 0.4 wt.% to 1.3 wt.% (94-548 µmol g^{-1} of meteorite). Other ions are individually below 0.1 wt. % (44 µmol g^{-1} of meteorite), among which NH_4^+ is the most abundant on average.

Ammonium is detected in all samples, between 0.060 ± 0.003 wt.% (OFb) and 0.079 ± 0.004 wt.% (OFa) (Table 2). The triplicate analysis of the OF sample allows us to infer a mean concentration of ammonium in OF of 0.070 ± 0.012 wt.%. The mean concentration from the four analyses gives 0.068 ± 0.011 wt.% of NH_4^+ in the Orgueil meteorite.

Notably, organic anions (acetate, formate, oxalate etc.) are also detected, the most concentrated being acetate (CH_3COO^-) with up to 0.098 ± 0.007 wt.% in OFa (Table 2 and Table S1). Taken together, acetate and formate carry 1 % of the total carbon in Orgueil.

The electrochemical equivalent mass ratios (Table 2) show that the ionic charge balance between cations and anions is roughly equilibrated for most samples.

The proportion of the total mass of ions extracted in the second rinse of the grinding jar and balls (see section 2.5 for details) is negligible for all ions, except for nitrates (NO_3^-) and nitrites (NO_2^-) (Table S2). This suggests that NO_3^- and NO_2^- may originate from a different source than the other ions. Since the concentrations of NO_2^- measured in the first extractions of OFb, OFc, and OMa are lower than the LoB (Table S2), it is likely that this ion comes from a contamination possibly due to the grinding jar and balls. The concentrations of NO_3^- measured in all the first extractions are larger than the LoB, but they are very variable from one sample to another, potentially indicative of sample heterogeneity. Moreover, we cannot exclude that a fraction of the NO_3^- detected may come from a contamination from the grinding jar and balls.

Therefore, the mean concentration of 0.012 ± 0.005 wt.% of NO_3^- in the Orgueil meteorite obtained from the four analyses should be considered as an upper limit.

3.2.2. Search for ions possibly associated with NH_4^+

In order to try to identify the carrier phase(s) of NH_4^+ in Orgueil, we searched for linear correlations between the total mole fraction of NH_4^+ and of other minor ions extracted from OFa, OFb, OFc and OMa. Figure 4 and Table S5 show the Pearson's correlation coefficients (r) and slopes of these linear regressions. NH_4^+ appears correlated to K^+ (r = 0.98), and to a lesser extent to Cl^- (r = 0.91, slope 1.0 ± 0.4) with a slope consistent with the presence of $NH_4^+Cl^-$. Interestingly, NH_4^+ is not correlated to NO_3^- (nor to NO_2^-, which probably comes from a contamination, see Table S2). However, this analysis would be insensitive to an association of NH_4^+ with some of the major ions (especially SO_4^{2-}) because of their large abundance differences. Therefore, in addition, for each sample, we also searched for correlations between the cumulative abundance of NH_4^+ and that of other ions extracted at each leaching step (Figure S5 and Table S6). The results show that, depending on the sample, a given couple of ions exhibit widely variable degrees of correlation during leaching. We interpret these differences as being mainly due to variations of the experimental protocol, and to variations of the ways the samples were ground and dissolved. Because the experimental protocol was optimised for OFc, data obtained from this sample are the most reliable. For OFc, the correlation obtained for $NH_4^+$and SO_4^{2-} (r = 0.999) suggests that some NH_4^+ may be in the form of $(NH_4^+)_2SO_4^{2-}$ in Orgueil. Finally, we cannot exclude an association of some NH_4^+ with carboxylate ions, especially with acetate CH_3COO^- (present in similar concentration as NH_4^+, and correlated to NH_4^+ – r = 0.989 for OFa), and possibly with methanesulfonate $CH_3SO_3^-$ ($r \geq 0.991$ for OFa and OFb).

3.2.3. Isotopic composition of NH_4^+

The $\delta^{15}N$ value of the nitrogen from NH_4^+ and NO_2^- in the first extraction of OFc (+71 ± 8 ‰) is indistinguishable within error from the $\delta^{15}N$ value of NH_4^+ isolated by a cationic resin (+73 ± 8 ‰), indicating that the presence of NO_2^- has a negligible influence on the measurement of the nitrogen isotopic composition of ammonium.

The $\delta^{15}N$ values of NH_4^+ ranges from +44 ± 8 ‰ (OMa) to +73 ± 8 ‰ (OFa and OFb) (Table 3, Table S4). Remarkably, the isotopic analyses of NH_4^+ extracted from OFa, OFb, and OFc give very similar results within uncertainty, with a $\delta^{15}N$ of +73 ± 8 ‰, +73 ± 8 ‰, and +71 ± 8 ‰ respectively. However, OMa, OMd, and OMe have significantly lower $\delta^{15}N$ of NH_4^+, with +44 ± 8 ‰, +54 ± 8 ‰, and +53 ± 8 ‰, respectively.

As discussed in section 2.7 and Text S2, given the difficulties inherent to the calibration of this measurement, these values should be considered as best estimates.

3.3. Nitrogen abundance and isotopic compositions in the bulk meteorite and in the IOM

The nitrogen abundances and isotopic compositions of the bulk and of the IOM are very similar for all OF and OM samples, with respective average values of 0.198 ± 0.012 wt.% and +47.8 ± 1.9 ‰ for the bulk, 2.5 ± 0.4 wt.% and +31.8 ± 0.9 ‰ for the IOM (Table 3).

Table 4 allows for the comparison of these average values with previous studies of Orgueil. The bulk nitrogen mass fraction of 0.198 ± 0.012 wt.% is in good agreement with other measurements reported in the literature, ranging from 0.148 wt.% to 0.530 wt.% (Robert and Epstein, 1982; Alexander et al., 2012; Pearson et al., 2006; Grady et al., 2002 ; Injerd and

555 Kaplan, 1974). The bulk nitrogen $\delta^{15}N$ of +47.8 ± 1.9 ‰ is consistent with the high range of
556 previous measurements, ranging from +32 to +46.2 ‰.

557 The nitrogen abundance and isotopic composition of the IOM are much more variable
558 in the literature, ranging from 1.4 wt.% to 2.75 wt.% and +14 ‰ to +30.7 ‰ (Alexander et al.,
559 1998, 2007; Pizzarello and Williams, 2012; Cronin et al., 1987; Remusat et al., 2005; Robert
560 and Epstein, 1982). Our results (2.5 wt.%, +31.8 ‰) are in good agreement with those of
561 Alexander et al. (2007) (2.7 wt.%, +30.7 ‰). One must bear in mind that the exact composition
562 of insoluble residue containing the IOM can vary depending on the sample heterogeneity and
563 on the details of the chemical extraction procedure, which may be different from one study to
564 another (see section 4.1).

565 The powders retrieved after leaching of Orgueil samples (Table S7), have nitrogen
566 abundances and isotopic compositions of 0.184 ± 0.044 wt.% and +40.4 ± 2.3 ‰ for the bulk,
567 2.3 ± 0.2 wt.% and +30.8 ± 2.1 ‰ for the IOM (Table S8). The bulk concentrations are lower
568 compared to those of the initial raw samples, because of the loss of water-soluble species after
569 leaching. However, the nitrogen isotopic composition of IOM is not significantly modified after
570 the leaching.

571

572 **3.4 Distribution of nitrogen in Orgueil, among different nitrogen-bearing phases**

573 Our analyses made it possible to establish the distribution of nitrogen among the
574 different nitrogen-bearing phases in Orgueil. Knowing the bulk nitrogen mass fraction, together
575 with the nitrogen mass fractions in IOM, NH_4^+ and NO_3^-, we calculated the respective
576 contributions of IOM, NH_4^+ and NO_3^- to the total nitrogen in Orgueil, and the amount of
577 remaining nitrogen. The results of these calculations are provided in Table 3 and in Figure 5.

3.4.1 Nitrogen in NH_4^+ and other water-soluble molecules

Water-soluble ammonium accounts for at least 23-31 % of the nitrogen in Orgueil, with a mean value of 27 ± 5 % (Table 3, Figure 5). Nitrate (NO_3^-) account for only 1.3 ± 0.6 % of the nitrogen in Orgueil on average. The nature of the NH_4^+-bearing compounds is discussed in section 4.4.

The decrease of the solid-to-water volume ratio in our extraction protocol of OFc (see section 2.5) enhanced the dissolution rate (Figure S4) and minimised the loss of solid powder during this leaching sequence compared for the other samples (the mass loss was 16 % vs. 50-67 %, respectively, cf. Table S7). This allowed us to estimate the total fraction of water-soluble compounds and its nitrogen content and isotopic composition, by analysing the powder remaining after the leaching sequence (Table S8, Table S9). The nitrogen budget calculated for OFc is reported in the Table S9. It shows that water-soluble species make up 30 ± 2 % of the total nitrogen in Orgueil, mainly in the form of ammonium (90 ± 10 %). Molecules other than NH_4^+ and NO_3^-, including water-soluble amino acids and amines, make up 3 ± 3 % of the total nitrogen in Orgueil according to this budget. The large relative uncertainty on this value comes from the mass loss during the leaching. The real value may be much lower than 3 %, as literature data show that amines, amino acids, and nucleobases only contain 0.29 %, 0.03 % and 0.001 % of the total nitrogen in Orgueil, respectively (Ehrenfreund et al., 2001; Callahan et al., 2011; Burton et al., 2014; Aponte et al., 2015).

3.4.2. Nitrogen (and carbon) in IOM

We have retrieved a percentage of mass of insoluble residue per mass of bulk meteorite of 2.7 ± 0.6 wt.%, and we find that IOM makes up 56 ± 12 % of the carbon (Figure S7) and 35 ± 5 % of the nitrogen in Orgueil (Table 3, Figure 5), and has a N/C atomic ratio of 0.035 ± 0.011 (Figure S7).

We have obtained Scanning Electron Microscopy images (not shown) of the insoluble residue, showing that it still contains some undissolved minerals, mainly iron sulfides. However, the presence of minerals (≈15 wt.% of the insoluble residue, according to Yang et Epstein, 1983) should not interfer with our estimates for how much nitrogen and carbon in the bulk samples is present in the IOM.

3.4.3. The remaining nitrogen

IOM and NH_4^+ represent 62 ± 10 % of the total nitrogen content of the Orgueil meteorite (Table 3), and the other water-soluble compounds (NO_3^-, organics etc.) 4 ± 4 % (Table 3, Table S9). If the loss of IOM during extraction is negligible, this implies the existence of one or several other nitrogen-bearing phases that are insoluble in water but soluble in organic solvents and/or acids (HF, HCl), and that account for 34 ± 14 % of the nitrogen.

4. Discussion

4.1. Comparisons of IOM yield and composition with previous studies

The percentage of mass of insoluble residue per mass of bulk meteorite (2.7 ± 0.6 wt.%), the fraction of bulk carbon in IOM (56 ± 12 %), and the N/C atomic ratio of IOM (0.035) retrieved in the present work are all comparable with those reported in Alexander et al. (2007) (Table 4, Figure S7). Other studies have higher percentages of mass of insoble residue per mass of bulk meteorite, ranging from 3 % to 11 % (Table 4), probably because they used different protocols. The protocol we have used may be more efficient at hydrolysing and dissolving in acids some minerals and/or some organic moieties bound to the macromolecular organic matter,

which do not end up in the final insoluble residue, and/or it results in more losses of very fine-grained IOM that is hard to recover during the isolation because it remains in suspension or is stuck on surfaces of the containers (Alexander et al., 2017). Compared to these studies, we have performed a first dissolution with HCl only, before the HF-HCl dissolution, and we used higher concentrations of HCl (see section 2.4; Huss and Lewis, 1995; Pizzarello and Williams, 2012). The loss of IOM would lead to an under-estimation of the masses of nitrogen and carbon in the bulk meteorite that is in IOM. We were not able to quantify the uncertainty induced by this potential loss of IOM. This would require a detailed study dedicated to the IOM extraction, which is out of the scope of the present work. Since we get similar fractions of nitrogen in IOM to that reported in Alexander et al. (2007) using a different protocol, the loss of IOM –if any– is comparable to this previous study.

We find that IOM accounts for 35 ± 5 % of the nitrogen in Orgueil, which is lower than the previous estimate from Kung and Clayton (1978), reporting 47 % of the nitrogen in IOM (Figure 5). More recent studies do not estimate the proportion of the bulk nitrogen that is in IOM, and giving the variations of bulk nitrogen and of mass of IOM per mass of bulk meteorite from one study to another (Table 4), a calculation using values from different studies would be misleading.

4.2. Extra-terrestrial NH_4^+ in Orgueil and potential effects of terrestrial alteration

The NH_4^+ content of 0.068 ± 0.011 wt.% we measured in the Orgueil meteorite (Table 2) is indistinguishable within error to the 0.061 ± 0.006 wt.% reported by Yoshimura et al. (2023), using a different experimental protocol and a lower mass of meteorite. These recent reanalyses confirm the chemical analysis carried out by Cloëz (1864), who reported an "ammoniaque" content of 0.098 wt.%. The term "ammoniaque" may designate NH_3H_2O or

NH_4^+, so the NH_4^+ content measured by Cloëz was either of 0.050 wt.% or 0.098 wt.%, respectively, but of the same order of magnitude than the recent measurements. This similarity highlights the quality of the research performed by the skilled scientists of the 19th century (Daubrée, Cloëz, Pisani etc.), although none of the present sophisticated analytical techniques were available to them (Gounelle and Zolensky, 2014). Results presented in such ancient papers should be trusted, rather than disregarded and forgotten. In addition to its detection, Cloëz (1864) reported that "ammoniaque" still represents 0.1042 wt.% of the rock after drying at 110°C (383 K), indicating the thermal stability of the NH_4^+ carrier(s).

The nitrogen isotopic composition of NH_4^+ is similar within uncertainty for all OF samples, with a mean $\delta^{15}N$ value of +72 ± 9 ‰. These samples, stored in a tiny flask found in an attic, are supposed to be the best-preserved samples of Orgueil available to date. Our isotopic analysis confirms the extra-terrestrial origin of NH_4^+ in OF, since the isotope ratio for terrestrial "NH_x" varies from about -50 ‰ to +50 ‰ with an average at 0 ‰ (Coplen et al., 2002; Felix et al., 2013; Bhattarai et al., 2021). However, the $\delta^{15}N$ of NH_4^+ is significantly lower in the OM sample displayed in the Museum Victor Brun of Montauban with +50 ± 12 ‰, while the overall quantity of NH_4^+ in OF and OM is similar within the error bars (ranging from 0.060 wt.% to 0.079 wt.% depending on the chip, with a 1σ error of 0.004, Table 2). This suggests that OM underwent contamination and/or alteration of nitrogen-bearing material. Assuming that nitrogen exchange can occur at room temperature (25°C) between atmospheric N_2 and NH_4^+ from Orgueil, the equilibrium constants of isotope exchange calculated by Urey (1947) suggest that a decrease of the $\delta^{15}N$ of NH_4^+ from +72 ‰ to +50 ‰ would require all of the N atoms of NH_4^+ in Orgueil to have been in equilibrium with the air, which seems difficult to conceive. Moreover, more recent calculations (Li et al., 2021 and references therein) have obtained even lower equilibrium constants of isotope exchange. Therefore, isotopic exchange between N_2 and NH_4^+ at 25°C does not seem to explain the $\delta^{15}N$ of NH_4^+ in OM. A contamination of terrestrial

673 NH_4^+, or a fixation of atmospheric N_2 into NH_4^+ via reactions with oxides or sulfides (Doane,
674 2017 and references herein), without loss of the extra-terrestrial NH_4^+ would require an increase
675 of NH_4^+ content by 0.029 wt.%. This additional amount of NH_4^+ appears barely incompatible
676 with the observed values (Table 2), but it could be compatible given the fact that NH_4^+ was
677 quantified in only one sample of OM while this sample is certainly more heterogeneous than
678 OF (more veins of remobilized materials, and more variable $\delta^{15}N$ of NH_4^+ in OM, see Table
679 S4). The decomposition of IOM ($\delta^{15}N$ of +32 ‰) into an additional amount of NH_4^+ of 0.080
680 wt.% is more clearly incompatible with the observed values. Alternatively, an exchange of 31
681 % of the extra-terrestrial NH_4^+ with terrestrial NH_4^+, required to explain these observations,
682 seems unlikely given the thermal stability of the NH_4^+ carrier(s) (Cloëz, 1864), although
683 humidity may facilitate exchanges over the long term. Therefore, an atmospheric contamination
684 of OM is our preferred explanation. Another possibility would be that the variations in the
685 nitrogen isotopic compositions of NH_4^+ between OM and OF samples could result from
686 differences in the mineral composition of the matrix, which could potentially lead to distinct
687 isotopic fractionations of NH_4^+ during the extraction and analytical procedures (Text S2).

688 The nitrogen mass fractions and isotopic compositions of the bulk and of the IOM are
689 very similar for OF and OM (Table 3), indicating that their different storage conditions had no
690 major influence on their bulk and IOM nitrogen composition. In the next sections of the
691 discussion, the average $\delta^{15}N$ value of +72 ± 9 ‰ obtained from the OF samples is retained as
692 the best estimate for NH_4^+ in Orgueil (see also section 2.7 and Text S2).

693 Other carbonaceous chondrites contain ammonium that is possibly extra-terrestrial like
694 in Orgueil. Berzelius (1834) reported the presence of water-soluble ammonium in another CI
695 chondrite, the Alais meteorite, that fell in 1806. Furthermore, Mautner (2014) reported the
696 presence of NH_4^+ in several other groups of carbonaceous chondrites, with CM and CR being

the most concentrated (0.02-0.03 wt.%), and CO, CV, CK containing less than 0.004 wt.% water-soluble ammonium. It seems that the concentration in NH_4^+ decreases with the increasing thermal metamorphism experienced by carbonaceous chondrites. Indeed, CO, CV and CK chondrites have been heated to temperatures higher than 573 K, in contrast to CI, CM and CR chondrites (Huss et al., 2006). Moreover, type 3 carbonaceous chondrites have been radiogenically heated for a very long time, whereas some type 2 had a short-duration heating. The decreasing concentration of NH_4^+ for CI, CM, and CR chondrites may be related to their decreasing matrix abundance of > 99 %, 70 % and 30-50 %, respectively (Krot et al., 2014).

Moreover, Mautner (2014) also reported the presence of NO_3^-, with concentrations generally higher in CO, CV, and CK (0.0004-0.0046 wt.%) than in CM and CR chondrites (0.0003-0.0008 wt.%). We have found 0.012 ± 0.005 wt.% in Orgueil. Since OM contains roughly as much nitrates as OF (Table 3), and Ryugu grains contain 3 times to 5 times more (Yoshimura et al., 2023), the formation of nitrates via terrestrial alteration during storage of the meteorite seems unlikely. However, some reactions could form NO_3^- (or NH_4^+) from N_2, NH_4^+ or organic matter, in the presence of metal oxides (Doane, 2017), or from the reaction of organic matter with atmospheric O_3 (de Vera et al., 2017). Isotopic analyses of NO_3^- would be needed to investigate its origin.

4.3. Composition of the remaining nitrogen

Our results show the existence of one or several other nitrogen-bearing phases that account for 34 ± 14 % of the nitrogen. The exact nature of this remaining nitrogen, which is not in IOM, NH_4^+ and other water-soluble compounds, is unknown.

Presolar grains (nanodiamonds, SiC, graphite, nitrides) have low abundance (≤ 0.1 wt.%), so they should hold a negligible fraction of the total nitrogen in the Orgueil meteorite (Huss and Lewis, 1995; Alexander et al., 1998).

Organic polar solvents, such as methanol, can dissolve organic compounds and a limited fraction of water-soluble ions, including ammonium. According to Becker and Epstein (1982), the evaporation of a methanol extract of Orgueil yields a large mass of white precipitate having a H/C > 4, so probably mainly composed of hydrated inorganic salts, and having a $\delta^{15}N$ ranging from +57 ‰ to +71 ‰, compatible within error bars with that of NH_4^+ (+72 ± 9 ‰). The presence of NH_4^+ in methanol extracts from Orgueil and Ryugu grains was confirmed by Yoshimura et al. (2023) and Schmitt-Kopplin et al. (2023), along with nitrogen-bearing organic compounds. Using data from Becker and Epstein (1982) and Robert and Epstein (1982), we calculate that this methanol extract contained 0.9 and 1.6 % of the total nitrogen and carbon atoms in Orgueil, respectively. The fraction of this methanol extract that is soluble in dichloromethane contained no or very little nitrogen. Another analysis of Orgueil reported in Smith and Kaplan (1970) shows that organic molecules extracted after dissolution in benzene-methanol (80:20 vol%) and removal of the organic acids –so mostly apolar organic molecules– represent less than 3 % of the total carbon. It is thus unlikely that a significant amount of nitrogen is in apolar organic molecules in Orgueil.

Interestingly, as for nitrogen, a significant fraction of the total carbon in Orgueil, and in other carbonaceous chondrites, is not in the soluble and insoluble phases typically extracted (Smith and Kaplan, 1970; Alexander et al., 2015). The analyses of Orgueil reported in Smith and Kaplan (1970), Alexander et al. (2015) (and references therein), and in the present study show that carbonates, soluble organic molecules (SOM), and IOM only account for about 2 to 3 %, 3 %, and 44 to 68 % of the carbon, respectively, with 32 to 56 % being in other material(s)

(Figure S7). According to Alexander et al. (2012), *"most of the remaining carbon appears to be insoluble in typical solvents, is not in inorganic carbon (e.g., carbonate or graphite), and is released by treatment with ≥1N HCl".* Most of this remaining carbon (and nitrogen) is then lost and/or dissolved/hydrolysed during the acid treatments used to extract the IOM (section 2.4). The remaining carbon and nitrogen could be bonded to IOM by acid hydrolysable functional groups (as suggested by Alexander et al., 2012 and Kebukawa et al., 2019) and/or they could have been in lost organic matter being hard to recover (because very fine-grained or having some other properties, as suggested by Alexander et al., 2017), and/or they could be trapped within phyllosilicates and/or nano-carbonates, as part of the diffuse organic matter revealed in the works of Garvie and Buseck (2007) and Le Guillou et al. (2014). Although Alexander et al. (2015, 2017) pointed out that this missing carbon is present in samples that contain little if any phyllosilicates (e.g., the most primitive CRs, the CV3.1 Kaba and the CO3.0 ALH 77307), some of it could be trapped in phyllosilicates of more altered meteorites such as Orgueil.

Based on the carbon and nitrogen budgets from the present study, together with data from Becker and Epstein (1982), Smith and Kaplan (1970) and Alexander et al. (2015) (and references therein) (to account for the parts of nitrogen in SOM, and the parts of carbon in SOM and carbonates), we estimate that the phase(s) (insoluble in water, other than IOM, SOM and carbonates) containing the remaining carbon and nitrogen should have a N/C atomic ratio of 0.054 (and a $\delta^{13}C$ of -16 ± 6 ‰, an elemental and isotopic estimate similar to that in Alexander et al., 2015) (Table S10). If we assume that all these remaining carbon and nitrogen atoms are in a unique organic phase, the unidentified organic matter (UOM), having a N/C ratio of 0.054, it should account for about 34 % of the total nitrogen in Orgueil. However, we cannot exclude the presence of remaining inorganic nitrogen (NH_4^+, NO_3^- etc.) not extracted by our protocol, which would contribute to this N/C ratio, so the real N/C ratio of this UOM might be lower. Alternatively, under the assumption of a N/C ratio of UOM equal to that of IOM (0.035), the

UOM should in that case make up about 23 % of the total nitrogen in Orgueil. In summary, it is possible that at least 60 % of the remaining nitrogen in Orgueil is either in IOM that was lost during isolation and/or in an organic matter that has not been isolated yet (hydrolysable organic matter, and/or organic molecules trapped in inorganic phases).

Considering a bulk $\delta^{15}N$ of +47.8 ‰, with IOM at +31.8 ‰ comprising at least 35 % of the bulk nitrogen and NH_4^+ at +72 ‰ comprising 27 % of nitrogen, the remaining 38 % of nitrogen (including other nitrogen-bearing water-soluble compounds, ≈3 %) necessarily has a lower $\delta^{15}N$ ranging from +23 ‰ to +55 ‰ (Table 3). If most of this remaining nitrogen is in the form of organic matter, it is interesting to note that this organic matter may have a $\delta^{15}N$ comparable to that of IOM. So it may actually be IOM that was lost during extraction possibly because very fine-grained, and/or an acid hydrolysable fraction of IOM.

In summary, the nitrogen budget of Orgueil reveals the presence of one or several yet unidentified nitrogen carrier(s) having a $\delta^{15}N$ ranging from +23 ‰ to +55 ‰. The main part of this remaining nitrogen (> 60 %) may be in an UOM, either very small organic grains that were lost during IOM extraction, and/or in acid hydrolysable functional groups bounded to the IOM and/or organic nitrogen trapped within minerals and released during acid hydrolysis. The range of $\delta^{15}N$ of the UOM suggests that this organic matter may have a nitrogen isotopic composition close (or similar) to that of IOM, so it could be related to one of the original reservoirs of nitrogen. The rest of the remaining nitrogen (< 40 %) could be made of nitrogen-bearing water-soluble compounds, potentially including some NH_4^+ (and NO_3^-) not extracted by our protocol.

4.4. Nature of the NH_4^+-bearing phase(s)

The nature of the phases carrying the water-soluble NH_4^+ remains an open question. Ammonium could be present in salts, associated with inorganic or organic anions, and/or associated with minerals, especially phyllosilicates. Correlations between the concentrations of NH_4^+ relative to Cl^- and SO_4^{2-} (Figure 4, Table S5, Table S6) indicate NH_4^+ might be carried in phases with similar solubilities and/or might be present in the same carrier phases as Cl^-, SO_4^{2-}, K^+ and possibly CH_3COO^- and $CH_3SO_3^-$. In addition, these results do not exclude the possibility that NH_4^+ is distributed among several carrier phases. Since NH_4^+ and K^+ have the same charge and a similar ionic radius, they are likely to occupy identical adsorption sites. These sites may be on the surface and/or within minerals and/or organic grains. Orgueil is made of 83 vol.% of phyllosilicate minerals (King et al., 2015), mainly smectites (Viennet et al., 2023). Smectites are expansive clay minerals that provide the largest adsorption surface areas available to water-soluble species in Orgueil. Organic grains composing IOM, SOM or UOM are less abundant, but their sub-micrometer-size may offer a large surface area with functional groups particularly attractive to NH_4^+. Moreover, a fraction of NH_4^+ could also be present in the form of salts such as ammonium chloride $NH_4^+Cl^-$, ammonium sulfate $(NH_4^+)_2SO_4^{2-}$, ammonium acetate $NH_4^+CH_3COO^-$ and ammonium methanesulfonate $NH_4^+CH_3SO_3^-$ (see section 3.2.2). Interestingly, NH_4^+ is not correlated with NO_3^- (Table S5). If most of the NO_3^- does not come from a contamination (Table S2), this would suggest that NH_4^+ and NO_3^- are associated with different phase(s) that might have independent origins. The modest correlation between NO_3^- and Ca^{2+} ($r = 0.89$) suggests an association of NO_3^- with Ca^{2+}, and therefore possibly with carbonates (especially dolomite) as they are the major carrier of Ca^{2+} in CI chondrites (Moynier et al., 2022 and references herein).

Finally, an important point is that the main carriers of NH_4^+ in Orgueil do not appear to be very volatile and easily lost from the rock, even after heating at 383 K (Cloëz, 1864). Notably, $NH_4^+Cl^-$, $(NH_4^+)_2SO_4^{2-}$ or ammoniated phyllosilicates are relatively stable at this

815 temperature (Petit et al., 1998; Haynes and Lide, 2010), which is consistent with their presence
816 in Orgueil.

817

818 **4.5. Origin(s) of NH_4^+**

819 This ammonium found in carbonaceous chondrites could be a tracer of the ices and/or
820 semi-volatile compounds (e.g., hydrates, salts etc.) that accreted in their parent bodies, and/or
821 of the post-accretion processes experienced by the primordial materials.

822 A first possibility is that NH_4^+ originates from the decomposition of the organic matter
823 via heating and/or aqueous alteration on the parent bodies. The IOMs found in carbonaceous
824 chondrites have been proposed to derive from a common organic precursor inherited from pre-
825 solar environments (Alexander et al., 1998, 2007). The differences in morphology, elemental
826 and isotopic compositions of the IOM among carbonaceous chondrites are then interpreted as
827 mostly resulting from alteration of this precursor in their respective parent bodies. CR
828 chondrites appear to host the least altered IOM, sharing compositional similarities with the
829 organic matter of chondritic porous interplanetary dust particles (CP-IDPs) and
830 comets (Alexander et al., 2017). The IOMs of CR chondrites have bulk $\delta^{15}N$ values ranging
831 from about +150 ‰ to +300 ‰ (Alexander et al., 2007, 2012) and are heterogeneous, as attested
832 by the presence of ^{15}N hotspots observed *in situ* (also present in the IOM of other chondrites;
833 Busemann et al., 2006 ; Bonal et al., 2010). The experimental hydrothermal alteration (300°C,
834 100 MPa, 6 days) of the IOMs of CR chondrites Renazzo and GRA 95229 was found to release
835 19 and 56 % of its nitrogen in the form of NH_3 having a $\delta^{15}N$ of +239 and +223 ‰, leaving a
836 solid residue of +133 and +162 ‰, respectively (Pizzarello and Williams, 2012). Both the
837 released NH_3 and the residual solid organic matter have $\delta^{15}N$ values much higher than that of
838 NH_4^+ (+72 ± 9 ‰) and IOM (+32 ± 1 ‰) in Orgueil, respectively. Moreover, Orgueil IOM is

not depleted in nitrogen compared to the IOMs of CR chondrites (Alexander et al., 2007), and it still contains as much hydrothermally releasable NH_3 as Renazzo IOM (24 % vs. 19 %, respectively) (Pizzarello and Williams 2012). If we add back the NH_4^+ to the Orgueil (OF) IOM, we find a N/C of about 0.064 and a $\delta^{15}N$ of about +50 ‰, higher and lower than the average values of CR IOM, respectively. Therefore, for all these reasons, it seems unlikely that the NH_4^+ of Orgueil was entirely derived from the alteration of an organic precursor similar to the IOM of CR chondrites, except if major isotopic exchanges occurred in an open system with an incorporation of ^{14}N and a net removal of ^{15}N while keeping a similar N/C. Among the CM chondrites, the more altered ones tend to have a lower bulk nitrogen abundance and $\delta^{15}N$, consistent with a removal of ^{15}N during alteration (Pearson et al., 2006). Hydrothermal alteration experiments show the release of NH_3 from Murchison (CM) IOM that is significantly more enriched in ^{15}N than the bulk IOM (Pizzarello and Williams 2012, Foustoukos et al., 2021). Moreover, Foustoukos et al. (2021) show that some nitrogen isotope exchange occurs between the IOM and NH_4^+ in solution. Orgueil material was possibly heated up to 150°C and altered by fluids for millions of years in its parent body (e.g., review by Brearley, 2006), the consequences of which for IOM are still poorly known. Therefore, we cannot exclude that NH_4^+ was totally or partially produced from an organic matter precursor, similar or different from the IOM of CR chondrites, via long-term processes.

Orgueil IOM (+31.8 ± 0.9 ‰), UOM (+39 ± 16 ‰) and NH_4^+ (+72 ± 9 ‰) appear to have increasing $\delta^{15}N$ values, with possibly close or similar values for IOM and UOM (see Table 3 and section 4.2), suggesting that these phases might be compositionally related. A possible interpretation would be that they result from successive transformations from one to another that decreased or increased their relative amount of ^{15}N. Alternatively, they might have been formed from different nitrogen isotopic reservoirs.

Some minor organic compounds, such as amines and amino acids, could be related to NH_4^+. Orgueil contains more amines than amino acids (Aponte et al. 2015), but to our knowledge, there was no measurement of the nitrogen isotopic composition of these compounds in Orgueil. Pizzarello et al. (1994) estimate the $\delta^{15}N$ of amines in Murchison (CM) to be higher than 93 ‰. The $\delta^{15}N$ of amino acids range from +12 ‰ to +184 ‰ in CM and from +48 ‰ to +326 ‰ in CR chondrites (Pizzarello et al., 1994; Engel and Macko, 1997; Pizzarello and Holmes, 2009; Elsila et al., 2012). Two measurements were made on the thermally metamorphosed CI-like chondrite Yamato 86029 (+121 ‰ and +145 ‰, Chan et al., 2016). The $\delta^{15}N$ values of amines and amino acids are generally higher than that of NH_4^+ in Orgueil, but some are comparable (glycine and isovaline in Murchison, Elsila et al., 2012). This suggests that NH_4^+ and some amino acids may be related, which would not be surprizing as NH_4^+ is involved in most of their formation mechanisms (Pizzarello and Holmes, 2009; Glavin et al. 2010; Elsila et al., 2012).

Another possibility is that NH_4^+ is a tracer of the accretion and/or later deposit of NH_3 ice and/or NH_3 hydrates ($2NH_3 \cdot H_2O$, $NH_3 \cdot H_2O$, $NH_3 \cdot 2H_2O$) or NH_4^+ salts on the CI primary parent body. In a protoplanetary disk, pure NH_3 should condense at 74-86 K and $NH_3 \cdot H_2O$ at 78-81 K (Zhang et al., 2015), whereas NH_4^+ salts form by thermal reactions of NH_3 in water ice, from 10-30 K to higher temperatures (Theulé et al., 2013; Bergner et al., 2016; Potapov et al., 2019). Pure NH_3 ice sublimates significantly above 80 K (Zheng and Kaiser, 2007) and many NH_4^+ salts only sublimate significantly above 160 K or even higher temperatures, depending on the anion (Bossa et al., 2008; Danger et al., 2011). CI chondrites have the highest abundance of volatile elements and water of all meteorites, implying that they accreted in a relatively cold region of the solar nebula, so probably relatively far from the Sun (Alexander et al., 2013; Desch et al., 2018; Lodders, 2021). Consequently, they may have accreted and/or later received significant amounts of NH_3 ice, NH_3 hydrates or NH_4^+ salts. The ^{15}N enrichment

888 of NH_4^+ in Orgueil may thus partly be a heritage of interstellar and/or nebular NH_3 ice
889 chemistry, although it is low compared to the extreme values (thousand(s) per mille) predicted
890 by some theoretical models of ion-molecule exchange reactions and isotopologue selective
891 photodissociation (Rodgers and Charnley, 2008a,b; Wirström et al., 2012; Heays et al., 2014;
892 Chakraborty et al., 2014) and seen in organic grains (hotspots) in chondrites (Busemann et al.
893 2006 ; Bonal et al. 2010). CN, HCN and NH_2 in cometary comae observed so far have $\delta^{15}N$
894 ranging from +650 ± 400 ‰ to +940 ± 500 ‰ (short- and long-period comets seem to have
895 similar isotopic composition in nitrogen, cf. Füri and Marty, 2015 and references therein), much
896 higher than the $\delta^{15}N$ of NH_4^+ in Orgueil (+72 ± 9 ‰). Obviously, Orgueil is devoid of the
897 extremely volatile molecules contributing to the gases in comae. Therefore, the NH_4^+ found in
898 Orgueil might be a ^{15}N-depleted refractory remnant cometary ices, or it may have other
899 origin(s), as discussed above.

900 Nevertheless, before being able to propose reasonable hypotheses for the origins of
901 Orgueil nitrogen-bearing phases, more analytical work is needed, especially to reveal the nature
902 of the UOM, measure the nitrogen isotopic composition of UOM directly (here we have only
903 estimated it indirectly) and confirm that of NH_4^+ independently (see Text S2). We note that the
904 stepwise combustion data of Orgueil exhibit a plateau of similar $\delta^{15}N$ values between +40 ‰
905 and +49 ‰ over consecutive temperature steps between 600°C and 700°C, which could be
906 consistent with the combustion of UOM (+39 ± 16 ‰) (Grady et al., 2002; Hashizume et al.,
907 2024).

908

909 **4.6. Comparisons with Ryugu grains**

910 Although CI chondrites are rare among meteorites, the bodies from which they derived
911 may not be rare among the Solar System's small bodies. Indeed, the petrologic and chemical

properties of the samples returned from the C-type asteroid Ryugu by the Hayabusa2 mission are strongly similar, although not identical, to CI chondrites (Nakamura et al. 2023; Yokoyama et al., 2023). Chemical analyses show the presence of fifteen amino acids of abiotic origin, as well as aliphatic amines (such as methylamine) and carboxylic acids (such as acetic acid), likely in the form of salts (Naraoka et al., 2023; Parker et al., 2023). Amines and carboxylic acids were also found in Orgueil, as reported in Aponte et al. (2014, 2015) and in the present study, with the detection of formic and acetic acids (Table 2). Notably, water-soluble formic and acetic acids represent 0.7 wt.% of the total carbon in Ryugu grain A0106 (Yoshimura et al., 2023), while they represent 1 wt.% of the total carbon in Orgueil (Table 2). In addition, we report methanesulfonate in Orgueil and a large variety of organic acids (Table S1), which were also detected in Ryugu grains (Yoshimura et al., 2023; Takano et al., 2024). The variety of soluble molecules containing the atoms CHNOS, found in Orgueil and Ryugu grains, along with ammonium, are indicative of their high degree of aqueous alteration (Naraoka et al., 2023; Yoshimura et al., 2023, Schmitt-Kopplin et al., 2023, Takano et al., 2024). Yoshimura et al. (2023) reported NH_4^+ at 3 ± 2 µg g^{-1} and less than 0.4 µg g^{-1} in Ryugu grains A0106 and C0107, respectively, after treatment for 20 h in ultra-pure water at 105°C. The abundance of NH_4^+ in Ryugu thus seems heterogeneous, and when present it is ≈200 times less abundant than in Orgueil. The NH_4^+ and/or NH-bearing compounds, including amines, could contribute to the faint 3.06-µm absorption band present in average spectra of several Ryugu grains, and to the strong 3.06-µm and 3.24-µm absorption bands observed on some rare grains (Pilorget et al., 2022; Viennet et al., 2023). Broadley et al. (2023) pointed out the lower abundance of nitrogen and lower $\delta^{15}N$ in some Ryugu grains compared to CI chondrites, and the heterogeneity of nitrogen abundance and $\delta^{15}N$ among Ryugu grains. They attributed these differences to the preferential loss of a ^{15}N-rich component, potentially during heterogeneous aqueous alteration in the parent planetesimal of Ryugu. Given the abundance and $\delta^{15}N$ of NH_4^+ in Orgueil, it is

likely that NH_4^+ was (part of) this ^{15}N-rich soluble component, possibly lost during the aqueous alteration of some Ryugu material. However, we have no evidence for a more intense aqueous alteration of Ryugu compared to Orgueil. Both appear to have been highly aqueously altered, although some Ryugu grains experienced less aqueous alteration (Nakamura et al., 2022; Nakamura et al., 2023). Localized short-duration, weak heating via collisions and solar heating might help to explain a loss of NH_4^+ from Ryugu (Bonal et al., 2024, Tomioka et al. 2023, Nakamura E. et al. 2022, Nakamura T. et al. 2023). Another possibility would be that some Ryugu grains lack ^{15}N-rich NH_4^+ compared to Orgueil because they did not form from exactly the same material and/or their chemical conditions of aqueous alteration (pH, temperature, and ionic strength of the fluid) were less favourable to the formation of NH_4^+ salts, as discussed in Yoshimura et al. (2023). Hashizume et al. (2024) report a positive correlation between nitrogen concentrations and $\delta^{15}N$ values among several Ryugu samples and CI chondrites, with samples with lower nitrogen concentrations exhibiting lower $\delta^{15}N$. They explain this trend by a two-component mixing model: one component with a $\delta^{15}N$ around 0 ‰ or lower, possibly in IOM, at a constant abundance in all samples, and another component of variable abundance between samples exhibiting a $\delta^{15}N$ value of +56 ± 4 ‰. According to Hashizume et al. (2024), this latter component should represent about two third of the bulk nitrogen in CI falls and ^{15}N-rich Ryugu grains. Based on our results, this "component" should comprise NH_4^+, UOM and soluble nitrogen species such as NO_3^-, the sum of which represents 61 ± 19 % of the bulk nitrogen and have a $\delta^{15}N$ of +58 ± 4 ‰ in Orgueil. Variable amounts of NH_4^+, UOM or NO_3^- between samples possibly explain the correlation reported by Hashizume et al. (2024).

Although Ryugu grains studied up to now contain no or ≈200 times less NH_4^+, they contain 3 times to 5 times more NO_3^- than Orgueil (Table 3). Yoshimura et al. (2023) reported 0.07 ± 0.01 wt.% and 0.04 ± 0.01 wt.% water-soluble NO_3^- in Ryugu grains A0106 and C0107, respectively. In Ryugu water-soluble extracts, nitrate appears to be the dominant carrier of

nitrogen, while in Orgueil water-soluble extracts ammonium is dominant. Measurements of the isotopic compositions of NO_3^- and NH_4^+ in Ryugu and CI chondrites would help to constrain their genetic links, and the alteration history of Ryugu material.

5. Conclusion

The ammonium detected in the Orgueil meteorite by Cloëz (1864) and Pisani (1864) is still present in the meteorite today. Water-soluble ammonium extracted via cryogenic grinding and leaching comprises 0.068 ± 0.011 wt.% of the stone, and 27 ± 5 % of its total nitrogen. The isotopic composition of the ammonium nitrogen ($\delta^{15}N$ = +72 ± 9 ‰) confirms its extra-terrestrial origin, and it should be considered as a best estimate so far (see section 2.7 and Text S2). The carrier phase(s) of this water-soluble ammonium is (are) still unknown, but our data are compatible with the presence of ammonium salts $NH_4^+Cl^-$, $(NH_4^+)_2SO_4^{2-}$, possibly $NH_4^+CH_3COO^-$, $NH_4^+CH_3SO_3^-$, and of ammoniated phyllosilicates. The main carrier(s) of NH_4^+ are not volatilized when Orgueil is heated at 110°C (383 K) (Cloëz, 1864).

Ammonium seems to be present on other carbonaceous chondrites as well (Berzelius, 1834; Mautner, 2014), but is at least two times more abundant in Orgueil than in CK, CO, CV, CR and CM chondrites. Ammonium was also observed on Ceres, comet 67P/Chyurumov-Gerasmenko, and is possibly present on many other small bodies (King et al., 1992; De Sanctis et al., 2015; Poch et al., 2020; Altwegg et al., 2022). Notably, reflectance spectra of the surface of comet 67P/Chyurumov-Gerasimenko are consistent with the presence of $(NH_4^+)_2SO_4^{2-}$ (Poch et al., 2020), and mass spectrometry data indicate the presence of abundant $NH_4^+SH^-$, along with $NH_4^+CN^-$ or $NH_4^+OCN^-$ in its dust grains (Altwegg et al., 2022), which are unstable under terrestrial conditions (Raunier et al., 2003; Friend et al., 2007). If these salts were initially present in the Orgueil meteoroid, they may have been lost during its entry in the Earth

atmosphere or rapidly after. Therefore, it is possible that the Orgueil parent body contained even more nitrogen in the form of ammonium.

In Orgueil, nitrogen is distributed among diverse phases: 27 ± 5 % is in water-soluble ammonium, 1.3 ± 0.6 % in nitrate, and about 3 ± 3 % in other water-soluble molecules (including amines, amino acids and nucleobases, which represent less than 0.4 % altogether). The IOM accounts for 35 ± 5 % of the nitrogen (and 56 ± 12 % of the carbon) in Orgueil. The remaining 34 ± 14 % of nitrogen is mainly (60-90 %) in an unidentified organic matter (UOM). This UOM is either a fraction of IOM that was lost during isolation and/or an acid-soluble organic matter that has not been isolated yet (hydrolysable functional groups bounded to the IOM, and/or in organic nitrogen trapped within phyllosilicates and/or nanocarbonates), and the rest is possibly in inorganic nitrogen trapped in minerals. From our nitrogen budget, we can estimate that the nitrogen in this (these) remaining phase(s) and in water-soluble species other than NH_4^+ have a $\delta^{15}N$ ranging from +23 ‰ to +55 ‰.

The ammonium found in Orgueil could have several origins. It could be a tracer of the accretion and/or later deposit of NH_3 ice and/or NH_3 hydrates or NH_4^+ salts on the CI parent body, which may have formed relatively far from the Sun (Alexander et al., 2013; Desch et al., 2018; Lodders, 2021). However, it is poorer in ^{15}N than nitrogen-bearing gases measured in cometary comae (Füri and Marty, 2015 and references therein). In addition, or alternatively, ammonium could have been produced via heating and/or aqueous alteration processes of primordial organic matter, occurring after the formation of the CI parent body. It was proposed that the organic matter in chondrites derived from a common organic precursor similar to the IOM of CR chondrites (Alexander et al., 1998, 2007), but such an origin of NH_4^+ would require major nitrogen isotopic exchanges in an open system. This seems unlikely, but it cannot be totally excluded given the unknown effects of long-term alteration processes on chemical

properties of N-bearing species. Orgueil IOM has the lowest ($\delta^{15}N = +32 \pm 1$ ‰) and NH_4^+ the highest ^{15}N-enrichment ($\delta^{15}N = +72 \pm 9$ ‰), whereas that of UOM appears to be intermediate, although closer to that of IOM ($\delta^{15}N = +39 \pm 16$ ‰). Based on these measurements and on the fact that IOM is heterogenous (having ^{15}N hotspots) and possibly UOM too, we cannot exclude that these phases could be compositionally related, or they have been formed from different nitrogen isotopic reservoirs.

Millimetre-size grains of the asteroid Ryugu have shown large variations in nitrogen concentrations and $\delta^{15}N$ (Broadley et al., 2023; Hashizume et al., 2024). Compared to Orgueil, the nitrogen concentration in Ryugu grains varies from similar values down to about 4 times lower, the grains with lower nitrogen concentrations exhibiting lower $\delta^{15}N$ (Hashizume et al., 2024). NH_4^+ was chemically extracted from one Ryugu grain, at a concentration ≈200 times less than in Orgueil (Yoshimura et al., 2023). The lower nitrogen abundance and ^{15}N-enrichment of some Ryugu grains may thus be at least partly due to the lack or the loss of ^{15}N-rich NH_4^+. Ryugu and Orgueil either originate from compositionally distinct materials, because of the heterogeneity of the CI parent body, or they originate from a compositionally similar material that has undergone different chemical or thermal conditions of alteration. Measurements of the isotopic compositions of NH_4^+ and NO_3^-, which is 3 to 5 times more abundant in Ryugu grains than in Orgueil (Yoshimura et al., 2023), are needed to constrain the genetic links and the alteration history of Ryugu material among CI chondrites. Importantly, one should bear in mind that Ryugu samples are about 10 to 100 times smaller than Orgueil samples, so the analytical results on Ryugu material may be more affected by its heterogeneity at the scale of the millimetre.

Additional investigations are planned to further constrain the nature of the nitrogen-bearing phases in Orgueil and particularly ammonium-bearing compounds, via investigations

using microscopy at the scale of the grains (nanometres). The present study demonstrates the importance of investigating the total budget of a volatile element (nitrogen, carbon etc.) and its distribution among several of its carrier phases, in order to better constrain the origin and evolution of carbonaceous chondrites and ultimately of the proto-planetary disk.

In addition, our quantifications of some of the major and minor water-soluble ions extractable from the Orgueil meteorite provide data of potential interest to constrain the aqueous chemistry occurring on the parent body. Moreover, the amount of ammonium accreted or delivered to planetary bodies via Orgueil-like objects could have strongly influenced their habitability, i.e. the existence of a surface or sub-surface liquid water ocean and its physico-chemistry.

Declaration of Competing Interest

The authors declare no conflict of interest.

Acknowledgments

The authors acknowledge Pierre Hily-Blant and Alexandre Faure for discussions about the incorporation of nitrogen in the Solar System. The authors also acknowledge the comments of Conel Alexander and two anonymous reviewers that greatly improved this manuscript. This work has been supported by a grant from Labex OSUG@2020 (Investissements d'avenir - ANR10 LABX56), by the Programme National de Planétologie (PNP) of CNRS-INSU co-funded by CNES, and by the French National Research Agency in the framework of the Investissements d'Avenir program (ANR-15-IDEX-02), through the funding of the "Origin of

Life" project of the Univ. Grenoble-Alpes. This research was also supported by the H2020 European Research Council (ERC) (SOLARYS ERC-CoG2017_771691).

CRediT authorship contribution statement

Lucie Laize-Générat: Investigation, Methodology, Validation, Data curation, Formal analysis, Visualization, Writing - original draft. **Lison Soussaintjean:** Investigation, Methodology, Data curation, Formal analysis, Writing - original draft. **Olivier Poch:** Conceptualization, Funding acquisition, Resources, Methodology, Investigation, Validation, Supervision, Writing - original draft. **Lydie Bonal:** Resources, Methodology, Supervision, Writing - review & editing. **Joël Savarino:** Resources, Methodology, Supervision, Writing - review & editing. **Nicolas Caillon:** Resources, Methodology, Writing - review & editing. **Patrick Ginot:** Resources, Methodology, Writing - review & editing. **Anthony Vella:** Resources, Methodology. **Alexis Lamothe**: Resources, Methodology. **Rhabira Elazzouzi**: Investigation, Resources. **Laurène Flandinet:** Investigation, Resources, Methodology, Writing - review & editing. **Lionel Vacher:** Investigation, Methodology, Writing - review & editing. **Matthieu Gounelle:** Resources, Writing - review & editing. **Martin Bizzaro:** Resources, Writing - review & editing. **Pierre Beck:** Funding acquisition, Resources, Writing - review & editing. **Eric Quirico:** Writing - review & editing. **Bernard Schmitt:** Resources.

Data availability

Reflectance spectra shown on Figure 2 and their associated sample information are freely available through the GhOSST database of the SSHADE infrastructure for solid spectroscopy at https://doi.org/10.26302/SSHADE/EXPERIMENT_LB_20231006_001 (Soussaintjean et

al., 2021). All other data are available through Zenodo at https://doi.org/10.5281/zenodo.11554136 (Laize-Générat et al., 2024).

Appendix A. Supplementary Material

The supplemental file includes pictures of the samples and extraction solutions, a text explaining a preliminary test of the extraction protocol, another text along with a figure and tables detailing the calibrations performed to estimate the nitrogen isotopic composition of ammonium, and several figures and tables showing the cumulative mole fractions of ions during the successive extraction steps and their correlation with ammonium mole fractions, the total abundance of the soluble ions in the different samples and their correlations with the total abundance of ammonium, the concentration of some ions in the first extraction solution and the fraction of total mass of ion extracted in the second rinse of the grinding jar and ball indicating that NO_3^- and NO_2^- probably comes from different sources than the other ions and NO_2^- is likely from a contamination, the analyses performed on the leached powders of Orgueil, and the distribution of the carbon in the meteorite.

References

Aléon J. (2010) Multiple origins of nitrogen isotopic anomalies in meteorites and comets. *Astrophys. J.* **722**, 1342–1351.

Alexander C.M.O'D., Russell S., Arden J., Ash R., Grady M. and Pillinger C. (1998) The origin of chondritic macromolecular organic matter: A carbon and nitrogen isotope study. *Meteorit. Planet. Sci.* **33**, 603–622.

Alexander C.M.O'D, Fogel M., Yabuta H. and Cody G. D. (2007) The origin and evolution of chondrites recorded in the elemental and isotopic compositions of their macromolecular organic matter. *Geochim. Cosmochim. Acta* **71**, 4380–4403.

Alexander C.M.O'D., Bowden R., Fogel M. L., Howard K. T., Herd C. D. K. and Nittler L. R. (2012) The provenances of asteroids, and their contributions to the volatile inventories of the terrestrial planets. *Science* **337**, 721–723.

Alexander C.M.O'D., Howard K. T., Bowden R. and Fogel M. L. (2013) The classification of CM and CR chondrites using bulk H, C and N abundances and isotopic compositions. *Geochim. Cosmochim. Acta* **123**, 244–260.

Alexander C.M.O'D., Bowden R., Fogel M.L. and Howard K.T. (2015) Carbonate abundances and isotopic compositions in chondrites. *Meteoritics & Planetary Science* **50**, 810–833.

Alexander C.M.O'D., Cody G. D., De Gregorio B. T., Nittler L. R. and Stroud R. M. (2017) The nature, origin and modification of insoluble organic matter in chondrites, the major source of Earth's C and N. *Geochemistry* **77**, 227–256.

Altwegg K., Balsiger H., Hänni N., Rubin M., Schuhmann M., Schroeder I., Sémon T., Wampfler S., Berthelier J.-J., Briois C., Combi M., Gombosi T. I., Cottin H., De Keyser J., Dhooghe F., Fiethe B. and Fuselier S. A. (2020) Evidence of ammonium salts in comet 67P as explanation for the nitrogen depletion in cometary comae. *Nat. Astron.* **4**, 533–540.

Altwegg K., Combi M., Fuselier S. A., Hänni N., De Keyser J., Mahjoub A., Müller D. R., Pestoni B., Rubin M. and Wampfler S. F. (2022) Abundant ammonium hydrosulphide embedded in cometary dust grains. *Mon. Not. R. Astron. Soc.* **516**, 3900-3910.

Ansdell G. and Dewar J. (1886) XIII. On the gaseous constituents of meteorites. *Proc. R. Soc. Lond.* **40**, 549–559.

Aponte J. C., Tarozo R., Alexandre M. R., Alexander C.M.O'D, Charnley S. B., Hallmann C., Summons R. E. and Huang Y. (2014) Chirality of meteoritic free and IOM-derived monocarboxylic acids and implications for prebiotic organic synthesis. *Geochim. Cosmochim. Acta* **131**, 1–12.

Aponte J. C., Dworkin J. P. and Elsila J. E. (2015) Indigenous aliphatic amines in the aqueously altered Orgueil meteorite. *Meteorit. Planet. Sci.* **50**, 1733–1749.

Armbruster D. A. and Pry T. (2008) Limit of Blank, Limit of Detection and Limit of Quantitation. *Clin Biochem Rev* **29**, S49–S52.

Becker R. H. and Epstein S. (1982) Carbon, hydrogen and nitrogen isotopes in solvent-extractable organic matter from carbonaceous chondrites. *Geochimica et Cosmochimica Acta* **46**, 97–103.

Bergin E. A., Blake G. A., Ciesla F., Hirschmann M. M. and Li J. (2015) Tracing the ingredients for a habitable earth from interstellar space through planet formation. *Proc. Natl. Acad. Sci.* **112**, 8965–8970.

Bergner J. B., Öberg K. I., Rajappan M. and Fayolle E. C. (2016) Kinetics and Mechanisms of the Acid-base Reaction Between NH3 and HCOOH in Interstellar Ice Analogs. *ApJ* **829**, 85-98.

Berzelius J. J. (1834) Ueber Meteorsteine. *Ann. Phys. Chem.* **109**, 113–148.

Bhattarai N., Wang S., Pan Y., Xu Q., Zhang Y., Chang Y. and Fang Y. (2021) δ^{15}N-stable isotope analysis of NHx: An overview on analytical measurements, source sampling and its source apportionment. *Front. Environ. Sci. Eng.* **15**, 126.

Bonal L., Huss G. R., Krot A. N., Nagashima K., Ishii H. A. and Bradley J. P. (2010) Highly 15N-enriched chondritic clasts in the CB/CH-like meteorite Isheyevo. *Geochim. Cosmochim. Acta* **74**, 6590–6609.

Bonal L., Quirico E., Montagnac G., Komatsu M., Kebukawa Y., Yabuta H., Amano K., Barosch J., Bejach L., Cody G. D., Dartois E., Dazzi A., De Gregorio B., Deniset-Besseau A., Duprat J., Engrand C., Hashiguchi M., Kamide K., Kilcoyne D., Martins Z., Mathurin J., Mostefaoui S., Nittler L., Ohigashi T., Okumura T., Remusat L., Sandford S., Shigenaka M., Stroud R., Suga H., Takahashi Y., Takeichi Y., Tamenori Y., Verdier-Paoletti M., Yamashita S., Nakamura T., Naraoka H., Noguchi T., Okazaki R., Yurimoto H., Tachibana S., Abe M., Miyazaki A., Nakato A., Nakazawa S., Nishimura M., Okada T., Saiki T., Sakamoto K., Tanaka S., Terui F., Tsuda Y., Usui T., Watanabe S., Yada T., Yogata K. and Yoshikawa M. (2024) The thermal history of Ryugu based on Raman characterization of Hayabusa2 samples. *Icarus* **408**, 115826.

Bossa J.-B., Borget F., Duvernay F., Theulé P. and Chiavassa T. (2008) Formation of Neutral Methylcarbamic Acid ($CH_3NHCOOH$) and Methylammonium Methylcarbamate [$CH_3NH_3^+$][$CH_3NHCO_2^-$] at Low Temperature. *J. Phys. Chem. A* **112**, 5113–5120.

Brearley A. J. (2006) The action of water. In *Meteorites and the early solar system II* (eds. D. S. Lauretta and H. Y. McSween). University of Arizona Press, Tucson. pp. 587–624.

Broadley M. W., Byrne D. J., Füri E., Zimmermann L., Marty B., Okazaki R., Yada T., Kitajima F., Tachibana S., Yogata K., Sakamoto K., Yurimoto H., Nakamura T., Noguchi T., Naraoka H., Yabuta H., Watanabe S., Tsuda Y., Nishimura M., Nakato A., Miyazaki A., Abe M., Okada T., Usui T., Yoshikawa M., Saiki T., Tanaka S., Terui F., Nakazawa S., Busemann H., Hashizume K., Gilmour J. D., Meshik A., Riebe M. E. I., Krietsch D., Maden C., Ishida A., Clay P., Crowther S. A., Fawcett L., Lawton T., Pravdivtseva O., Miura Y. N., Park J., Bajo K., Takano Y., Yamada K., Kawagucci S., Matsui Y., Yamamoto M., Righter K., Sakai S., Iwata N., Shirai N., Sekimoto S., Inagaki M., Ebihara M., Yokochi R., Nishiizumi K., Nagao K., Lee J. I., Kano A., Caffee M. W. and Uemura R. (2023) The noble gas and nitrogen relationship between Ryugu and carbonaceous chondrites. *Geochim. Cosmochim. Acta* **345**, 62–74.

Burcar B., Pasek M., Gull M., Cafferty B. J., Velasco F., Hud N. V. and Menor-Salván C. (2016) Darwin's warm little pond: a one-pot reaction for prebiotic phosphorylation and the mobilization of phosphate from minerals in a urea-based solvent. *Angew. Chem. Int. Ed.* **55**, 13249–13253.

Burton A. S., Grunsfeld S., Elsila J. E., Glavin D. P. and Dworkin J. P. (2014) The effects of parent-body hydrothermal heating on amino acid abundances in CI-like chondrites. *Polar Sci.* **8**, 255–263.

Busemann H., Young A. F., Alexander C. M. O., Hoppe P., Mukhopadhyay S. and Nittler L. R. (2006) Interstellar Chemistry Recorded in Organic Matter from Primitive Meteorites. *Science* **312**, 727–730.

Callahan M. P., Smith K. E., Cleaves H. J., Ruzicka J., Stern J. C., Glavin D. P., House C. H. and Dworkin J. P. (2011) Carbonaceous meteorites contain a wide range of extraterrestrial nucleobases. *Proc. Natl. Acad. Sci.* **108**, 13995–13998.

Chakraborty S., Muskatel B. H., Jackson T. L., Ahmed M., Levine R. D. and Thiemens M. H. (2014) Massive isotopic effect in vacuum UV photodissociation of N2 and implications for meteorite data. *Proc. Natl. Acad. Sci.* **111**, 14704–14709.

Chan Q. H. S., Chikaraishi Y., Takano Y., Ogawa N. O. and Ohkouchi N. (2016) Amino acid compositions in heated carbonaceous chondrites and their compound-specific nitrogen isotopic ratios. *Earth Planets Space* **68**, 7.

Cloëz S. (1864) Analyse chimique de la pierre météoritique d'Orgueil. *Comptes Rendus de l'Académie des Sciences Paris* **59**, 37–40.

Cloutis E. A., Hiroi T., Gaffey M. J., Alexander C.M.O'D and Mann P. (2011) Spectral reflectance properties of carbonaceous chondrites: 1. CI chondrites. *Icarus* **212**, 180–209.

Coplen T., Hopple J., Böhlke J., Peiser H., Rieder S., Krouse H., Rosman K., Ding T., Vocke Jr R., Révész K., and others (2002) *Compilation of Minimum and Maximum Isotope Ratios of Selected Elements in Naturally Occurring Terrestrial Materials and Reagents*., U.S. Geological Survey Water-Resources Investigations Report 01-4222.

Cronin J. R., Pizzarello S. and Frye J. S. (1987) ^{13}C NMR spectroscopy of the insoluble carbon of carbonaceous chondrites. *Geochim. Cosmochim. Acta* **51**, 299–303.

Danger G., Borget F., Chomat M., Duvernay F., Theulé P., Guillemin J.-C., Le Sergeant d'Hendecourt L. and Chiavassa T. (2011) Experimental investigation of aminoacetonitrile formation through the Strecker synthesis in astrophysical-like conditions: reactivity of methanimine (CH_2NH), ammonia (NH_3), and hydrogen cyanide (HCN). *Astron. Astrophys.* **535**, A47-A56.

Daubrée (1864) Note sur les météorites tombées le 14 mai aux environs d'Orgueil (Tarn & Garonne). *Comptes Rendus de l'Académie des Sciences Paris* **58**, 984–986.

De Sanctis M. C., Ammannito E., Raponi A., Marchi S., McCord T. B., McSween H. Y., Capaccioni F., Capria M. T., Carrozzo F. G., Ciarniello M., Longobardo A., Tosi F., Fonte S., Formisano M., Frigeri A., Giardino M., Magni G., Palomba E., Turrini D., Zambon F., Combe J.-P., Feldman W., Jaumann R., McFadden L. A., Pieters C. M., Prettyman T., Toplis M., Raymond C. A. and Russell C. T. (2015) Ammoniated phyllosilicates with a likely outer Solar System origin on (1) Ceres. *Nature* **528**, 241–244.

Desch S. J., Kalyaan A. and Alexander C.M.O'D (2018) The effect of Jupiter's formation on the distribution of refractory elements and inclusions in meteorites. *Astrophys. J. Suppl. Ser.* **238**, 11.

De Vera G. A., Gernjak W., Weinberg H., Farré M. J., Keller J. and von Gunten U. (2017) Kinetics and mechanisms of nitrate and ammonium formation during ozonation of dissolved organic nitrogen. *Water Research* **108**, 451–461.

Doane T. A. (2017) The Abiotic Nitrogen Cycle. *ACS Earth Space Chem.* **1**, 411–421.

Dufresne E. R. and Anders E. (1962) On the chemical evolution of the carbonaceous chondrites. *Geochim. Cosmochim. Acta* **26**, 1085–1114.

Durand B. and Nicaise G. (1980) Procedures for kerogen isolation. In *Kerogen-insoluble organic matter from sedimentary rocks* (ed. B. Durand). Editions technip. pp. 33–53.

Dziedzic P., Bartoszewicz A. and Córdova A. (2009) Inorganic ammonium salts as catalysts for direct aldol reactions in the presence of water. *Tetrahedron Letters* **50**, 7242–7245.

Ehrenfreund P., Glavin D. P., Botta O., Cooper G. W. and Bada J. L. (2001) Extraterrestrial amino acids in Orgueil and Ivuna: Tracing the parent body of CI type carbonaceous chondrites. *Proc. Natl. Acad. Sci.* **98**, 2138–2141.

Elsila J. E., Charnley S. B., Burton A. S., Glavin D. P. and Dworkin J. P. (2012) Compound-specific carbon, nitrogen, and hydrogen isotopic ratios for amino acids in CM and CR chondrites and their use in evaluating potential formation pathways. *Meteorit. Planet. Sci.* **47**, 1517–1536.

Engel M. H. and Macko S. A. (1997) Isotopic evidence for extraterrestrial non- racemic amino acids in the Murchison meteorite. *Nature* **389**, 265–268.

Felix J. D., Elliott E. M., Gish T. J., McConnell L. L. and Shaw S. L. (2013) Characterizing the isotopic composition of atmospheric ammonia emission sources using passive samplers and a combined oxidation-bacterial denitrifier approach. *Rapid Commun. Mass Spectrom.* **27**, 2239–2246.

Foustoukos D. I., Alexander C. M. O. and Cody G. D. (2021) H and N systematics in thermally altered chondritic insoluble organic matter: An experimental study. *Geochimica et Cosmochimica Acta* **300**, 44–64.

Fray N., Bardyn A., Cottin H., Baklouti D., Briois C., Engrand C., Fischer H., Hornung K., Isnard R., Langevin Y., Lehto H., Le Roy L., Mellado E. M., Merouane S., Modica P., Orthous-Daunay F.-R., Paquette J., Rynö J., Schulz R., Silén J., Siljeström S., Stenzel O., Thirkell L., Varmuza K., Zaprudin B., Kissel J. and Hilchenbach M. (2017) Nitrogen-to-carbon atomic ratio measured by COSIMA in the particles of comet 67P/Churyumov–Gerasimenko. *Mon. Not. R. Astron. Soc.* **469**, S506–S516.

Fredriksson K. and Kerridge J. F. (1988) Carbonates and sulfates in CI chondrites: formation by aqueous activity on the parent body. *Meteoritics* **23**, 35–44.

Friend D. G., Poling B. E., Thomson G. H., Daubert T. E. and Buck E. (2007) Physical and chemical data, section 2. *NIST*, 2–517.

Füri E. and Marty B. (2015) Nitrogen isotope variations in the Solar System. *Nat. Geosci.* **8**, 515–522.

Gardinier A., Derenne S., Robert F., Behar F., Largeau C. and Maquet J. (2000) Solid state CP/MAS ^{13}C NMR of the insoluble organic matter of the Orgueil and Murchison meteorites: quantitative study. *Earth Planet. Sci. Lett.* **184**, 9–21.

Garvie L. A. J. and Buseck P. R. (2007) Prebiotic carbon in clays from Orgueil and Ivuna (CI), and Tagish Lake (C2 ungrouped) meteorites. *Meteorit. Planet. Sci.* **42**, 2111–2117.

Geiss J. (1987) Composition measurements and the history of cometary matter. In *Exploration of Halley's Comet* (eds. M. Grewing, F. Praderie, and R. Reinhard). Springer Berlin Heidelberg, Berlin, Heidelberg. pp. 859–866.

Glavin D. P., Callahan M. P., Dworkin J. P. and Elsila J. E. (2010) The effects of parent body processes on amino acids in carbonaceous chondrites. *Meteorit. Planet. Sci.* **45**, 1948–1972.

Gonfiantini R. (1984) I.A.E.A. advisory group meeting on stable isotope reference samples for geochemical and hydrological investigations. *Chemical Geology* **46**, 85.

Gounelle M. and Zolensky M. E. (2001) A terrestrial origin for sulfate veins in CI1 chondrites. *Meteorit. Planet. Sci.* **36**, 1321–1329.

Gounelle M. and Zolensky M. E. (2014) The Orgueil meteorite: 150 years of history. *Meteorit. Planet. Sci.* **49**, 1769–1794.

Grady M. M., Verchovsky A. B., Franchi I. A., Wright I. P. and Pillinger C. T. (2002) Light dement geochemistry of the Tagish Lake CI2 chondrite: Comparison with CI1 and CM2 meteorites. *Meteorit. Planet. Sci.* **37**, 713–735.

Hashizume K., Ishida A., Chiba A., Okazaki R., Yogata K., Yada T., Kitajima F., Yurimoto H., Nakamura T., Noguchi T., Yabuta H., Naraoka H., Takano Y., Sakamoto K., Tachibana S., Nishimura M., Nakato A., Miyazaki A., Abe M., Okada T., Usui T., Yoshikawa M., Saiki T., Terui F., Tanaka S., Nakazawa S., Watanabe S., Tsuda Y., Broadley M. W., Busemann H., the Hayabusa2 Initial Analysis Volatile Team. (2024) The Earth atmosphere-like bulk nitrogen isotope composition obtained by stepwise combustion analyses of Ryugu return samples, *Meteorit. Planet. Sci.* **59**, 2117–2133.

Haynes W. M. and Lide D. R. (2010) *CRC Handbook of Chemistry and Physics*., CRC Press Boca Raton, FL.

Heays A. N., Visser R., Gredel R., Ubachs W., Lewis B. R., Gibson S. T. and Van Dishoeck E. F. (2014) Isotope selective photodissociation of N_2 by the interstellar radiation field and cosmic rays. *Astron. Astrophys.* **562**, A61.

Huss G. R., Rubin A. E. and Grossman J. N. (2006) Thermal metamorphism in chondrites. In *Meteorites and the Early Solar System II* (eds. D. S. Lauretta and H. Y. McSween). Tucson. pp. 567–586.

Huss R. and Lewis R. S. (1995) Presolar diamond, SiC, and graphite in primitive chondrites: Abundances as a function of meteorite class and petrologic type. *Geochim. Cosmochim. Acta* **59**, 115–160.

Injerd W. G. and Kaplan I. R. (1974) Nitrogen isotope distribution in meteorites. *Meteoritics* **9**, 352-353.

Kebukawa Y., Alexander C.M.O'D and Cody G.D. (2019) Comparison of FT-IR spectra of bulk and acid insoluble organic matter in chondritic meteorites: An implication for missing carbon during demineralization. *Meteorit. Planet. Sci.* **54**, 1632-1641.

King T.V.V., Clark R.N., Calvin W.M., Sherman D.M. and Brown R.H. (1992) Evidence for Ammonium-Bearing Minerals on Ceres. *Science* **255**, 1551–1553.

King A. J., Schofield P. F., Howard K. T. and Russell S. S. (2015) Modal mineralogy of CI and CI-like chondrites by X-ray diffraction. *Geochim. Cosmochim. Acta* **165**, 148–160.

Krot A. N., Keil K., Scott E. R. D., Goodrich C. A. and Weisberg M. K. (2014) 1.1 - Classification of meteorites and their genetic relationships. In *Treatise on Geochemistry (Second Edition)* (eds. H. D. Holland and K. K. Turekian). Elsevier, Oxford. pp. 1–63.

Kung C.-C. and Clayton R. N. (1978) Nitrogen abundances and isotopic compositions in stony meteorites. *Earth Planet. Sci. Lett.* **38**, 421–435.

[dataset] Laize-Générat, L., Soussaintjean, L., & Poch, O. (2024). Nitrogen in the Orgueil meteorite: abundant ammonium among other reservoirs of variable isotopic compositions. Zenodo. Dataset. https://doi.org/10.5281/zenodo.11554136

Lamothe A., Savarino J., Ginot P., Soussaintjean L., Gautier E., Akers P. D., Caillon N. and Erbland J. (2023) An extraction method for nitrogen isotope measurement of ammonium in a low-concentration environment. *Atmospheric Measurement Techniques* **16**, 4015–4030.
Le Guillou C., Bernard S., Brearley A. J. and Remusat L. (2014) Evolution of organic matter in Orgueil, Murchison and Renazzo during parent body aqueous alteration: In situ investigations. *Geochim. Cosmochim. Acta* **131**, 368–392.

Li L., He Y., Zhang Z. and Liu Y. (2021) Nitrogen isotope fractionations among gaseous and aqueous NH_4^+, NH_3, N_2, and metal-ammine complexes: Theoretical calculations and applications. *Geochim. Cosmochim. Acta* **295**, 80-97.

Lodders K. (2004) Jupiter formed with more tar than ice. *Astrophys. J.* **611**, 587–597.

Lodders K. (2021) Relative atomic solar system abundances, mass fractions, and atomic masses of the elements and their isotopes, composition of the solar photosphere, and compositions of the major chondritic meteorite groups. *Space Sci. Rev.* **217**, 44.

Lyons J. R., Gharib-Nezhad E. and Ayres T. R. (2018) A light carbon isotope composition for the Sun. *Nat. Commun.* **9**, 908.

Mariotti A., Lancelot C. and Billen G. (1984) Natural isotopic composition of nitrogen as a tracer of origin for suspended organic matter in the Scheldt estuary. *Geochim. Cosmochim. Acta* **48**, 549–555.

Mautner M. N. (2014) In situ biological resources: Soluble nutrients and electrolytes in carbonaceous asteroids/meteorites. Implications for astroecology and human space populations. *Planet. Space Sci.* **104**, 234–243.

McIlvin M. R. and Altabet M. A. (2005) Chemical conversion of nitrate and nitrite to nitrous oxide for nitrogen and oxygen isotopic analysis in freshwater and seawater. *Anal. Chem.* **77**, 5589–5595.

Morin S., Savarino J., Frey M. M., Domine F., Jacobi H.-W., Kaleschke L. and Martins J. M. F. (2009) Comprehensive isotopic composition of atmospheric nitrate in the Atlantic Ocean boundary layer from 65°S to 79°N. *J. Geophys. Res.* **114**, D05303.

Moynier F., Dai W., Yokoyama T., Hu Y., Paquet M., Abe Y., Aléon J., Alexander C. M. O., Amari S., Amelin Y., Bajo K.-I., Bizzarro M., Bouvier A., Carlson R. W., Chaussidon M., Choi B.-G., Dauphas N., Davis A. M., Di Rocco T., Fujiya W., Fukai R., Gautam I., Haba M.

K., Hibiya Y., Hidaka H., Homma H., Hoppe P., Huss G. R., Ichida K., Iizuka T., Ireland T. R., Ishikawa A., Ito M., Itoh S., Kawasaki N., Kita N. T., Kitajima K., Kleine T., Komatani S., Krot A. N., Liu M.-C., Masuda Y., McKeegan K. D., Morita M., Motomura K., Nakai I., Nagashima K., Nesvorný D., Nguyen A., Nittler L., Onose M., Pack A., Park C., Piani L., Qin L., Russell S. S., Sakamoto N., Schönbächler M., Tafla L., Tang H., Terada K., Terada Y., Usui T., Wada S., Wadhwa M., Walker R. J., Yamashita K., Yin Q.-Z., Yoneda S., Young E. D., Yui H., Zhang A.-C., Nakamura T., Naraoka H., Noguchi T., Okazaki R., Sakamoto K., Yabuta H., Abe M., Miyazaki A., Nakato A., Nishimura M., Okada T., Yada T., Yogata K., Nakazawa S., Saiki T., Tanaka S., Terui F., Tsuda Y., Watanabe S.-I., Yoshikawa M., Tachibana S. and Yurimoto H. (2022) The Solar System calcium isotopic composition inferred from Ryugu samples. *Geochem. Perspect. Lett.* **24**, 1–6.

Nagy B., Fredriksson K., Urey H. C., Claus G., Andersen C. A. and Percy J. (1963) Electron probe microanalysis of organized elements in the Orgueil meteorite. *Nature* **198**, 121–125.

Nakamura E., Kobayashi K., Tanaka R., Kunihiro T., Kitagawa H., Potiszil C., Ota T., Sakaguchi C., Yamanaka M., Ratnayake D. M., Tripathi H., Kumar R., Avramescu M.-L., Tsuchida H., Yachi Y., Miura H., Abe M., Fukai R., Furuya S., Hatakeda K., Hayashi T., Hitomi Y., Kumagai K., Miyazaki A., Nakato A., Nishimura M., Okada T., Soejima H., Sugita S., Suzuki A., Usui T., Yada T., Yamamoto D., Yogata K., Yoshitake M., Arakawa M., Fujii A., Hayakawa M., Hirata Naoyuki, Hirata Naru, Honda R., Honda C., Hosoda S., Iijima Y., Ikeda H., Ishiguro M., Ishihara Y., Iwata T., Kawahara K., Kikuchi S., Kitazato K., Matsumoto K., Matsuoka M., Michikami T., Mimasu Y., Miura A., Morota T., Nakazawa S., Namiki N., Noda H., Noguchi R., Ogawa N., Ogawa K., Okamoto C., Ono G., Ozaki M., Saiki T., Sakatani N., Sawada H., Senshu H., Shimaki Y., Shirai K., Takei Y., Takeuchi H., Tanaka S., Tatsumi E., Terui F., Tsukizaki R., Wada K., Yamada M., Yamada T., Yamamoto Y., Yano H., Yokota Y., Yoshihara K., Yoshikawa M., Yoshikawa K., Fujimoto M., Watanabe S. and Tsuda Y. (2022) On the origin and evolution of the asteroid Ryugu: A comprehensive geochemical perspective. *Proceedings of the Japan Academy, Series B* **98**, 227–282.

Nakamura T., Matsumoto M., Amano K., Enokido Y., Zolensky M. E., Mikouchi T., Genda H., Tanaka S., Zolotov M. Y., Kurosawa K., Wakita S., Hyodo R., Nagano H., Nakashima D., Takahashi Y., Fujioka Y., Kikuiri M., Kagawa E., Matsuoka M., Brearley A. J., Tsuchiyama A., Uesugi M., Matsuno J., Kimura Y., Sato M., Milliken R. E., Tatsumi E., Sugita S., Hiroi T., Kitazato K., Brownlee D., Joswiak D. J., Takahashi M., Ninomiya K., Takahashi T., Osawa T., Terada K., Brenker F. E., Tkalcec B. J., Vincze L., Brunetto R., Aléon-Toppani A., Chan Q. H. S., Roskosz M., Viennet J.-C., Beck P., Alp E. E., Michikami T., Nagaashi Y., Tsuji T., Ino Y., Martinez J., Han J., Dolocan A., Bodnar R. J., Tanaka M., Yoshida H., Sugiyama K., King A. J., Fukushi K., Suga H., Yamashita S., Kawai T., Inoue K., Nakato A., Noguchi T., Vilas F., Hendrix A. R., Jaramillo-Correa C., Domingue D. L., Dominguez G., Gainsforth Z., Engrand C., Duprat J., Russell S. S., Bonato E., Ma C., Kawamoto T., Wada T., Watanabe S., Endo R., Enju S., Riu L., Rubino S., Tack P., Takeshita S., Takeichi Y., Takeuchi A., Takigawa A., Takir D., Tanigaki T., Taniguchi A., Tsukamoto K., Yagi T., Yamada S., Yamamoto K., Yamashita Y., Yasutake M., Uesugi K., Umegaki I., Chiu I., Ishizaki T., Okumura S., Palomba E., Pilorget C., Potin S. M., Alasli A., Anada S., Araki Y., Sakatani N., Schultz C., Sekizawa O., Sitzman S. D., Sugiura K., Sun M., Dartois E., De Pauw E., Dionnet Z., Djouadi Z., Falkenberg G., Fujita R., Fukuma T., Gearba I. R., Hagiya

K., Hu M. Y., Kato T., Kawamura T., Kimura M., Kubo M. K., Langenhorst F., Lantz C., Lavina B., Lindner M., Zhao J., Vekemans B., Baklouti D., Bazi B., Borondics F., Nagasawa S., Nishiyama G., Nitta K., Mathurin J., Matsumoto T., Mitsukawa I., Miura H., Miyake A., Miyake Y., Yurimoto H., Okazaki R., Yabuta H., Naraoka H., Sakamoto K., Tachibana S., Connolly H. C., Lauretta D. S., Yoshitake M., Yoshikawa M., Yoshikawa K., Yoshihara K., Yokota Y., Yogata K., Yano H., Yamamoto Y., Yamamoto D., Yamada M., Yamada T., Yada T., Wada K., Usui T., Tsukizaki R., Terui F., Takeuchi H., Takei Y., Iwamae A., Soejima H., Shirai K., Shimaki Y., Senshu H., Sawada H., Saiki T., Ozaki M., Ono G., Okada T., Ogawa N., Ogawa K., Noguchi R., Noda H., Nishimura M., Namiki N., Nakazawa S., Morota T., Miyazaki A., Miura A., Mimasu Y., Matsumoto K., Kumagai K., Kouyama T., Kikuchi S., Kawahara K., Kameda S., Iwata T., Ishihara Y., Ishiguro M., Ikeda H., Hosoda S., Honda R., Honda C., Hitomi Y., Hirata N., Hirata N., Hayashi T., Hayakawa M., Hatakeda K., Furuya S., Fukai R., Fujii A., Cho Y., Arakawa M., Abe M., Watanabe S. and Tsuda Y. (2023) Formation and evolution of carbonaceous asteroid Ryugu: Direct evidence from returned samples. *Science* **379**, eabn8671.

Naraoka H., Takano Y., Dworkin J. P., Oba Y., Hamase K., Furusho A., Ogawa N. O., Hashiguchi M., Fukushima K., Aoki D., Schmitt-Kopplin P., Aponte J. C., Parker E. T., Glavin D. P., McLain H. L., Elsila J. E., Graham H. V., Eiler J. M., Orthous-Daunay F.-R., Wolters C., Isa J., Vuitton V., Thissen R., Sakai S., Yoshimura T., Koga T., Ohkouchi N., Chikaraishi Y., Sugahara H., Mita H., Furukawa Y., Hertkorn N., Ruf A., Yurimoto H., Nakamura T., Noguchi T., Okazaki R., Yabuta H., Sakamoto K., Tachibana S., Connolly H. C., Lauretta D. S., Abe M., Yada T., Nishimura M., Yogata K., Nakato A., Yoshitake M., Suzuki A., Miyazaki A., Furuya S., Hatakeda K., Soejima H., Hitomi Y., Kumagai K., Usui T., Hayashi T., Yamamoto D., Fukai R., Kitazato K., Sugita S., Namiki N., Arakawa M., Ikeda H., Ishiguro M., Hirata Naru, Wada K., Ishihara Y., Noguchi R., Morota T., Sakatani N., Matsumoto K., Senshu H., Honda R., Tatsumi E., Yokota Y., Honda C., Michikami T., Matsuoka M., Miura A., Noda H., Yamada T., Yoshihara K., Kawahara K., Ozaki M., Iijima Y., Yano H., Hayakawa M., Iwata T., Tsukizaki R., Sawada H., Hosoda S., Ogawa K., Okamoto C., Hirata Naoyuki, Shirai K., Shimaki Y., Yamada M., Okada T., Yamamoto Y., Takeuchi H., Fujii A., Takei Y., Yoshikawa K., Mimasu Y., Ono G., Ogawa N., Kikuchi S., Nakazawa S., Terui F., Tanaka S., Saiki T., Yoshikawa M., Watanabe S. and Tsuda Y. (2023) Soluble organic molecules in samples of the carbonaceous asteroid (162173) Ryugu. *Science* **379**, eabn9033.

Parker E. T., McLain H. L., Glavin D. P., Dworkin J. P., Elsila J. E., Aponte J. C., Naraoka H., Takano Y., Tachibana S., Yabuta H., Yurimoto H., Sakamoto K., Yada T., Nishimura M., Nakato A., Miyazaki A., Yogata K., Abe M., Okada T., Usui T., Yoshikawa M., Saiki T., Tanaka S., Nakazawa S., Tsuda Y., Terui F., Noguchi T., Okazaki R., Watanabe S. and Nakamura T. (2023) Extraterrestrial amino acids and amines identified in asteroid Ryugu samples returned by the Hayabusa2 mission. *Geochim. Cosmochim. Acta* **347**, 42–57.

Oba Y., Takano Y., Naraoka H., Furukawa Y., Glavin D. P., Dworkin J. P. and Tachibana S. (2020) Extraterrestrial hexamethylenetetramine in meteorites—a precursor of prebiotic chemistry in the inner solar system. *Nat. Commun.* **11**, 6243.

Pearson V. K., Sephton M. A., Franchi I. A., Gibson J. M. and Gilmour I. (2006) Carbon and nitrogen in carbonaceous chondrites: Elemental abundances and stable isotopic compositions. *Meteoritics & Planetary Science* **41**, 1899–1918.

Petit S., Righi D., Madejova J. and Decarreau A. (1998) Layer charge estimation of smectites using infrared spectroscopy. *Clay Miner.* **33**, 579–591.

Pilorget C., Okada T., Hamm V., Brunetto R., Yada T., Loizeau D., Riu L., Usui T., Moussi-Soffys A., Hatakeda K., Nakato A., Yogata K., Abe M., Aléon-Toppani A., Carter J., Chaigneau M., Crane B., Gondet B., Kumagai K., Langevin Y., Lantz C., Le Pivert-Jolivet T., Lequertier G., Lourit L., Miyazaki A., Nishimura M., Poulet F., Arakawa M., Hirata N., Kitazato K., Nakazawa S., Namiki N., Saiki T., Sugita S., Tachibana S., Tanaka S., Yoshikawa M., Tsuda Y., Watanabe S. and Bibring J.-P. (2022) First compositional analysis of Ryugu samples by the MicrOmega hyperspectral microscope. *Nat. Astron.* **6**, 221–225.

Pisani (1864) Etude chimique et analyse de l'aérolithe d'Orgueil. *Comptes Rendus de l'Académie des Sciences Paris* **59**, 132–135.

Pizzarello S., Feng X., Epstein S. and Cronin J. R. (1994) Isotopic analyses of nitrogenous compounds from the Murchison meteorite: ammonia, amines, amino acids, and polar hydrocarbons. *Geochim. Cosmochim. Acta* **58**, 5579–5587.

Pizzarello S. and Holmes W. (2009) Nitrogen-containing compounds in two CR2 meteorites: ^{15}N composition, molecular distribution and precursor molecules. *Geochim. Cosmochim. Acta* **73**, 2150–2162.

Pizzarello S. and Williams L. B. (2012) Ammonia in the early solar system: an account from carbonaceous meteorites. *Astrophys. J.* **749**, 161-167.

Poch O., Istiqomah I., Quirico E., Beck P., Schmitt B., Theulé P., Faure A., Hily-Blant P., Bonal L., Raponi A., Ciarniello M., Rousseau B., Potin S., Brissaud O., Flandinet L., Filacchione G., Pommerol A., Thomas N., Kappel D., Mennella V., Moroz L., Vinogradoff V., Arnold G., Erard S., Bockelée-Morvan D., Leyrat C., Capaccioni F., Sanctis M. C. D., Longobardo A., Mancarella F., Palomba E. and Tosi F. (2020) Ammonium salts are a reservoir of nitrogen on a cometary nucleus and possibly on some asteroids. *Science* **367**, eaaw7462.

Pontoppidan K. M., Salyk C., Bergin E. A., Brittain S., Marty B., Mousis O. and Öberg K. I. (2014) Volatiles in protoplanetary disks. In *Protostars and Planets VI*, University of Arizona Press.

Potapov A., Theulé P., Jäger C. and Henning T. (2019) Evidence of Surface Catalytic Effect on Cosmic Dust Grain Analogs: The Ammonia and Carbon Dioxide Surface Reaction. *ApJL* **878**, L20-L25.

Potin S., Brissaud O., Beck P., Schmitt B., Magnard Y., Correia J.-J., Rabou P. and Jocou L. (2018) SHADOWS: A spectro-gonio radiometer for bidirectional reflectance studies of dark meteorites and terrestrial analogues. Design, calibrations and performances on challenging surfaces. *Applied Optics* **57**, 8279–8296.

Raunier S., Chiavassa T., Marinelli F., Allouche A. and Aycard J. P. (2003) Reactivity of HNCO with NH_3 at low temperature monitored by FTIR spectroscopy: formation of $NH_4^+OCN^-$. *Chem. Phys. Lett.* **368**, 594–600.

Remusat L., Derenne S., Robert F. and Knicker H. (2005) New pyrolytic and spectroscopic data on Orgueil and Murchison insoluble organic matter: A different origin than soluble? *Geochim. Cosmochim. Acta* **69**, 3919–3932.

Rivkin A. S., Emery J. P., Howell E. S., Kareta T., Noonan J. W., Richardson M., Sharkey B. N. L., Sickafoose A. A., Woodney L. M., Cartwright R. J., Lindsay S. and Mcclure L. T. (2022) The nature of low-albedo small bodies from 3 μm spectroscopy: one group that formed within the ammonia snow line and one that formed beyond it. *Planet. Sci. J.* **3**, 153.

Robert F. and Epstein S. (1982) The concentration and isotopic composition of hydrogen, carbon and nitrogen in carbonaceous meteorites. *Geochimica et Cosmochimica Acta* **46**, 81–95.

Rodgers S. D. and Charnley S. B. (2008a) Nitrogen isotopic fractionation of interstellar nitriles. *Astrophys. J.* **689**, 1448-1455.

Rodgers S. D. and Charnley S. B. (2008b) Nitrogen superfractionation in dense cloud cores. *Mon. Not. R. Astron. Soc. Lett.* **385**, L48–L52.

Schmitt-Kopplin P., Hertkorn N., Harir M., Moritz F., Lucio M., Bonal L., Quirico E., Takano Y., Dworkin J. P., Naraoka H., Tachibana S., Nakamura T., Noguchi T., Okazaki R., Yabuta H., Yurimoto H., Sakamoto K., Yada T., Nishimura M., Nakato A., Miyazaki A., Yogata K., Abe M., Usui T., Yoshikawa M., Saiki T., Tanaka S., Terui F., Nakazawa S., Okada T., Watanabe S. and Tsuda Y. (2023) Soluble organic matter Molecular atlas of Ryugu reveals cold hydrothermalism on C-type asteroid parent body. *Nat. Commun.* **14**, 6525.

Smith J. W. and Kaplan I. R. (1970) Endogenous carbon in carbonaceous meteorites. *Science* **167**, 1367–1370.

[dataset] Soussaintjean, L., Laize-Générat, L., Poch, O. (2021). Vis-NIR reflectance spectra (i = 0°, e = 30°) of three raw chips of the Orgueil CI chondrite under ambient conditions. SSHADE/GhoSST (OSUG Data Center). Dataset/Spectral Data. https://doi.org/10.26302/SSHADE/EXPERIMENT_LB_20231006_001

Takano Y., Naraoka H., Dworkin J.P., Koga T., Sasaki K., Sato H., Oba Y., Ogawa N.O., Yoshimura T., Hamase K., Ohkouchi N., Parker E.T., Aponte J.C., Glavin D.P., Furukawa Y., Aoki J., Kano K., Nomura S.M., Orthous-Daunay F–R, Schmitt-Kopplin P., Hayabusa2-initial-analysis SOM team, Yurimoto H., Nakamura T., Noguchi T., Okazaki R., Yabuta H., Sakamoto K., Yada T., Nishimura M., Nakato A., Miyazaki A., Yogata K., Abe M., Okada T., Usui T., Yoshikawa M., Saiki T., Tanaka S., Terui F., Nakazawa S., Watanabe S., Tsuda Y. and Tachibana S. (2024) Primordial aqueous alteration recorded in water-soluble organic molecules from the carbonaceous asteroid (162173) Ryugu. *Nature communication* **15**, 5708.

Theulé P., Duvernay F., Danger G., Borget F., Bossa J. B., Vinogradoff V., Mispelaer F. and Chiavassa T. (2013) Thermal reactions in interstellar ice: A step towards molecular complexity in the interstellar medium. *Advances in Space Research* **52**, 1567–1579.

Tomioka N., Yamaguchi A., Ito M., Uesugi M., Imae N., Shirai N., Ohigashi T., Kimura M., Liu M.-C., Greenwood R. C., Uesugi K., Nakato A., Yogata K., Yuzawa H., Kodama Y., Hirahara K., Sakurai I., Okada I., Karouji Y., Okazaki K., Kurosawa K., Noguchi T., Miyake A., Miyahara M., Seto Y., Matsumoto T., Igami Y., Nakazawa S., Okada T., Saiki T., Tanaka

S., Terui F., Yoshikawa M., Miyazaki A., Nishimura M., Yada T., Abe M., Usui T., Watanabe S. and Tsuda Y. (2023) A history of mild shocks experienced by the regolith particles on hydrated asteroid Ryugu. *Nat. Astron.* **7**, 669–677.

Urey H. C. (1947) The Thermodynamic Properties of Isotopic Substances. *Journal of the Chemical Society (Resumed)*, 562-581.

Urey H. C. (1966) Biological material in meteorites: a review. *Science* **151**, 157–166.

Vdovykin G. P. (1970) Carbonaceous Matter in Meteorites (Organic Compounds, Diamonds, Graphite), *National Aeronautics and Space Administration Technical Translation TT F*-582.

Viennet, M. Roskosz, T. Nakamura, P. Beck, B. Baptiste, B. Lavina, E.E. Alp, M.Y. Hu, J. Zhao, M. Gounelle, R. Brunetto, H. Yurimoto, T. Noguchi, R. Okazaki, H. Yabuta, H. Naraoka, K. Sakamoto, S. Tachibana, T. Yada, M. Nishimura, A. Nakato, A. Miyazaki, K. Yogata, M. Abe, T. Okada, T. Usui, M. Yoshikawa, T. Saiki, S. Tanaka, F. Terui, S. Nakazawa, S.-I. Watanabe, and Y. Tsuda (2023) Interaction between clay minerals and organics in asteroid Ryugu. *Geochem. Perspect. Lett.* **25**, 8–12.

Weber A. L. (2007) The sugar model: autocatalytic activity of the triose–ammonia reaction. *Orig. Life Evol. Biospheres* **37**, 105–111.

Werner R. A. and Brand W. A. (2001) Referencing strategies and techniques in stable isotope ratio analysis. *Rapid Commun. Mass Spectrom.* **15**, 501–519.

Wiik H. B. (1956) The chemical composition of some stony meteorites. *Geochim. Cosmochim. Acta* **9**, 279–289.

Wirström E. S., Charnley S. B., Cordiner M. A. and Milam S. N. (2012) Isotopic anomalies in primitive solar system matter: spin-state dependent fractionation of nitrogen and deuterium in interstellar clouds. *Astrophys. J.* **757**, L11-L16.

Yang J. and Epstein S. (1983) Interstellar organic matter in meteorites. *Geochimica et Cosmochimica Acta* **47**, 2199–2216.

Yokoyama T., Nagashima K., Nakai I., Young E. D., Abe Y., Aléon J., Alexander C. M. O., Amari S., Amelin Y., Bajo K., Bizzarro M., Bouvier A., Carlson R. W., Chaussidon M., Choi B.-G., Dauphas N., Davis A. M., Di Rocco T., Fujiya W., Fukai R., Gautam I., Haba M. K., Hibiya Y., Hidaka H., Homma H., Hoppe P., Huss G. R., Ichida K., Iizuka T., Ireland T. R., Ishikawa A., Ito M., Itoh S., Kawasaki N., Kita N. T., Kitajima K., Kleine T., Komatani S., Krot A. N., Liu M.-C., Masuda Y., McKeegan K. D., Morita M., Motomura K., Moynier F., Nguyen A., Nittler L., Onose M., Pack A., Park C., Piani L., Qin L., Russell S. S., Sakamoto N., Schönbächler M., Tafla L., Tang H., Terada K., Terada Y., Usui T., Wada S., Wadhwa M., Walker R. J., Yamashita K., Yin Q.-Z., Yoneda S., Yui H., Zhang A.-C., Connolly H. C., Lauretta D. S., Nakamura T., Naraoka H., Noguchi T., Okazaki R., Sakamoto K., Yabuta H., Abe M., Arakawa M., Fujii A., Hayakawa M., Hirata Naoyuki, Hirata Naru, Honda R., Honda C., Hosoda S., Iijima Y., Ikeda H., Ishiguro M., Ishihara Y., Iwata T., Kawahara K., Kikuchi S., Kitazato K., Matsumoto K., Matsuoka M., Michikami T., Mimasu Y., Miura A., Morota T., Nakazawa S., Namiki N., Noda H., Noguchi R., Ogawa N., Ogawa K., Okada T., Okamoto C., Ono G., Ozaki M., Saiki T., Sakatani N., Sawada H., Senshu H., Shimaki Y., Shirai K., Sugita S., Takei Y., Takeuchi H., Tanaka S., Tatsumi E., Terui F., Tsuda Y.,

Tsukizaki R., Wada K., Watanabe S., Yamada M., Yamada T., Yamamoto Y., Yano H., Yokota Y., Yoshihara K., Yoshikawa M., Yoshikawa K., Furuya S., Hatakeda K., Hayashi T., Hitomi Y., Kumagai K., Miyazaki A., Nakato A., Nishimura M., Soejima H., Suzuki A., Yada T., Yamamoto D., Yogata K., Yoshitake M., Tachibana S. and Yurimoto H. (2023) Samples returned from the asteroid Ryugu are similar to Ivuna-type carbonaceous meteorites. *Science* **379**, eabn7850.

Yoshimura T., Takano Y., Naraoka H., Koga T., Araoka D., Ogawa N. O., Schmitt-Kopplin P., Hertkorn N., Oba Y., Dworkin J. P., Aponte J. C., Yoshikawa T., Tanaka Satoru, Ohkouchi N., Hashiguchi M., McLain H., Parker E. T., Sakai S., Yamaguchi M., Suzuki T., Yokoyama T., Yurimoto H., Nakamura T., Noguchi T., Okazaki R., Yabuta H., Sakamoto K., Yada T., Nishimura M., Nakato A., Miyazaki A., Yogata K., Abe M., Okada T., Usui T., Yoshikawa M., Saiki T., Tanaka Satoshi, Terui F., Nakazawa S., Watanabe S., Tsuda Y. and Tachibana S. (2023) Chemical evolution of primordial salts and organic sulfur molecules in the asteroid 162173 Ryugu. *Nat. Commun.* **14**, 5284.

Zhang L., Altabet M. A., Wu T. and Hadas O. (2007) Sensitive measurement of NH_4^+ $^{15}N/^{14}N(\delta^{15}NH_4^+)$ at natural abundance levels in fresh and saltwaters. *Anal. Chem.* **79**, 5297–5303.

Zhang K., Blake G. A. and Bergin E. A. (2015) Evidence of fast pebble growth near condensation fronts in the HL Tau protoplanetary disk. *ApJL* **806**, L7–L13.

Zheng W. and Kaiser R. I. (2007) An infrared spectroscopy study of the phase transition in solid ammonia. *Chemical Physics Letters* **440**, 229–234.

Figures

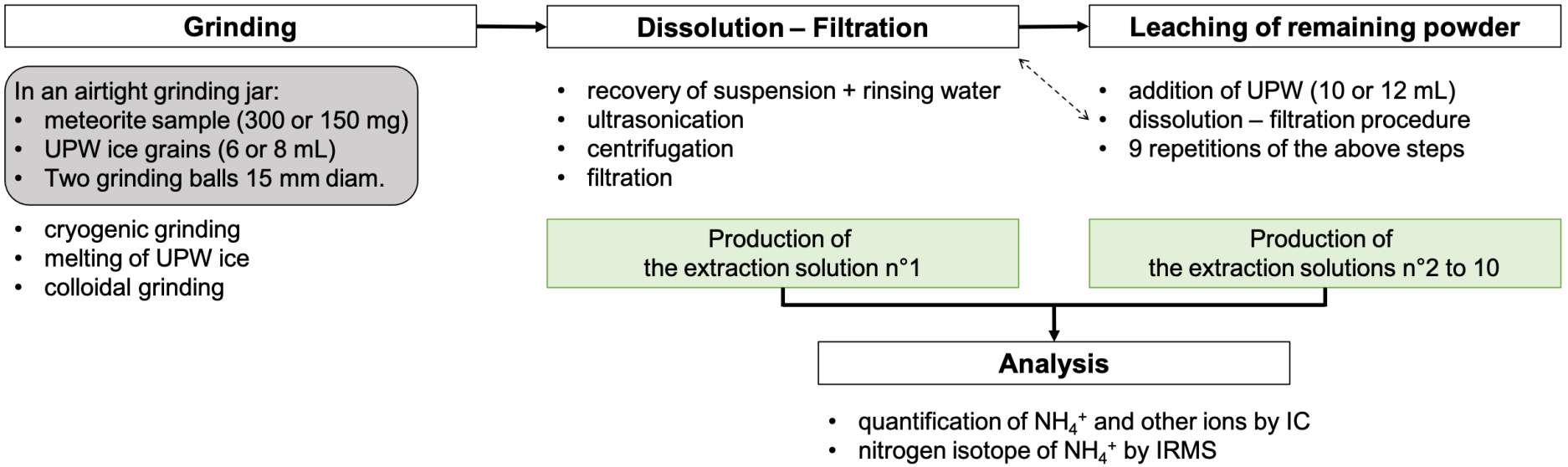

Figure 1: Flowchart of procedures for water-soluble ions extraction, quantification, and NH_4^+ isotope analysis. To avoid contamination, all transfers of sample or solutions are performed in a glove box under an argon atmosphere. Apart from these operations, the solutions are always in airtight vessels. UPW = ultra-pure water. Images of the samples and leaching steps are provided in the Supplementary Material document.

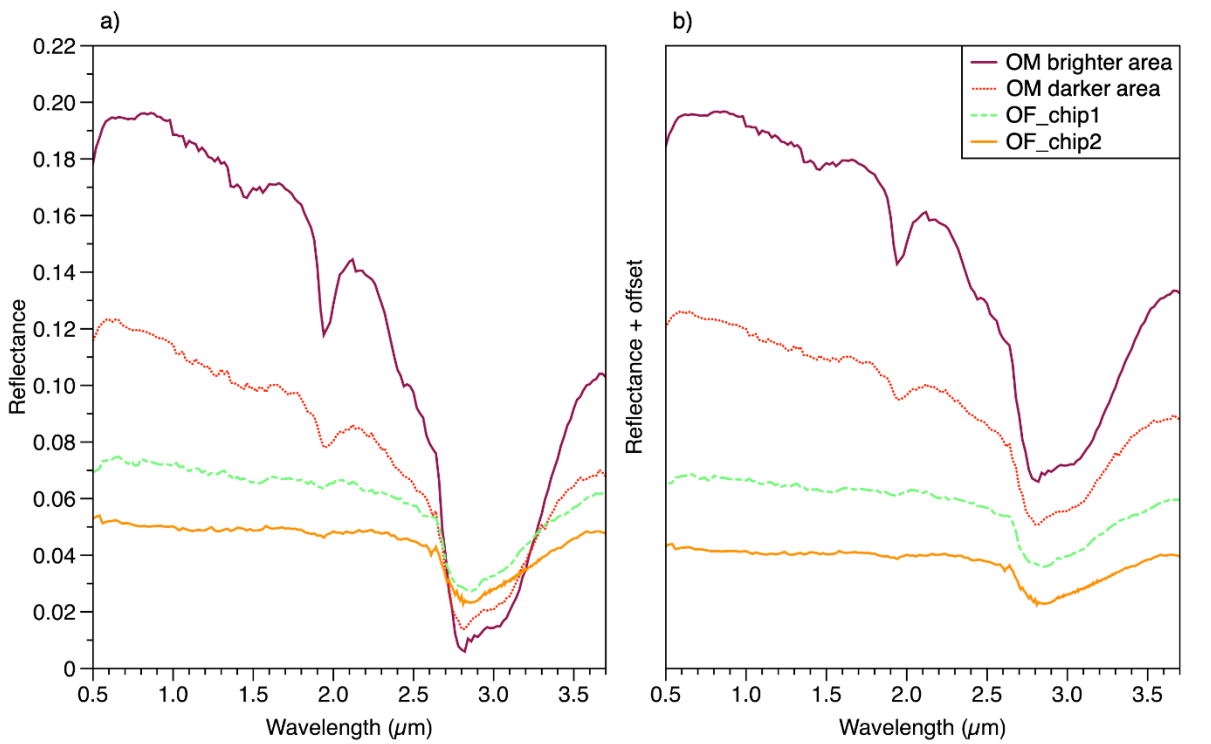

Figure 2: Reflectance spectra of raw chips of the Orgueil samples, **(a)** plotted on a same reflectance scale, and **(b)** with an offset. The 3-µm absorption feature is due to adsorbed H_2O and structural OH and H_2O in minerals. The 1.94-µm absorption band is attributed to H_2O in sulfate minerals. These minerals are more abundant on the surface of OM, scattering the light and causing a higher reflectance and a bluer spectral slope compared to the two chips of OF, which have similar spectra. Therefore, OM appears to be more terrestrially altered than OF. These spectra can be visualized and downloaded on the GhoSST database from the SSHADE infrastructure (Soussaintjean et al., 2021).

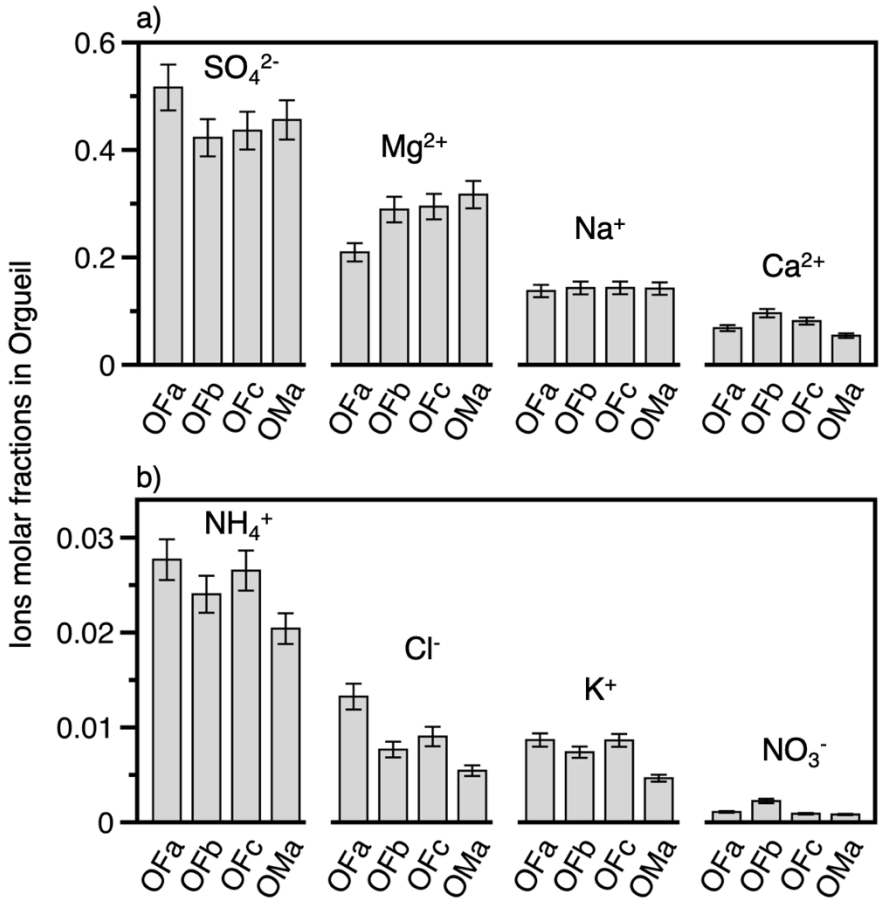

Figure 3: Histograms of the mole fraction of water-soluble ions (mole of an ion divided by mole of total ions) for **(a)** major ions, and **(b)** minor ions, plotted for the four Orgueil samples OFa, OFb, OFc and OMa (Table 1). SO_4^{2-} dominates the major ions, accounting for 40 to 50 mol% of total water-soluble ions. NH_4^+ dominates the minor ions, accounting for 2 to 3 mol% of the total water-soluble ions. For each ion, variations between samples probably reflect the compositional heterogeneity of the Orgueil meteorite. Interestingly, NH_4^+, Cl^- and K^+ exhibit quite similar relative variations between samples (see also Figure 4 and Table S5), and Ca^{2+} and NO_3^- also appear to do so. This is indicative of a release of these ions by carrier phases with similar solubilities and/or by the same phases.

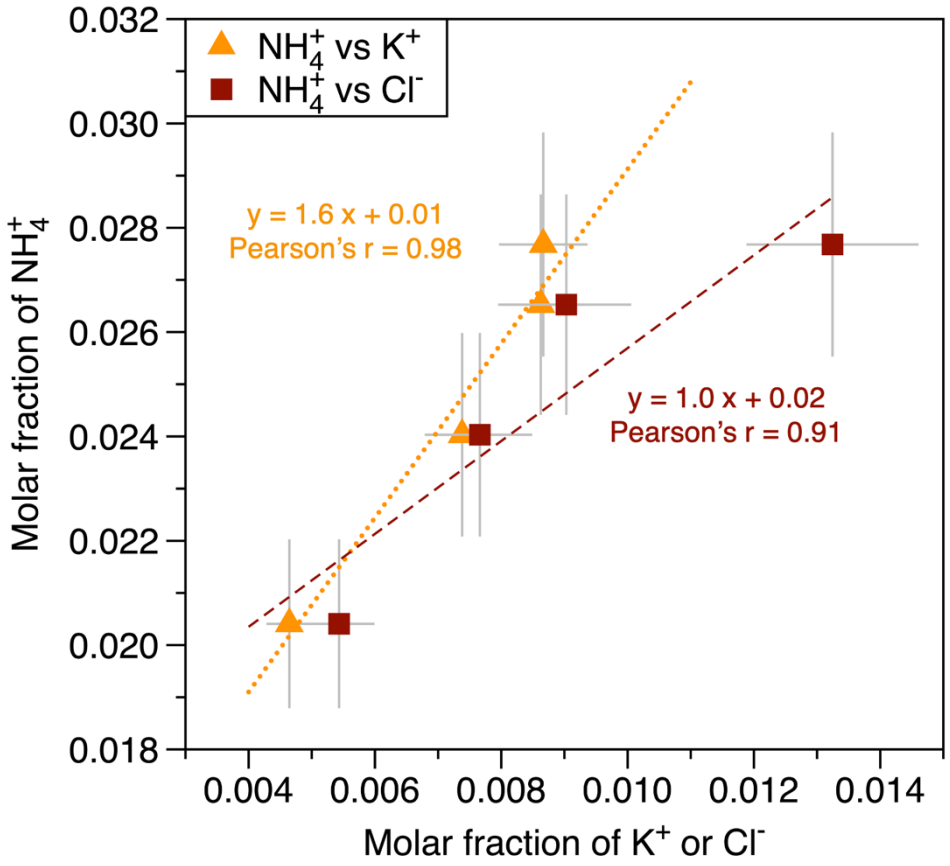

Figure 4: Linear correlation between the molar fraction of NH_4^+ (mole of NH_4^+ divided by mole of total ions) and that of K^+ (triangles, dotted line) and Cl^- (squares, dashed line) found after extraction and analysis of OMa, OFb, OFc and OFa (listed here by increasing mole fraction of NH_4^+). NH_4^+ mole fraction appears to be correlated with K^+ and Cl^- mole fractions, indicating that NH_4^+ might be associated with phases with similar solubilities and/or might be present in the same phases as Cl^- and K^+. The slope of 1 for NH_4^+ vs. Cl^- suggests the presence of $NH_4^+Cl^-$.

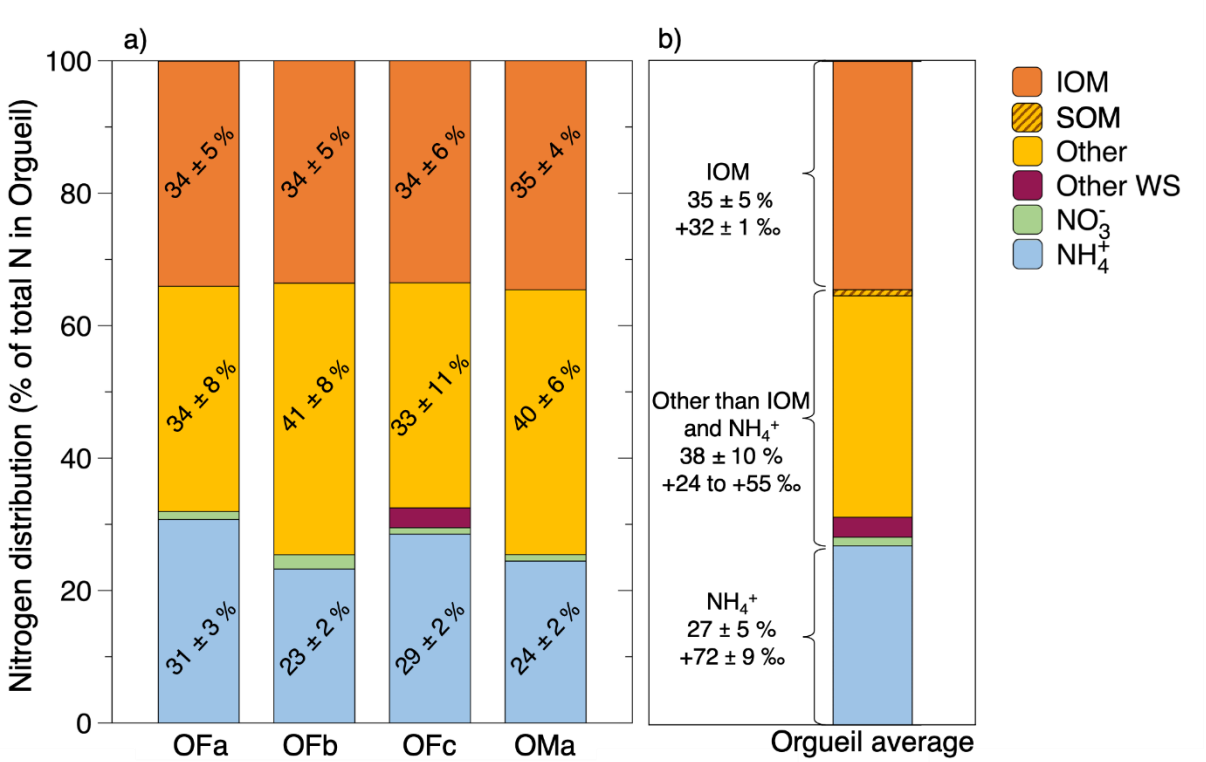

1627

1628 **Figure 5:** Distribution of nitrogen among the nitrogen-bearing phases in the Orgueil meteorite,
1629 from values in Table 3. **(a)** Distribution of nitrogen in OFa, OFb, OFc and OMa samples (Table
1630 1). **(b)** Average distribution calculated from the data of this study. The hashed area corresponds
1631 to the fraction of nitrogen in the SOM reported by Becker and Epstein (1982).
1632 IOM = Insoluble Organic Matter.
1633 SOM = Soluble Organic Matter. It only represents 0.9 % of the total nitrogen according to
1634 Becker and Epstein (1982).
1635 "Other than IOM and NH_4^+" = remaining nitrogen (not in the extracted IOM nor in NH_4^+),
1636 which is mainly (60-90 %) in an unidentified organic matter (UOM) as shown in Figure S7 and
1637 discussed in section 4.3. This UOM may be IOM lost during its extraction and/or acid
1638 hydrolysable functional groups bounded to the IOM and/or organic nitrogen trapped within
1639 minerals. The rest of the remaining nitrogen may be in inorganic species not extracted by our
1640 protocol. Here, NO_3^- is included in this remaining nitrogen because its $\delta^{15}N$ was not measured.
1641 Other WS = part of nitrogen in water-soluble compounds other than NH_4^+ and NO_3^-, estimated
1642 (only for OFc) to be 3 ± 3 % (see Table S9).
1643

Tables

Sample name	Storage condition	Piece name	Mass (mg)	Experiments performed
Orgueil-Flask (OF)	Sealed flask in private attic	**OFa**	303.1 ± 0.1	- Leaching followed by IC and IRMS analysis on the water-soluble solutions - IRMS on the leached powder (3 replicates of ~3 mg)
		OFb	302.3 ± 0.1	- Leaching followed by IC and IRMS analysis on the water-soluble solutions - IRMS on the leached powder (3 replicates of ~3 mg)
		OFc	150.0 ± 0.1	- Leaching followed by IC and IRMS analysis on the water-soluble solutions - IRMS on the leached powder (3 replicates of ~3 mg)
		OFd	160.0 ± 0.1	- IRMS on bulk meteorite powder (2 replicates of ~2.5 mg) - IOM extraction (1.9 mg extracted from 81 mg) followed by IRMS on the extracted IOM (2 replicates of ~0.8 mg)
		OFe	68.0 ± 0.1	- IRMS on bulk meteorite (3 replicates of ~3 mg) - IOM extraction (1.2 mg extracted from 46 mg) followed by IRMS on the extracted IOM (2 replicates of ~0.6 mg)
Orgueil Museum (OM)	Sealed bell-jar (possibly leaking) in Museum Victor Brun of Montauban	**OMa**	306.8 ± 0.1	- Leaching followed by IC and IRMS analysis on the water-soluble solutions - IRMS on the leached powder (3 replicates of ~3 mg)
		OMb	9.9 ± 0.1	- IRMS on bulk meteorite (3 replicates of ~3 mg)
		OMc	37.8 ± 0.1	- IOM extraction (1.2 mg extracted from 37.8 mg) followed by IRMS on the extracted IOM (2 replicates of ~0.6 mg)
		OMd	139.0 ± 0.1	- Leaching followed by IRMS analysis on the water-soluble solutions
		OMe	122.4 ± 0.1	- Leaching followed by IRMS analysis on the water-soluble solutions

Table 1: Names and masses of the different studied samples and pieces of Orgueil, and experiments performed on these samples.

1648

	OFa		OFb		OFc		OMa		Orgueil average	
	(wt.%)	sd	(wt.%)	sd	(wt.%)	sd	(wt.%)	sd	(wt.%)	sd
SO_4^{2-}	7.83	0.46	5.59	0.32	6.12	0.347	7.58	0.43	6.78	1.34
Mg^{2+}	0.804	0.045	0.966	0.056	1.05	0.059	1.33	0.08	1.04	0.25
Na^{+}	0.499	0.030	0.452	0.027	0.481	0.028	0.565	0.033	0.499	0.071
Ca^{2+}	0.433	0.024	0.530	0.030	0.477	0.027	0.377	0.021	0.454	0.082
NH_4^{+}	0.0789	0.0040	0.0596	0.0034	0.0699	0.004	0.0638	0.0035	0.0681	0.0109
CH_3COO^{-}	0.0978	0.0073	0.0314	0.0029		n.a.		n.a.	0.0646	0.0383
Cl^{-}	0.0742	0.0063	0.0374	0.0034	0.0468	0.005	0.0334	0.0029	0.0479	0.0202
K^{+}	0.0535	0.0030	0.0397	0.0022	0.0493	0.003	0.0314	0.0017	0.0435	0.0109
$HCOO^{-}$	0.0282	0.0017	0.0137	0.0012		n.a.		n.a.	0.0209	0.0087
NO_3^{-}	0.0106	0.0006	0.0191	0.0016	0.00812	0.001	0.00876	0.00047	0.0117	0.0052
$C_2O_4^{2-}$	0.0121	0.0007	0.0068	0.0004		n.a.		n.a.	0.00944	0.00324
$CH_3SO_3^{-}$	0.00174	0.00018	0.0076	0.0008		n.a.		n.a.	0.00468	0.00344
Total	**9.93**	**0.58**	**7.75**	**0.45**	**8.30**	**0.47**	**10.0**	**0.6**	**9.05**	**1.84**
	(meq/g)	sd	(meq/g)	sd	(meq/g)	sd	(meq/g)	sd	(meq/g)	sd
Σ^{-}	1.68	0.10	1.19	0.07	1.29	0.07	1.59	0.09	1.45	0.30
Σ^{+}	1.15	0.07	1.30	0.08	1.36	0.08	1.57	0.09	1.35	0.29

1649

Table 2: Mass fraction of ions measured in water-soluble extraction solutions of Orgueil samples OFa, OFb, OFc and OMa and corrected from the LoB. "Orgueil average" corresponds to the average value calculated from the data on the four samples (when present). The total amount of ions includes minor ions that are not presented in this table but available in the Table S1. Variations of ion mass fraction from one sample to another is mainly due to the heterogeneity of composition of Orgueil at the mm/cm-scales. As OMa contains as much NH_4^+ as the other samples, NH_4^+ does not appear to have been lost after being exposed to terrestrial weathering. Electrochemical equivalent mass ratios are indicated for anions (Σ^-) and cations (Σ^+).

n.a.: values were not acquired

	Sample	Nitrogen mass fraction		$\delta^{15}N$	
		(wt.%)	sd	(‰)	sd
Bulk					
	OFd (*n=2*)	0.200	0.008	+48.1	0.2
	OFe (*n=2*)	0.190	0.006	+48.8	1.0
	OMb (*n=3*)	0.203	0.006	+46.5	1.5
	Average	***0.198***	***0.012***	***+47.8***	***1.9***

Phase	**Sample**	**Phase mass fraction in Orgueil**		**Nitrogen mass fraction in phase**		**Nitrogen fraction in Orgueil**		δ^{15}**N**	
Molecule		(wt.%)	sd	(wt.%)	sd	(%)	sd	(‰)	sd
IOM									
	OFd (*n=2*)	2.4	0.4	2.9	0.1	34	5	+31.9	0.1
	OFe (*n=1*)	2.7	0.4	2.4	0.2	34	6	+31.3	1.1
	OMc (*n=2*)	3.1	0.4	2.3	0.1	35	4	+32.3	0.2
	Average	***2.7***	***0.6***	***2.5***	***0.4***	***35***	***5***	***+31.8***	***0.9***
Water-soluble species									
NH_4^+									
	OFa (*n=1*)	0.079	0.004			31	3	+73	8 [a]
	OFb (*n=1*)	0.060	0.003			23	2	+73	8 [a]
	OFc (*n=1*)	0.070	0.004	90	10	29	2	+71	8 [a]
	OM [b]	0.064	0.004 [b]			24	2 [b]	+50	12 [a,b]
	Average	***0.068***	***0.011***	***90***	***10***	***27***	***5***	***+72***	***9*** [a,c]
NO_3^-									
	OFa (*n=1*)	0.011	0.001			1.2	0.1		
	OFb (*n=1*)	0.019	0.002			2.2	0.3		
	OFc (*n=1*)	0.0081	0.0005	3.3	0.6	1.0	0.1		
	OMa (*n=1*)	0.0088	0.0005			1.0	0.1		
	Average	***0.012***	***0.005***	***3.3***	***0.6***	***1.3***	***0.6***		
Other than IOM and NH_4^+ [d]						***38***	***10***	***+39***	***16*** [e]

Table 3: Nitrogen elemental and isotopic analyses of the bulk Orgueil meteorite samples, and of the nitrogen-bearing phases.

[a] These $\delta^{15}N$ values are those for NH_4^+, with potential contributions of nitrogen-bearing water-soluble organic molecules oxidized or partly oxidized by the azide method (section 2.7).

[b] For OM, the ammonium mass fractions in Orgueil and in nitrogen-bearing phases were measured only in OMa. The $\delta^{15}N$ value is the average of those measured in NH_4^+ extracted from OMa, OMd and OMe (Table S4).

[c] As the isotopic composition of OMa is not in the same range as OFa, OFb and OFc probably due to terrestrial alteration (see section 4.2), its value is excluded from the calculation of the average value.

[d] "Other than IOM and NH_4^+" is the remaining nitrogen (not in the extracted IOM nor in NH_4^+), which is mainly (60-90 %) in an unidentified organic matter (UOM) as shown in Figure S7 and discussed in section 4.3. This UOM may be IOM lost during its extraction and/or acid hydrolysable functional groups bounded to the IOM and/or organic nitrogen trapped within minerals. The rest of the remaining nitrogen may be in inorganic species not extracted by our protocol. Here, NO_3^- is included in this remaining nitrogen because its $\delta^{15}N$ was not measured.

[e] The isotopic composition of nitrogen in other nitrogen-bearing phases than IOM and NH_4^+ (but including NO_3^-) is calculated (see section 4.3).

	Bulk					IOM							
	N_{Bulk} mass fraction	**$\delta^{15}N_{Bulk}$**	**C_{Bulk} mass fraction**	**$\delta^{13}C_{Bulk}$**	**N/C**	**Insoluble residue mass fraction**	**N_{IOM} mass fraction in insoluble residue**	**N_{IOM} mass fraction in bulk rock**	**$\delta^{15}N_{IOM}$**	**C_{IOM} mass fraction in insoluble residue**	**C_{IOM} mass fraction in bulk rock**	**$\delta^{13}C_{IOM}$**	**N/C**
	(wt.%)	(‰)	(wt.%)	(‰)	(at.)	(wt.%)	(wt.%)	(wt.%)	(‰)	(wt.%)	(wt.%)	(‰)	(at.)
This study *(average)*	0.198	+47.8	3.02	-12.9	0.057	2.7	2.5	0.068	+31.8	62	1.67	-17.5	0.035
and Epstein (1982)	0.272	+39	2.85	-15.6	0.082*	11*			+27	20.7*	2.28	-19.4	
Smith et Kaplan *et al.* (1970)			3.75	-11.6							2.15	-16.9	
Alexander *et al.* (2012) *(average)*	0.179	+40.0	3.72	-12.9	0.041*								
Pearson *et al.* (2006) *(average)*	0.530	+44.6	4.88	-17.5	0.093*								
Grady *et al.* (2002)	0.19996	+32	4.35	-15.2	0.039*								
Injerd and Kaplan (1974)	0.1476	+46.2											
Alexander *et al.* (2007)						2.98*	2.73*	0.0814*	+30.7	67.0	2.00	-17.05	0.0349
Alexander *et al*. (1998)						3.03*	1.55*	0.0471	+14			-16	
Pizzarello and Williams (2012)						8	1.4		+29.4				
Cronin *et al.* (1987)							2.74			68.46			
Huss and Lewis (1995)						3.62							
Remusat *et al.* (2005) *(average)*							2.75						
Kung and Clayton (1978)								0.07					
Alexander *et al.* (2015) *(average)*											2.00		
Yang and Epstein (1983)			2.3	-15.4		4.1				58.0	2.38*	-16.3	

1697

1698 **Table 4:** Orgueil average nitrogen and carbon abundances and isotopic compositions in bulk and IOM, from this study and from previous works.
1699 * Value calculated from the data available in the original paper.

Supplementary Material

Nitrogen in the Orgueil meteorite: abundant ammonium among other reservoirs of variable isotopic compositions

Lucie Laize-Générat, Lison Soussaintjean, Olivier Poch, Lydie Bonal, Joël Savarino, Nicolas Caillon, Patrick Ginot, Anthony Vella, Alexis Lamothe, Rhabira Elazzouzi, Laurène Flandinet, Lionel Vacher, Matthieu Gounelle, Martin Bizzaro, Pierre Beck, Eric Quirico, Bernard Schmitt

2 Texts

7 Figures

10 Tables

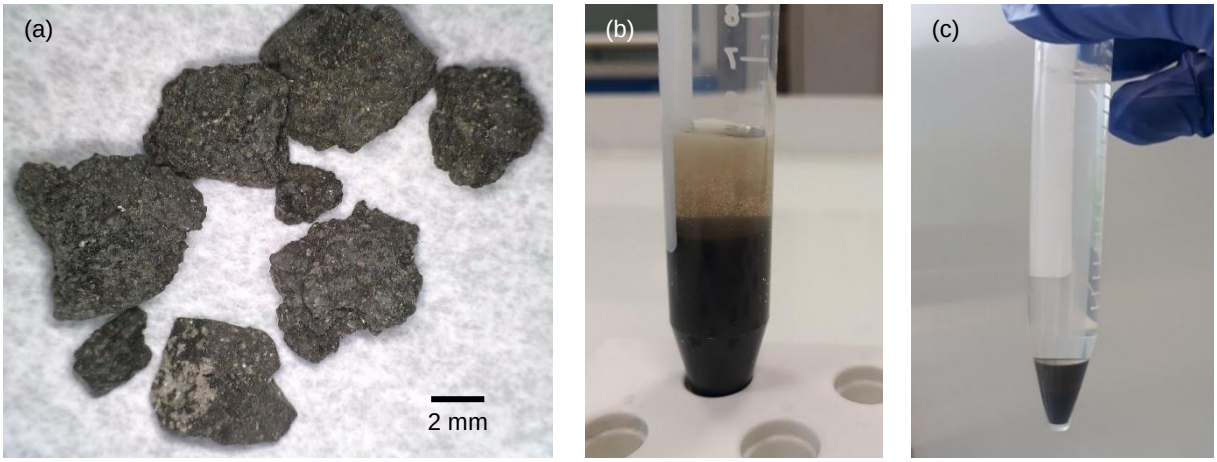

Figure S1: Illustrations of the extraction of NH_4^+ and water-soluble ions from Orgueil (OFa). **(a)** Orgueil sample chips. **(b)** Suspension collected after cryogenic grinding of the chips with UPW ice grains and **(c)** after centrifugation. The supernatant liquid phase corresponding to the extraction solution n°1 was collected and analysed for its content in NH_4^+ (and other ions) and the isotopic composition of nitrogen in NH_4^+ was also measured.

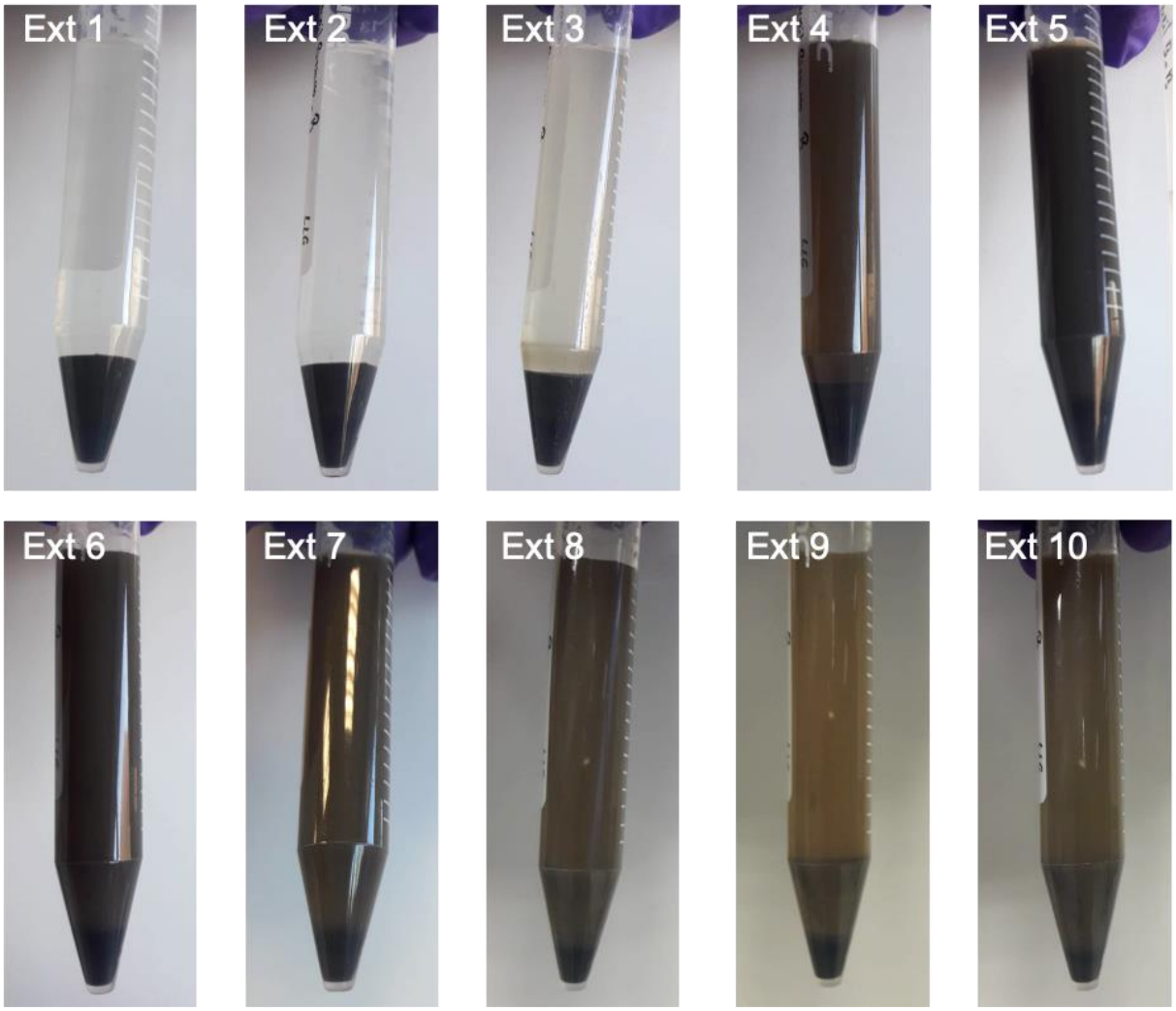

Figure S2: Images of the suspensions of meteorite powder in liquid water obtained for the sample OFb after centrifugation, before filtration. The supernatant water is transparent in extraction solutions n°1, 2 and 3 (Ext 1, 2, 3), but it is more opaque in the following ones due to the presence of sub-micrometre-size grains that stay in suspension because they are too lightweight to be centrifuged. These small grains were possibly produced by disaggregation of Orgueil components by ultrasonication and/or by desalting. A similar behaviour was observed for the other samples.

Text S1: Preliminary test of the extraction efficiency of NH_4^+ from a clay mineral

The extraction efficiency of the protocol used to extract NH_4^+ from the meteorite was first tested on a mixture of commercial clay minerals purchased from the Clay Mineral Society. The mixture consisted of powders of 0.4 mg of a synthetic ammoniated Barasym clay mineral SYn-1 (containing 2.4 wt.% NH_4^+ as measured by an IRMS analysis of the solid powder) and 299.6 mg of the nitrogen-free Na-montmorillonite SWy-3 (the absence of nitrogen was checked by an IRMS analysis). The influence of the solubilisation time on the extraction yield was investigated by performing two sample preparations in 10 mL of UPW. In the first experiment, the mineral mixture was maintained in liquid water under constant stirring for 15 hours prior to the extraction sequence. In the second experiment, the mineral mixture was poured in liquid water and directly underwent the extraction protocol, with no solubilisation time.

Figure S3 shows the extraction yields of NH_4^+ obtained after each extraction of the protocol, for both experiments. With no waiting time for solubilisation in UPW, only 75 % of the adsorbed ions were collected after 10 extractions, whereas following a 15-hour waiting period, 75 % were collected only after the first extraction and 100 % after 10 extractions.

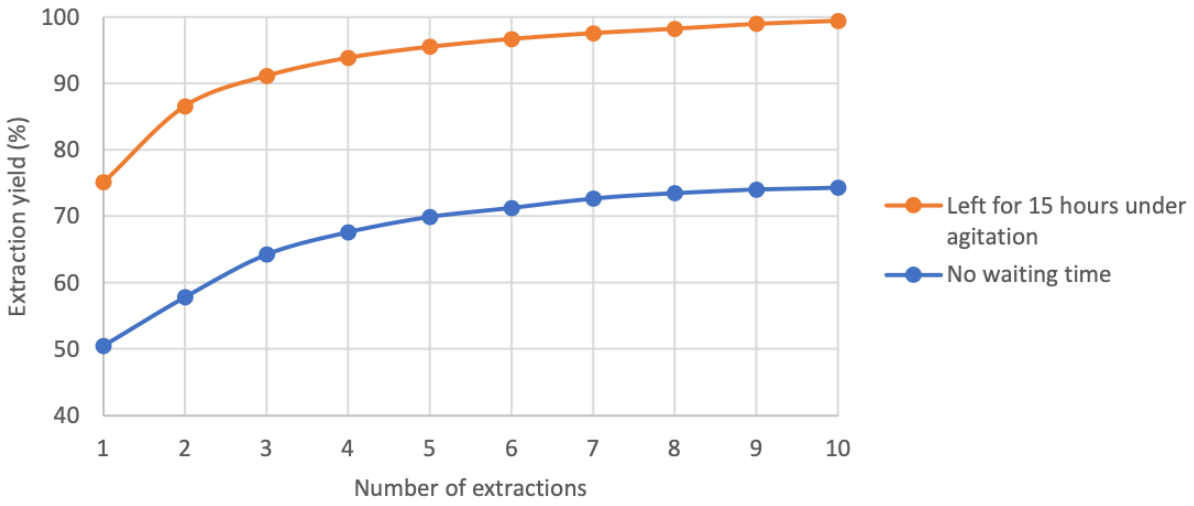

Figure S3: Extraction yields measured for two tests of NH_4^+ extraction from the ammoniated clay SYn-1 (2.4 wt.% NH_4^+) mixed with nitrogen-free SWy-3 clay mineral. The time elapsed between the addition of clay powder in water and the first extraction is the only parameter varying between the two tests. 10 successive extractions were performed for each test. The extracted solutions were analysed by ion chromatography. The extraction yield is the cumulative extracted mass of NH_4^+ divided by the initial mass of NH_4^+ adsorbed on the clay powder.

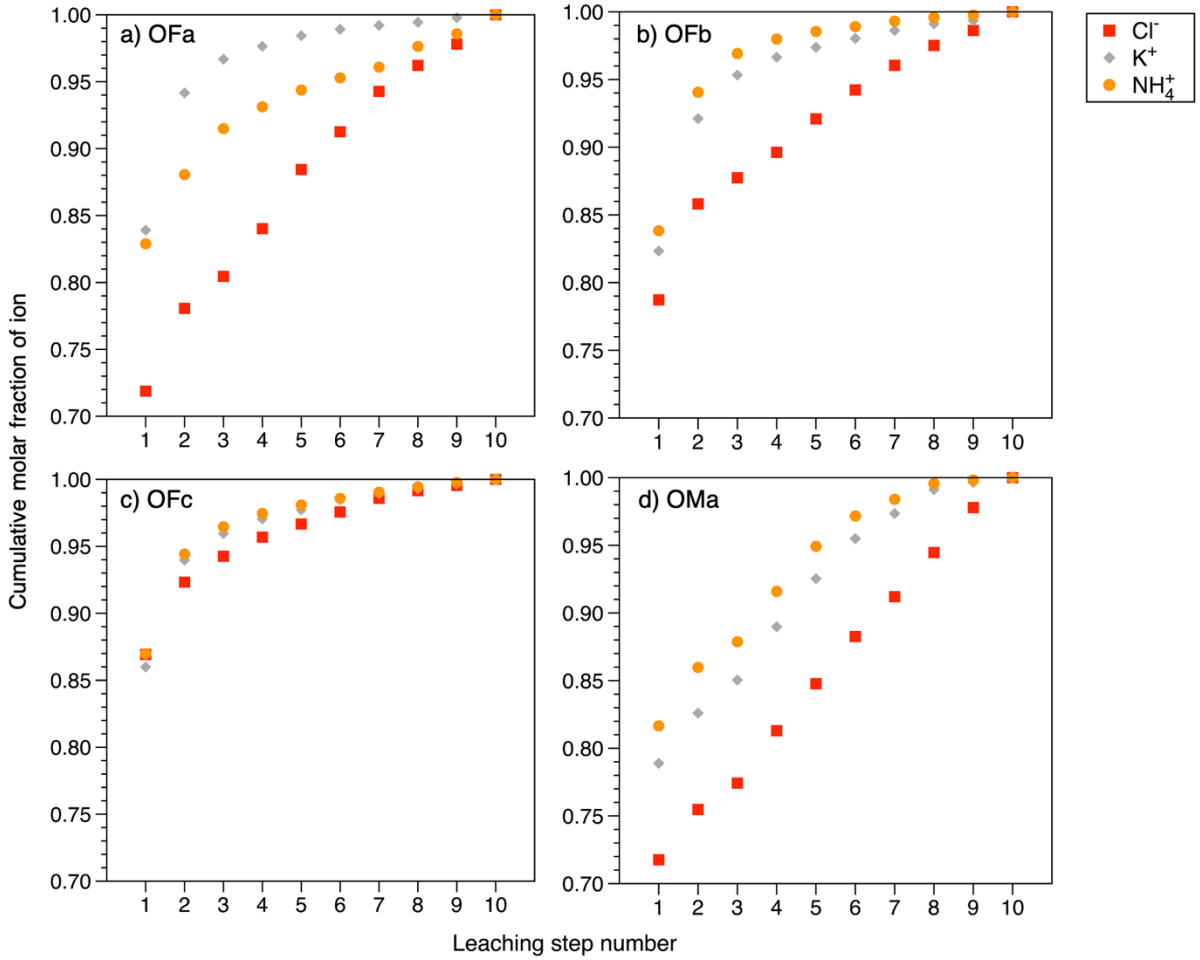

Figure S4: Cumulative mole of NH_4^+, K^+ and Cl^- ions extracted at each step of the leaching protocol normalized by the total extracted mole for **(a)** OFa, **(b)** OFb, **(c)** OFc, and **(d)** OMa. These curves show that most of the ions (77 to 91 %) are extracted in the first extraction solution (leaching step n°1), while the leaching solutions n°2 to 10 account for the remaining 9 to 23 %. A complete leaching would result in a plateauing of these curves, as additional leaching steps would not extract more ion. However, although the rate at which each ion is dissolved decreases, a plateau is not reached for all samples/ions here, suggesting that the reported concentration should be considered as lower values. The amounts of NH_4^+ and K^+ extracted during the leaching steps seem to follow similar (but not identical) trends. This suggests that NH_4^+ and K^+ might be present in phases of similar solubility and/or in the same phases. The trends of Cl^- differ from those of NH_4^+ and K^+ for most of the samples, except for OFc. Note that several factors may control the leaching and finally the shape of these curves: the heterogeneity of the samples (causing different composition, and different reactions to the grinding and leaching steps), the nature of the phase carrying the ion, the solubility of the carrier etc.

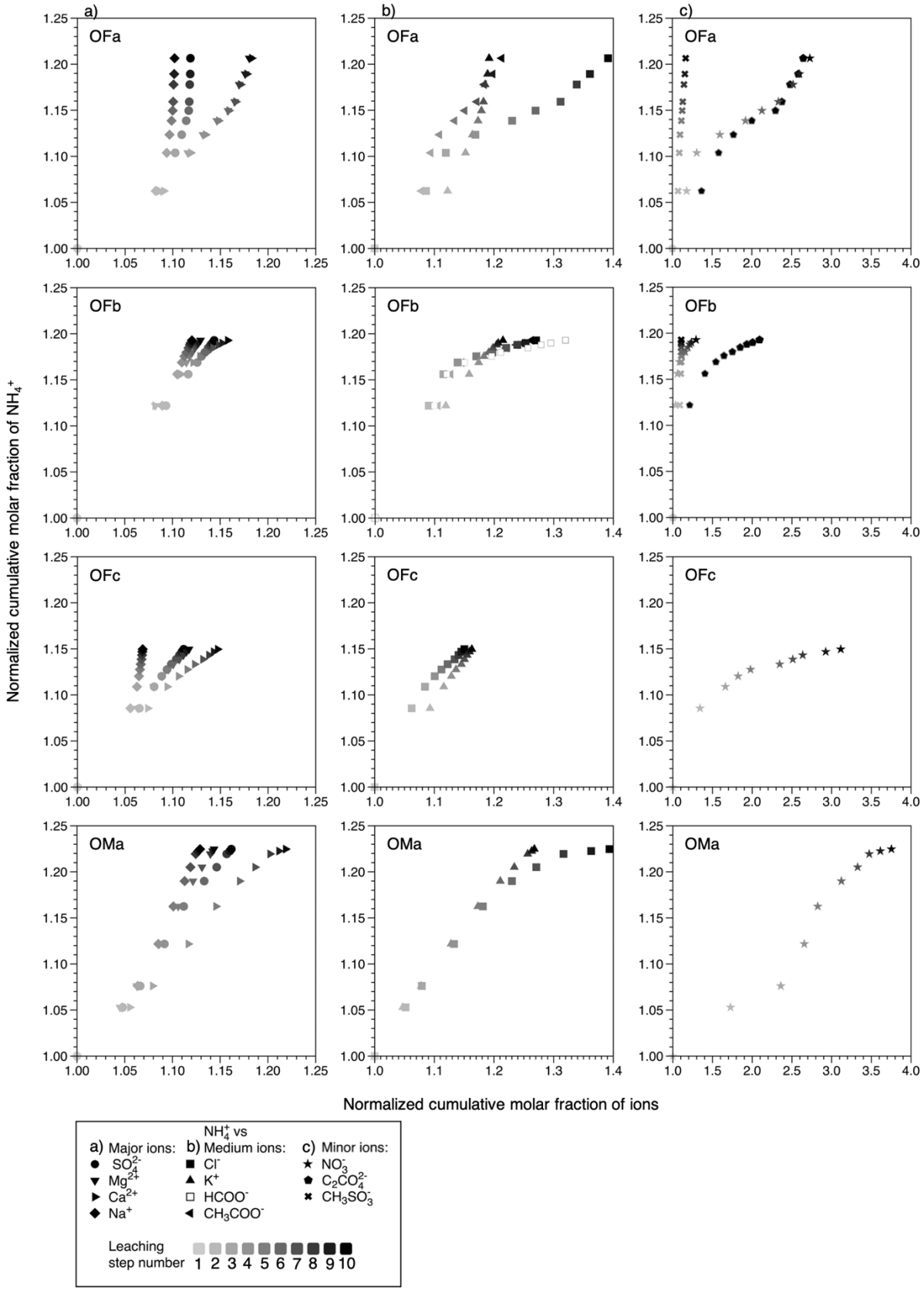

Figure S5: Normalized cumulative mole fraction of NH_4^+ (mole of NH_4^+ divided by mole of total ions and normalized by the molar fraction measured at the first extraction) extracted at each step of the leaching protocol plotted as a function of the normalized cumulative mole fraction of other ions of **(a)** major, **(b)** medium or **(c)** minor abundances. Absence of an ion in

a plot means that it was not measured or that the normalization could not have been calculated because no ion were measured in the first extraction.

Ions present in phases of similar solubility and/or in the same phases as NH_4^+ would show aligned points on these plots. However, one should note that these data may be affected by the fact that different samples would have different evolution during the grinding and leaching steps because of sample mass and heterogeneity differences. In particular, about 300 mg of meteorite were dissolved in 10 extractions of 10 mL UPW for the extractions of OFa, OFb and OMa whereas 150 mg of OFc were dissolved in 10 extractions of 12 mL UPW. This change was implemented to try to improve the water-soluble extraction efficiency and to try to decrease the mass loss during the process. We can see from this figure that these changes were effective as the normalized cumulative amounts of NH_4^+, K^+ and Cl^- at the tenth leaching are lower for OFc, meaning that more ions were extracted at the first leading step for OFc than for OFa, OFb and OMa. Table S6 gives the Pearson's correlation coefficients and the slopes of the linear regressions between the cumulated mole of NH_4^+ and that of other ions in extraction solutions.

	OFa		OFb		OFc		OMa		**Orgueil average**	
	(wt.%)	sd	(wt.%)	sd	(wt.%)	sd	(wt.%)	sd	**(wt.%)**	**sd**
Sulfate*	7.83	0.46	5.59	0.32	6.12	0.347	7.58	0.43	6.78	1.34
Magnesium*	0.804	0.045	0.966	0.056	1.05	0.059	1.33	0.08	1.04	0.25
Sodium*	0.499	0.030	0.452	0.027	0.481	0.028	0.565	0.033	0.499	0.071
Calcium*	0.433	0.024	0.530	0.030	0.477	0.027	0.377	0.021	0.454	0.082
Ammonium*	0.0789	0.0040	0.0596	0.0034	0.0699	0.004	0.0638	0.0035	0.0681	0.0109
Acetate*	0.0978	0.0073	0.0314	0.0029	n.a.		n.a.		0.0646	0.0383
Chloride*	0.0742	0.0063	0.0374	0.0034	0.0468	0.005	0.0334	0.0029	0.0479	0.0202
Potassium*	0.0535	0.0030	0.0397	0.0022	0.0493	0.003	0.0314	0.0017	0.0435	0.0109
Formate*	0.0282	0.0017	0.0137	0.0012	n.a.		n.a.		0.0209	0.0087
Nitrate*	0.0106	0.0006	0.0191	0.0016	0.00812	0.001	0.00876	0.00047	0.0117	0.0052
Oxalate*	0.0121	0.0007	0.0068	0.0004	n.a.		n.a.		0.00944	0.00324
MSA*	0.00174	0.00018	0.0076	0.0008	n.a.		n.a.		0.00468	0.00344
Glycolate	0.00116	0.00006	n.a.		n.a.		n.a.		0.00116	0.00006
Adipate	0.000895	0.000045	n.a.		n.a.		n.a.		0.000895	0.000045
Propionate*	0.000807	0.000076	n.a.		n.a.		n.a.		0.000807	0.000076
Bromide*	0.000660	0.000046	n.a.		0.000554	0.000052	$< 1.10^{-6}$		0.000607	0.000102
Succinate*	0.000552	0.000042	n.a.		n.a.		n.a.		0.000552	0.000042
Sebacate	0.000546	0.000039	n.a.		n.a.		n.a.		0.000546	0.000039
Phosphate*	0.000539	0.000045	n.a.		n.a.		n.a.		0.000539	0.000045

Glutarate*	0.000453	0.000028	n.a.	n.a.	n.a.	0.000453	0.000028
Tartrate	0.000348	0.000035	n.a.	n.a.	n.a.	0.000348	0.000035
Malonate	0.000335	0.000027	n.a.	n.a.	n.a.	0.000335	0.000027
3-Hydroxybutyrate	0.000326	0.000031	n.a.	n.a.	n.a.	0.000326	0.000031
Citrate	0.000307	0.000025	n.a.	n.a.	n.a.	0.000307	0.000025
Lactate	0.000296	0.000017	n.a.	n.a.	n.a.	0.000296	0.000017
Pimelate	0.000282	0.000027	n.a.	n.a.	n.a.	0.000282	0.000027
2-Ketobutyrate	0.000184	0.000017	n.a.	n.a.	n.a.	0.000184	0.000017
Maleate	0.000112	0.000010	n.a.	n.a.	n.a.	0.000112	0.000010
Fluoride*	0.0000921	0.0000039	n.a.	n.a.	n.a.	0.0000921	0.0000039
Butyrate	0.0000913	0.0000055	n.a.	n.a.	n.a.	0.0000913	0.0000055
Chlorate	0.0000714	0.0000035	n.a.	n.a.	n.a.	0.0000714	0.0000035
Phtalate	0.0000667	0.0000049	n.a.	n.a.	n.a.	0.0000667	0.0000049
Azelaate	0.0000539	0.0000027	n.a.	n.a.	n.a.	0.0000539	0.0000027
Pyruvate*	0.0000401	0.0000023	n.a.	n.a.	n.a.	0.0000401	0.0000023
Glyoxylate	0.0000500	0.0000025	n.a.	n.a.	n.a.	0.0000500	0.0000025
Malate	0.0000403	0.0000020	n.a.	n.a.	n.a.	0.0000403	0.0000020
Citraconate	0.0000398	0.0000028	n.a.	n.a.	n.a.	0.0000398	0.0000028
4-Oxoheptanoate	0.0000385	0.0000018	n.a.	n.a.	n.a.	0.0000385	0.0000018
Suberate	0.0000265	0.0000026	n.a.	n.a.	n.a.	0.0000265	0.0000026
Cis-Pinonate	0.0000181	0.0000015	n.a.	n.a.	n.a.	0.0000181	0.0000015

Gluconate	0.0000130	0.0000007	n.a.		n.a.		n.a.		0.0000130	0.0000007
Vanillate	0.0000123	0.0000006	n.a.		n.a.		n.a.		0.0000123	0.0000006
Pinate	0.00000832	0.00000080	n.a.		n.a.		n.a.		0.00000832	0.00000080
MBTCA	0.00000793	0.00000048	n.a.		n.a.		n.a.		0.00000793	0.00000048
Bromate	0.00000645	0.00000057	n.a.		n.a.		n.a.		0.00000645	0.00000057
Pinonate	0.00000562	0.00000029	n.a.		n.a.		n.a.		0.00000562	0.00000029
Lithium*	0.000000443	0.000000032	n.a.		n.a.		n.a.		0.000000443	0.000000032
Total	**9.93**	**0.58**	**7.75**	**0.45**	**8.30**	**0.47**	**10.0**	**0.6**	**9.05**	**1.84**

Table S1: Mass fraction of water-soluble ions in OFa, OFb, OFc and OMa, and the averaged Orgueil value. *The concentration is corrected by the LoB.

n.a.: not acquired
MSA: methanesulfonate; MBTCA: 3-methylbutane-1,2,3-tricarboxylate

	Concentration measured in the first extraction (ppb) compared to the LoB (in brackets, ppb)			Fraction of the total mass of ion which is extracted in the second rinse of the grinding jar and balls (in wt.%)			
	NH_4^+	NO_3^-	NO_2^-	SO_4^{2-}	NH_4^+	NO_3^-	NO_2^-
OFa	18521 (21)	1136 (363)	317 (174)	1.0	9.2	33	24
OFb	15319 (21)	4447 (363)	148 (174)	1.4	1.4	9.7	35
OFc	7726 (21)	541 (363)	18 (174)	0.3	0.8	35	37
OMa	16347 (21)	914 (363)	0 (174)	0.2	0.4	23	58

Table S2: Left: Measured concentrations of ions in the first extraction solution (ppb) and the calculated Limit of Blank (LoB) in brackets (ppb) from 15 blanks of an extraction step (see section 2.6 for details). **Right:** Fractions of the total mass of ions, extracted in the second rinse of the grinding jar and balls (see section 2.5 for details).

Given that the concentrations of NO_2^- measured in the first extractions of OFb, OFc and OMa are lower than the LoB, this ion likely comes from a contamination. The concentrations of NO_3^- measured in the first extractions are all larger than the LoB, but very variable from one sample to another, potentially indicative of sample heterogeneity. Furthermore, the fractions of the total mass of NO_3^- and NO_2^- extracted in the second rinse of the jar and balls are approximately 30 times higher than those of NH_4^+ or SO_4^{2-} (the most concentrated ion). This suggests that NO_3^- and NO_2^- may originate from different sources than the NH_4^+ or SO_4^{2-}, potentially indicating contamination.

Text S2: Calibration experiments performed to measure the isotopic fractionation of NH_4^+ induced by the extraction protocol

Ammonium contained in meteorites undergoes isotopic fractionation during the ammonium extraction protocol described in section 2.5. To correct $\delta^{15}N_{\text{first correction}}$ for this fractionation, we have applied the principle of "identical treatment" (Werner and Brand, 2001), by which isotopic standards should undergo the same protocol as the samples. For this, the whole extraction protocol was run on reference samples consisting of a mineral powder and of UPW ice particles containing an isotopic standard of ammonium sulfate (J, K, L or M), at concentrations similar to the samples. The isotopic fractionation induced by the extraction protocol was determined by comparing the $\delta^{15}N_{\text{first correction}}$ with the true $\delta^{15}N$ of the isotopic standards.

Five experiments A, B, C, D and E were carried out. Experiments A and B were made only with isotopic standards in UPW, without mineral phase, at ammonium concentrations of 22 µmol.L^{-1} and 443 µmol.L^{-1}, respectively. Experiments C and D were made with isotopic standards in UPW and in presence of a mass *m* of Na-montmorillonite smectite phyllosilicate powder (SWy-3) with ammonium-to-*m* ratios ($[NH_4^+]/m$) of 0.07 µmol.L^{-1}.mg^{-1} and 2.96 µmol.L^{-1}.mg^{-1}, respectively. SWy-3 was used as a nitrogen-free simulant of Orgueil minerals, because Orgueil is essentially made of expandable smectite phyllosilicates (King et al., 2015; Viennet et al., 2023), possibly a smectite-rich serpentine mixed-layer-mineral (see Viennet et al., LPSC 2022). A last experiment (E) was carried out, using the M isotopic standard in UPW in presence of a mass *m* of a leached powder of Orgueil with a $[NH_4^+]/m$ ratio of 0.32 µmol.L^{-1}.mg^{-1}. This leached powder of Orgueil is composed of the powders remaining after the 10 extraction steps (ultrasonication, centrifugation, filtration, and recovery) performed on the OMd and OMe samples. In a previous experiment, we established that an 11^{th} extraction step still releases ammonium, comprising 7 % of the total mass of ammonium extracted during the preceding 10 extractions. Consequently, considering that this residual ammonium has a $\delta^{15}N_{\text{first correction}}$ of +56 ‰ (as measured in OMd and OMe, Table S4) while the standard has a $\delta^{15}N_{\text{true}}$ of +375 ‰, we calculated by mass balance the $\delta^{15}N_{\text{true}}$ of the total ammonium introduced in this experiment (Figure S6, plain square point).

No nitrogen isotopic fractionation was measured in experiments A and B, whereas experiments C, D and E show isotopic fractionations, much stronger in the case of experiment C and E performed at lower $[NH_4^+]/m$ ratios (Figure S6, Table S3). The absence of isotopic fractionation during experiments A and B (Figure S6, curves a and b; Table S3), indicates that isotopic fractionation occurs exclusively between ammonium and the mineral powder. Differences between experiments C and D indicate that the isotopic fractionation depends on the $[NH_4^+]/m$ ratio (42 times higher for D than C). The isotopic fractionation of experiment E (Figure S6, plain square point) is consistent with that observed in experiment C (Figure S6, empty diamonds). Experiment E was made with a $[NH_4^+]/m$ ratio a factor of 4 higher than that of experiment C. Given the trend observed for experiments C and D, an experiment with the powder SWy-3 and a $[NH_4^+]/m$ ratio of 0.32 µmol.L^{-1}.mg^{-1} would have likely resulted in a slightly lower fractionation than that observed in experiment E, with the meteorite powder at the same ratio. Therefore, the meteorite powder may induce a higher fractionation than the SWy-3 powder. However, we ignore the detailed dependence of the fractionation with the $[NH_4^+]/m$ ratio. This would require to perform several additional experiments with Orgueil

meteorite powder, which is not conceivable given the rarity of this meteorite. Moreover, the leached powder of Orgueil is not perfectly equivalent to the raw Orgueil chips, which contain soluble ions that may contribute to the fractionation of the ammonium during this experimental protocol. Therefore, given these uncertainties and the fact that the $[NH_4^+]/m$ ratio is of the same order of magnitude for experiments E and C, we hypothesise that the fractionation induced by the Orgueil powder is comparable, although possibly slightly higher, than that induced by the Na-montmorillonite SWy-3.

Given that the $[NH_4^+]/m$ ratios of the first extraction solutions of OFa, OFb, OFc, OMa and the solution of experiment D are of the same order of magnitude (Table S3, Table S4), and that SWy-3 and Orgueil powders appear to induce similar nitrogen isotopic fractionation of NH_4^+, we have corrected the $\delta^{15}N_{\text{first correction}}$ from the isotopic fractionation induced by the ammonium extraction protocol with the calibration obtained in experiment D: $\delta^{15}N_{true} = 0{,}874 * \delta^{15}N_{first\ correction} + 4{,}568$.

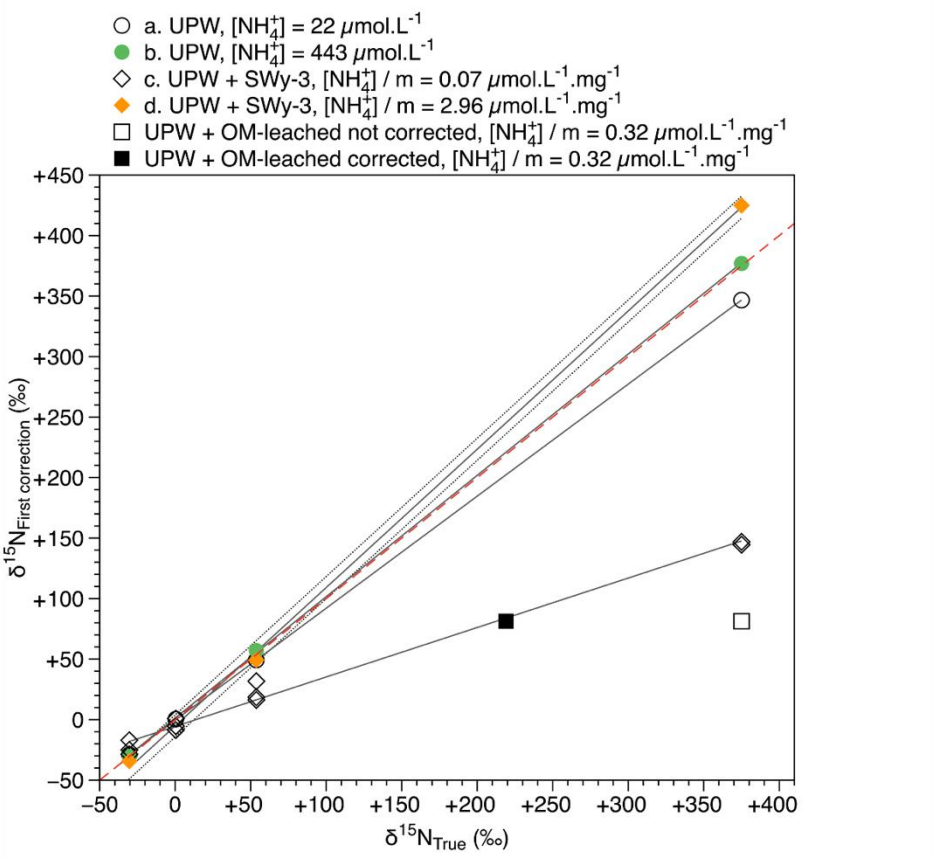

Figure S6: Calibration curves for the corrections of the $\delta^{15}N_{\text{First correction}}$ of NH_4^+. Experiments with NH_4^+isotopic standards K, L and M (with true $\delta^{15}N$ equal to -30.41, +53.75 and +375.3 ‰ respectively) and UPW are represented with circles (empty and green for concentrations $[NH_4^+]$ of 22 and 443 µmol.L^{-1}, respectively). Experiments with isotopic standards, UPW and the montmorillonite SWy-3 are represented with diamonds (empty and orange for $[NH_4^+]$/m of 0.07 and 2.96 µmol.L^{-1}.mg^{-1}, respectively). The result of the experiment led on the M isotopic standard with UPW and leached-OMa is plotted as a plain squared mark. The black lines show the linear regressions between the measured $\delta^{15}N$ of NH_4^+ and the true $\delta^{15}N$ of NH_4^+ in the standards (Table S3). As described in Text S2, the measurements on the samples were calibrated

using data from the experiment D. For this experiment D, the dotted lines indicate the 95 % confidence interval. The y = x function is represented with the red dashed line.

Linear regression	Composition	NH_4^+ concentrations ($\mu mol.L^{-1}$)	$[NH_4^+]$/m ratio ($\mu mol.L^{-1}.mg^{-1}$)	Slope	Intercept	R^2
a	UPW	22	N.A.	0.926	-0.472	1.000
b	UPW	443	N.A.	1.002	1.373	1.000
c	UPW + SWy-3	22	0.07	0.409	-5.600	0.988
d	UPW + SWy-3	443	2.96	1.143	-5.119	0.999
N.A.	UPW + leached-OMa	43	0.32	N.A.	N.A.	N.A.

Table S3: Slopes, intercepts and coefficient of correlation of the linear regressions calculated for the A, B, C, D and E calibration experiments (Figure S6).

	$[NH_4^+]$/m ratio ($\mu mol.L^{-1}.mg^{-1}$)	$\delta^{15}N_{measured}$ (‰)	NH_4^+ $\delta^{15}N_{first\ correction}$ (‰)	$\delta^{15}N_{meteorite}$ (‰)
OFa	3.38	-8	+78 ± 1.8	+73 ± 8
OFb	2.81	+24	+78 ± 0.3	+73 ± 8
OFc	2.85	+15	+76 ± 0.4	+71 ± 8
OMa	2.95	+29	+45 ± 0.4	+44 ± 8
OMd	N.A.	+19	+56 ± 0.3	+54 ± 8
OMe	N.A.	+19	+55 ± 0.3	+53 ± 8
Orgueil average			**+77 ± 1.8**	**+72 ± 9**

Table S4: Measured nitrogen isotopic compositions of the ammonium extracted from the Orgueil samples ($\delta^{15}N_{measured}$), corrected for the influences of contamination and isotopic fractionations occurring during the IRMS analysis ($\delta^{15}N_{first\ correction}$) and corrected from the isotopic fractionation induced during the extraction from the meteorite ($\delta^{15}N_{meteorite}$).

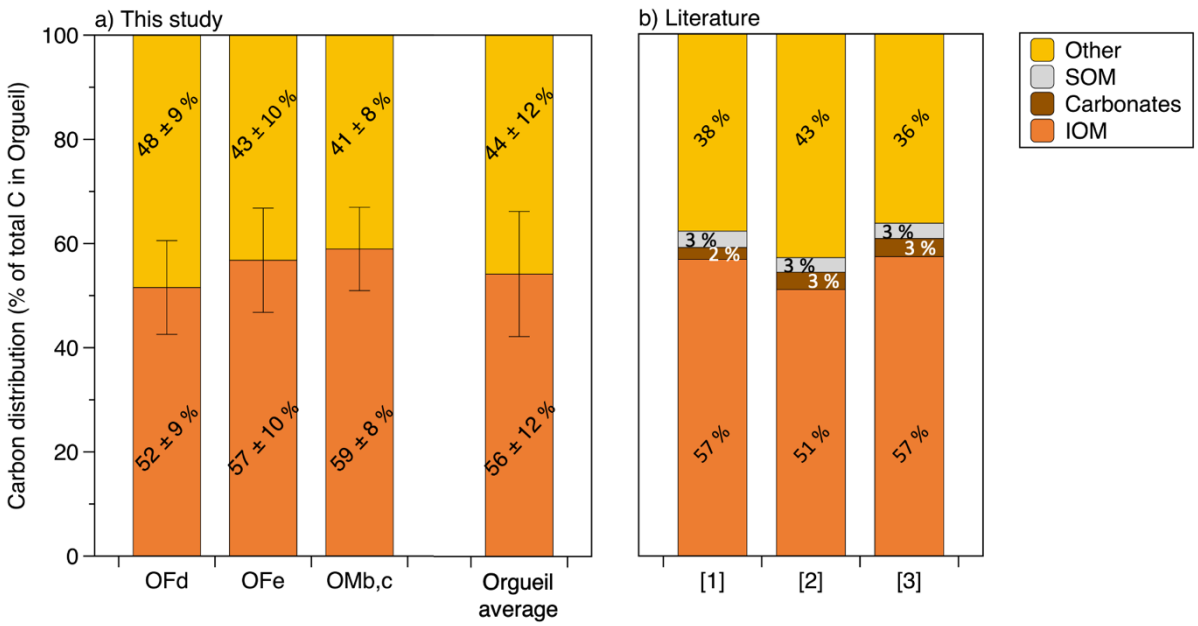

Figure S7: Distribution of the carbon in the Orgueil meteorite. **(a)** Distribution of the carbon in OFd, OFe and OMb,c samples (Table 1) and average distribution of the carbon in Orgueil from this study. IOM = Insoluble Organic Matter. Other = carbon in other carrier phases. **(b)** Distribution of the carbon among the IOM, the soluble organic matter (SOM), carbonates, and other carbon-bearing phase(s) in [1] Orgueil BM reported in Alexander et al. (2015), [2] Orgueil SI reported in Alexander et al. (2015) and [3] Orgueil reported in Smith and Kaplan (1970). A significant fraction of carbon (36 to 43 %) is not in IOM, carbonates or SOM, but is in an unidentified organic matter (UOM). This UOM may be IOM lost during its extraction and/or acid hydrolysable functional groups bounded to the IOM and/or organic nitrogen trapped within minerals (see discussion in section 4.3).

	NH_4^+ vs.		
	K^+	Cl^-	NO_3^-
Pearson's r	0.98	0.91	0.01
Slope	1.6 ± 0.6	1.0 ± 0.4	0.8 ± 3.6

Table S5: Pearson's correlation coefficients (denoted by Pearson's r) and slopes of the linear regressions between the normalized total mole fraction of NH_4^+ cumulated from the 10 extraction solutions (cumulated mole of NH_4^+ divided by mole of all measured ions) and that of other minor ions analysed after grinding and leaching of OFa, OFb, OFc and OMa in water. Best correlations are obtained between NH_4^+ vs. K^+ and NH_4^+ vs. Cl^- mole fractions, suggesting that NH_4^+ might be associated with phases with similar solubilities and/or might be present in the same phases as Cl^- and K^+. The slope of 1 for NH_4^+ vs. Cl^- suggests the presence of $NH_4^+Cl^-$.

	OFa		OFb		OFc		OMa	
NH_4^+ vs.	Pearson's r	slope	Pearson's r	slope	Pearson's r	slope	Pearson's r	slope
SO_4^{2-}	0.887	0.08 ± 0.04	0.999	0.07 ± 0.04	0.999	0.08 ± 0.05	0.997	0.06 ± 0.02
Mg^{2+}	0.977	0.13 ± 0.06	0.999	0.12 ± 0.06	0.998	0.11 ± 0.07	0.996	0.10 ± 0.04
Na^+	0.840	0.34 ± 0.23	0.993	0.25 ± 0.14	0.964	0.37 ± 0.34	0.987	0.2 ± 0.1
Ca^{2+}	0.976	0.4 ± 0.2	0.988	0.31 ± 0.15	0.993	0.34 ± 0.19	0.997	0.4 ± 0.1
CH_3COO^-	0.989	3.5 ± 2.2	0.914	5.3 ± 3.0	/	/	/	/
Cl^-	0.975	1.1 ± 0.5	0.888	2.6 ± 1.4	0.977	3.0 ± 2.6	0.962	2.7 ± 1.0
K^+	0.923	2.9 ± 1.3	0.996	3.1 ± 1.3	0.999	2.9 ± 1.6	0.997	3.8 ± 1.2
$HCOO^-$	/	/	0.863	7.9 ± 4.0	/	/	/	/
$C_2O_4^{2-}$	0.977	15.7 ± 5.1	0.854	13.2 ± 4.8	/	/	/	/
NO_3^-	0.946	8.3 ± 2.8	0.744	9.7 ± 5.6	0.856	9.8 ± 4.7	0.983	9.0 ± 2.4
$CH_3SO_3^-$	0.991	268 ± 219	0.994	59 ± 76	/	/	/	/

Table S6: Pearson's correlation coefficients (denoted by Pearson's r) and slopes of the linear regressions between the cumulative mole of NH_4^+ divided by the molar fraction of the first extraction and that of other ions after extraction solution n°1 to n°10. See Figure S5 caption for details.

	Mass before leaching (mg)	Mass after leaching (mg)	lost mass (%)
OFa	303.1 ± 0.1	100.1 ± 0.1	67
OFb	302.3 ± 0.1	110.8 ± 0.1	63
OFc	150.0 ± 0.1	125.3 ± 0.1	16
OMa	306.8 ± 0.1	154.0 ± 0.1	50

Table S7: Percentages of mass loss during the extraction of water-soluble ions (cryogenic grinding followed by leaching in liquid water) for OFa, OFb, OFc and OMa samples (Table 1). About 300 mg of meteorite were dissolved in 10 extractions of 10 mL UPW for the extractions of OFa, OFb and OMa, whereas 150 mg of OFc were dissolved in 10 extractions of 12 mL UPW. These changes in the protocol were implemented to try to improve the water-soluble extraction efficiency and to try to decrease the mass loss during the process. We can see in this table that these changes were effective as only 16% of the total mass of OFc was lost during the extraction protocol, opposed to 50 to 67 % for the other samples. This mass loss has to be taking into account for the interpretation of the results of elementary and isotopic composition analyses by IRMS on the leached powders of OFa, OFb, OFc and OMa and IOM extracted from the leached powders of OFb and OMa.

Sample		Nitrogen mass fraction		δ^{15}N	
		(wt.%)	sd	(‰)	sd
Bulk leached powder					
	OFa (*n=3*)	0.244	0.022	+40.5	0.7
	OFb (*n=3*)	0.159	0.008	+39.2	0.6
	OFc (*n=3*)	0.166	0.002	+38.7	0.5
	OMa (*n=3*)	0.169	0.003	+43.2	0.5
	Average	***0.184***	***0.044***	***+40.4***	***2.3***

Phase	Sample	Phase mass fraction in leached Orgueil		Nitrogen mass fraction in phase		Nitrogen fraction in leached Orgueil		δ^{15}N	
		(wt.%)	sd	(wt.%)	sd	(%)	sd	(‰)	sd
IOM									
	OFb (*n=2*)	3.4	0.4	2.11	0.03	46	6	+31.9	0.2
	OFc (*n=3*)	4.4	0.4	2.35	0.02	62	6	+28.8	1.2
	OMa (*n=2*)	3.3	0.4	2.34	0.22	46	7	+31.7	0.7
	Average	***3.7***	***0.9***	***2.27***	***0.20***	***51***	***14***	***+30.8***	***2.1***

Table S8: Nitrogen elemental and isotopic analyses of the powders retrieved after leaching of the Orgueil meteorite samples with liquid water. Insoluble organic matter (IOM) was also extracted and analysed from the leached powders.

N-bearing phase	N (%) [a]	N (%) [b]	δ^{15}N (‰)
IOM	**34 ± 6**		+31 ± 1
Water-Soluble (total)	**30 ± 2**	**100**	
NH_4^+	29 ± 2	90 ± 10	+71 ± 8 [c]
NO_3^-	1.0 ± 0.1	3.3 ± 0.6	
Other molecules [d]	3 ± 3	6 ± 6	
Other [e]	**36 ± 9**		

Table S9: Distribution of nitrogen in Orgueil OFc sample, for which the mass loss during the the extraction of water-soluble ions was minimal (16 %, Table S7).

[a] among the N-bearing phases in Orgueil.

[b] within the water-soluble N-bearing species.

[c] This δ^{15}N value is for NH_4^+, with potential contributions of nitrogen-bearing water-soluble organic molecules oxidized or partly oxidized by the azide method (section 2.7).

[d] The fraction of total nitrogen in other water-soluble molecules is estimated from the difference of bulk nitrogen in the leached meteorite powder (Table S8) compared to the raw meteorite (Table 3), also taking into account the measured amounts in NH_4^+ and NO_3^- .

[e] "Other" is the remaining nitrogen (not in the extracted IOM, NH_4^+ and water-soluble species), which is mainly (60-90 %) in an unidentified organic matter (UOM) as shown in Figure S7 and discussed in section 4.3. This UOM may be IOM lost during its extraction and/or acid hydrolysable functional groups bounded to the IOM and/or organic nitrogen trapped within minerals. The rest of the remaining nitrogen may be in inorganic species not extracted by our protocol.

		Bulk		**IOM**		**Other than IOM, NH_4^+, NO_3^-, SOM and carbonates**	
		N/C (at.)	sd	N/C (at.)	sd	N/C (at.)	sd
OF	**OFa**	0.061	0.003	0.040	0.009	0.048	0.020
	OFb					0.058	0.021
	OFc	0.058	0.002	0.035	0.008	0.056	0.024
OM		0.051	0.002	0.030	0.005	0.056	0.022
Orgueil Average		**0.057**	**0.006**	**0.035**	**0.011**	**0.055**	**0.026**

Table S10: Nitrogen-to-carbon atomic ratios (N/C) measured for Orgueil bulk, IOM and estimated for the fraction of Orgueil other than IOM, NH_4^+, NO_3^-, SOM and carbonates. The estimation of the N/C ratio of this latter fraction is made using data from the present study together with data from Becker and Epstein (1982), Smith and Kaplan (1970) and Alexander et al. (2015) (see section 4.3 for details).